Endo : Press®

ENDOSCOPE-ASSISTED MICRONEUROSURGERY

Principles, Methodology and Applications

Renato J. GALZIO

Manfred TSCHABITSCHER

Renato J. Galzio, M.D., is Professor and Chairman of Neurosurgery at the Medical School of the University of L'Aquila and Director of the Department of Neurosurgery of the San Salvatore City Hospital of L'Aquila, Italy. He has performed more than 7,500 major operative procedures and is a recognized expert in vascular and skull base surgery, in operative neuroendoscopy and in the use of image-guided techniques. In 1995, he introduced in its clinical practice, the use of the endoscope to assist and control microsurgical maneuvers during intracranial interventions, performing more than 500 procedures of this type, and has developed scopes and instruments dedicated to this particular methodology. He pioneered microsurgical and endoscopic hands-on courses in Italy. He is a member of several national and international neurosurgical societies and has published more than 50 peer-reviewed articles in international journals and numerous book chapters in specialized literature.

Manfred Tschabitscher, M.D., Ph.D., is fulltime Professor of Anatomy and Head of the Department of Systematic Anatomy and of the Microsurgical and Endoscopic Anatomy Study Group at the Medical University of Vienna, Austria. He is a member of the Anatomy Division of the German Society of Neurosurgeons and an honorary member of the Italian Society of Neurosurgery. In the past few years his research work has been focused on defining the fundamentals of anatomy with particular relevance to the use of endoscopes in various specialties, among them neurosurgery, ENT, maxillofacial surgery, plastic surgery and surgery of the hand. He is the author of several textbooks on endoscopic anatomy and has published more than 100 papers in medical literature. As an academic teacher he organized numerous postgraduate workshops (Neuroendoscopy, Microsurgery, Brain Injuries, etc.), has taught dissection work for decades and gives lectures to medical students, scrub nurse trainees and lab technicians in training.

Endo : Press®

ENDOSCOPE-ASSISTED MICRONEUROSURGERY

Principles, Methodology and Applications

Renato J. GALZIO, M.D.

Department of Life, Health and Environmental Sciences
Chair of Neurosurgery
Medical School of the University of L'Aquila

Prof. Manfred TSCHABITSCHER, M.D.

Human Anatomy
Section of Anatomy and Physiopathology
Department of Clinical and Experimental Sciences
University of Brescia

Collaborators:

Francesco Di COLA, M.D.

Department of Life, Health and
Environmental Sciences
Resident in Neurosurgery
University of L'Aquila

Danilo De PAULIS, M.D.

Department of Neurosurgery
"San Salvatore" City Hospital

Important notes:

Medical knowledge is ever changing. As new research and clinical experience broaden our knowledge, changes in treatment and therapy may be required. The authors and editors of the material herein have consulted sources believed to be reliable in their efforts to provide information that is complete and in accord with the standards accepted at the time of publication. However, in view of the possibility of human error by the authors, editors, or publisher, or changes in medical knowledge, neither the authors, editors, publisher, nor any other party who has been involved in the preparation of this booklet, warrants that the information contained herein is in every respect accurate or complete, and they are not responsible for any errors or omissions or for the results obtained from use of such information. The information contained within this booklet is intended for use by doctors and other health care profes sionals. This material is not intended for use as a basis for treatment decisions, and is not a substitute for professional consultation and/or use of peer-reviewed medical literature.

Some of the product names, patents, and registered designs referred to in this booklet are in fact registered trademarks or proprietary names even though specific reference to this fact is not always made in the text. Therefore, the appearance of a name without designation as proprietary is not to be construed as a representation by the publisher that it is in the public domain.

The use of this booklet as well as any implementation of the information contained within explicitly takes place at the reader's own risk. No liability shall be accepted and no guarantee is given for the work neither from the publisher or the editor nor from the author or any other party who has been involved in the preparation of this work. This particularly applies to the content, the timeliness, the correctness, the completeness as well as to the quality. Printing errors and omissions cannot be completely excluded. The publisher as well as the author or other copyright holders of this work disclaim any liability, particularly for any damages arising out of or associated with the use of the medical procedures mentioned within this booklet.

Any legal claims or claims for damages are excluded.

In case any references are made in this booklet to any 3rd party publication(s) or links to any 3rd party websites are mentioned, it is made clear that neither the publisher nor the author or other copyright holders of this booklet endorse in any way the content of said publication(s) and/or web sites referred to or linked from this booklet and do not assume any form of liability for any factual inaccuracies or breaches of law which may occur therein. Thus, no liability shall be accepted for content within the 3rd party publication(s) or 3rd party websites and no guarantee is given for any other work or any other websites at all.

Endoscope-Assisted Microneurosurgery
Principles, Methodology and Applications

Renato J. Galzio and **Manfred Tschabitscher**

Correspondence address of the author:

Renato J. Galzio, M.D.
Department of Life, Health and Environmental Sciences
Chair of Neurosurgery
Medical School of the University of L'Aquila
Piazza Salvatore Tommasi 1 (Coppito), 67100-L'Aquila, Italy
E-mail: renato.galzio@cc.univaq.it

Prof. **Manfred Tschabitscher,** M.D.
Human Anatomy
Section of Anatomy and Physiopathology
Department of Clinical and Experimental Sciences
University of Brescia
Viale Europa 11, 25123-Brescia, Italy

Microsurgical and Endoscopic Anatomy
Medical University of Vienna
Währinger Straße 13, 1090-Wien, Austria
E-mail: manfred.tschabitscher@meduniwien.ac.at

Collaborators:

Francesco Di Cola, M.D.
Department of Life, Health and Environmental Sciences
Resident in Neurosurgery
University of L'Aquila
Piazza Salvatore Tommasi 1 (Coppito), 67100-L'Aquila, Italy
E-mail: fra.dicola@hotmail.it
dicolafran@gmail.com

Danilo De Paulis, M.D.
Department of Neurosurgery
"San Salvatore" City Hospital
Via Vetoio snc (Coppito),
67100-L'Aquila, Italy
E-mail: d.depaulis@alice.it

1st edition 2012

P.O. Box, 78503 Tuttlingen, Germany
Phone: +49 (0) 74 61/1 45 90
Fax: +49 (0) 74 61/708-529
E-Mail: endopress@t-online.de

Editions in languages other than English and German are in preparation. For up-to-date information, please contact Endo:Press® GmbH at the address shown above.

Design and Composing:
Endo:Press® GmbH, Germany

Printing and Binding:
Straub Druck + Medien AG
Max-Planck-Straße 17, 78713 Schramberg, Germany

07.15-0.3

ISBN 978-3-89756-829-7

Table of Contents

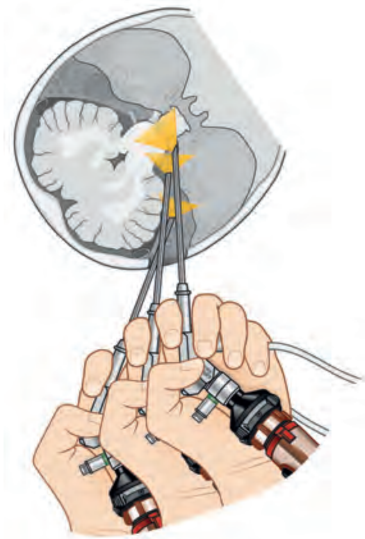

1

The endoscopes can be advanced into the operative area to enlarge the visual field of deeply located sectors.

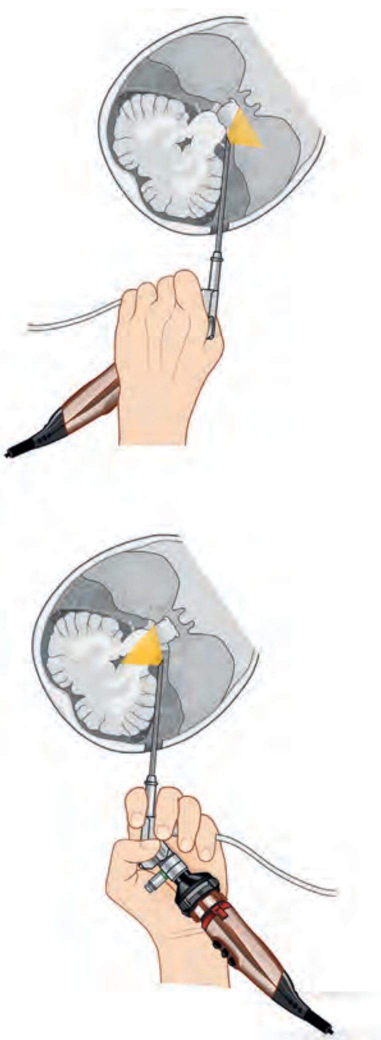

2

30° angled scopes allow visualization of structures located "around the corner" and obscured by foreground objects; on-axis rotation of the scope further enhances inspection.

1.0 Historical Background and General Aspects

During operative approaches to deeply located intracranial lesions, endoscopes may be employed to assist microsurgical maneuvers and to control their efficacy. This methodology is usually defined as **E**ndoscope-**A**ssisted **M**icroneurosurgery (**EAM**).

In the late 1970's *Apuzzo et al.*[1], as well as *Halves* and *Bushe*[2], reported the use of the endoscope as a technical adjunct in the microsurgical resection of pituitary lesions with extrasellar extension, with endoscopy used to view structures located out of the line of sight of the microscope (a view previously achieved with angled mirrors)[3]. In 1995 *Matula, Tschabitscher et al.* introduced the concept of endoscope-assisted microneurosurgery in the treatment of intracranial lesions, mainly located in the posterior fossa and in the parasellar region[4], but it was *Axel Perneczky* who essentially pioneered and popularized the use of the endoscope in intracranial neurosurgery, introducing the concept of minimally invasive neurosurgery[5–8].

During microsurgical procedures, the operative microscope provides direct illumination and magnification of the operative field; however, it allows detailed view only of superficially located structures. Visualization and dissection of structures underneath the surface plane is often associated with inadvertent manipulation and retraction of structures located in superficial anatomical sectors, which inevitably results in iatrogenic trauma. This can be obviated by using a combination of microsurgical and endoscope-assisted techniques, enabling minimally invasive visualization of structures adjacent to and behind the superficial anatomical plane, "*just behind the corner*". During EAM procedures, the operative microscope provides a straight-ahead view on-axis with the trajectory of penetration, and permits visual control of the endoscope, whereas endoscopes provide clear vision and allow for less traumatic dissection of structures located at a deeper level of the operative field. In order to allow adequate control, as with any microsurgical instrument, scopes used for endoscope-assisted microneurosurgery must be specifically designed, especially in terms of sturdiness and rigidity. For endoscope-assisted microneurosurgical procedures, semi-rigid fiberscopes have also been proposed, but the authors hold the opinion that rigid scopes are more suitable because they are superior in terms of image quality and because the rigid shaft allows them to be firmly fixed to a holding device mounted to the operating table. Rigid telescopes used for EAM are based on the rod-lens system patented by *H.H. Hopkins* in 1960, coupled with an external fiberoptic cold light system (first patented by *Karl Storz* in 1965)[9–11]. The videoendoscopic view is provided by chip cameras attached to the scope transmitting the images to external monitors[12].

Rigid endoscopes can be safely sterilized in an autoclave and can be focused on objects at varying distances. Different degrees of inclination of the front lens provide the scopes with different viewing directions; 0°-, 30°-, 45°-, 70°- and even 110°-angled scopes have been described. Essentially, only 0°- and 30°-angled scopes are used for endoscope-assisted microneurosurgical procedures, because angles of vision larger than 30° greatly distort the appearance of anatomical structures, making it difficult to match and adequately control the microsurgical and endoscopic views. 0°-telescopes to a certain degree also permit lateral viewing and can be used for inspection of deep-seated hidden structures; advancing the scope into the operative field permits inspection of a wide space beyond the structures located in the uppermost plane (**Fig. 1**); 30°-angled scopes allow visualization of structures located behind the uppermost object plane ("*just behind the corner*"). By on-axis rotation of the shaft, a wide panoramic view of lower sectors of the operative field can be obtained (**Fig. 2**).

Modern endoscopes capture a large field of view of about 80°, which becomes apparent by the so-called "fish-eye" effect and a 3D-like vision of structures in front of the scope's tip. Accordingly, even if a real three-dimensional view is not provided, small in-and-out movements of the tip of the scope can produce a 3D-like visual impression eliminating the need for more sophisticated optical devices. Indeed, three-dimensional videoendoscopic imaging systems have been developed and are applied in laparoscopic procedures[13,14], but, evidence favoring their use in intracranial procedures has been inconsistent, so far.

Endoscope-assisted microneurosurgical procedures can be performed by using the free-hand technique with the scope simply to visualize structures located "*just behind the corner*" and to assess the result of surgical maneuvers.

However, in most instances, it is necessary that the scope be fixed to a holding system enabling the surgeon to gain full control over the course of microsurgical maneuvers or, occasionally, to perform surgical maneuvers under direct endoscopic vision using both hands. Special holding devices are available to securely lock the scope in the correct intracranial position. In our opinion, mechanical holders are better suited for this purpose than pneumatic holders, because they allow delicate and precise scope repositioning without the inherent risk of inducing a dangerous rebound effect.

Endoscopes used for EAM procedures must have specific characteristics. The proximal eyepiece section of the endoscope has to be angled to prevent the connected camera from getting in between the microscope's light beam and to avoid that the scope itself obstructs the smooth flow of microsurgical maneuvers: endoscopes with a 45° angled eyepiece are suited best for this purpose; due to the well-balanced ergonomic design, the scope feels comfortable and stable in all operating conditions, whether it is manually operated by the free hand or used while mounted to a holder. The shaft of the scope should not be too long, but should enable access to any intracranial target site; the shaft diameter has to be small enough so as to minimize interference with surgical maneuvers, but it should be large enough to provide an adequate endoscopic view.

Essentially, three different endoscopes are required for proper performance of endoscope-assisted microneurosurgical procedures: a 0° scope and two 30° scopes, one with upward, and the other with downward vision.

Endoscopic illumination is best provided by use of a Xenon 300 cold light source, connected to the scope by a fiberoptic light cable. Endoscopic images are visualized through a video system comprising a digital video camera with camera control unit and monitors. A three-chip video camera, and even more so, a state-of-the art high definition (HD) camera can provide superior resolution, colour and clarity for a high quality video image, but it should be noted, that a single-chip camera may meet the needs of routine clinical practice just as well.

The video image is displayed on LCD monitors and may also be superimposed using the picture-in-picture mode of a dedicated device, such as the TWINVIDEO® System (KARL STORZ Tuttlingen, Germany). Storage of still images, video sequences and audio files is better obtained using specific medical recorders with the possibility of archiving and transferring data in digital high definition format.

The videoendoscopic system is mounted on a special mobile cart that can be placed in the most comfortable position. The main monitor is placed in front of the surgeon but it is advisable to have more than one video monitor strategically set up in the operative room, so that any member of the operative staff can watch the operation in real time throughout its stages.

Most of the microsurgical standard instruments are also well-suited for EAM procedures; special bayonet-shaped instruments have been specifically designed to reduce to a minimum the risk of iatrogenic injury during microsurgical maneuvers; malleable suction tubes with lateral openings have proven to be particularly useful. Irrigation and suction sheaths, specially designed for the scopes, can be used effectively to facilitate performing endoscope-assisted microneurosurgery via the transsphenoidal route for pituitary and other skull base lesions.

The recommended set for use in EAM procedures comprises scopes, sheaths, holders, instruments, videocameras, cold light source and a video documentation and storage system. It is based on our personal extensive experience and, in our opinion, substantially suitable for the purpose intended.

Because endoscopic vision is only possible in pre-existing anatomical spaces, the adjunctive use of the endoscope during microneurosurgical maneuvers is useful only in the treatment of intracranial lesions deeply located in the arachnoidal cisterns or in the ventricular cavities. The indications for EAM also include the treatment of sellar and parasellar lesions, although fully endoscopic transsphenoidal approaches have been proposed for this purpose.

Surgeons performing endoscope-assisted microneurosurgical procedures have to be familiar both with microsurgical anatomy (involving the special view of anatomical structures as seen through an operative microscope during specific microsurgical approaches) and with the endoscopic anatomy (which refers to the visualization of the same structures as seen through another optical device, taking into account that an endoscope's varying angle of view can generate quite a different visual appearance of the same anatomical site. Adequate training based on cadaveric dissections is mandatory to acquire adequate practical knowledge of surgical anatomy and microsurgical dissection techniques, but it takes even more effort to achieve a sufficient level of expertise in handling endoscopes and to gain adequate knowledge of the endoscopic anatomy of the various approaches used in the field of EAM. Accordingly, before discussing methodology and clinical applications of EAM, the endoscopic anatomy of the intracranial basal cisterns and of the fourth ventricle, as seen through microsurgical approaches, will be briefly addressed.

2.0 Endoscopic Anatomy of the Intracranial Basal Cisterns and the Fourth Ventricle

Main indications for EAM are the treatment of expansive lesions, aneurysms and neurovascular conflicts located in the basal cisterns. Endoscopic assistance to microsurgical maneuvers is of limited value in the treatment of lesions located in the third and in the lateral ventricles; for lesions located within these cavities, fully endoscopic neurosurgery yields more effective results; the method has evolved to become the gold standard in the treatment of cystic and small tumoral lesions, i.e. colloid cysts, and it has also proven to be particularly useful in the sampling of biopsies from large expansive lesions. Conversely, endoscope-assisted microneurosurgery has been shown to be especially effective in the treatment of neoplastic lesions located in the fourth ventricle. Endoscope-assisted microneurosurgery is also well-suited for the treatment of sellar and parasellar lesions treated via the transsphenoidal route. Nowadays, the fully neuroendoscopic management of these types of lesions is gaining increasingly wider acceptance, but has not yet demonstrated a clear superiority. On the other hand, endoscopic anatomy of the third, lateral and fourth ventricles, as seen through the operative scopes, has been described in a number of publications[15–21]. Apart from that, endoscopic anatomy of skull base structures, as visualized via the transsphenoidal approach, has been widely reported in literature[22–27]. We will restrict our presentation to the description of endoscopic anatomy of the basal cisterns, and of the fourth ventricle, as seen during a standard microsurgical approach because only a few papers cover these topics[28–32].

Anatomical studies on cadaveric specimens were performed in the *Microsurgical and Endoscopic Anatomy Department of the Center of Anatomy and Cell Biology of the Medical University of Vienna, Austria*. Fresh (non-fixed) cadaver heads were used, and only the arterial system was injected with colored rubber. Access to each region was established using a similar technique as in standard neurosurgical procedures. The videoendoscopic equipment comprised HOPKINS® rod lens telescopes with 0° and 30° direction of view, diameter 2.7 mm and 4 mm (KARL STORZ Tuttlingen, Germany), cold light fountains and additional systems for video documentation (KARL STORZ IMAGE1 video camera system) and data storage.

2.1 Endoscopic Inspection of the Anterolateral Basal Cisterns via the Supraorbital Approach

Vision of the anterolateral basal cisterns, and of the structures contained inside, is quite similar in approaches using the supraorbital or pterional routes. In the following, we will restrict our description to the first approach, which on the one hand is of relatively low invasiveness, and secondly, is considered a useful approach for training with cadaveric specimens. The supraorbital approach is prepared through an eyebrow incision and a small craniotomy as originally performed by *Perneczky*[33, 34]. The approach described below is performed on the right side.

Once the dura has been opened, a 0°-scope with straight-ahead view (28162 AUA) may be inserted to begin with endoscopic inspection (**Fig. 3a**); gravitation causes the frontal lobe to descend, and the olfactory nerve (Icn) can be visualized (**Fig. 3b**); the course of the olfactory nerve is followed toward its proximal extremity, where it crosses the optic nerve (IIcn) behind the planum sphenoidale (PSph) (**Fig. 3c**); more laterally, the deeper portion of the Sylvian fissure (SF) can be identified (**Fig. 3d**) and opened from distal to proximal, causing the frontal lobe to descend

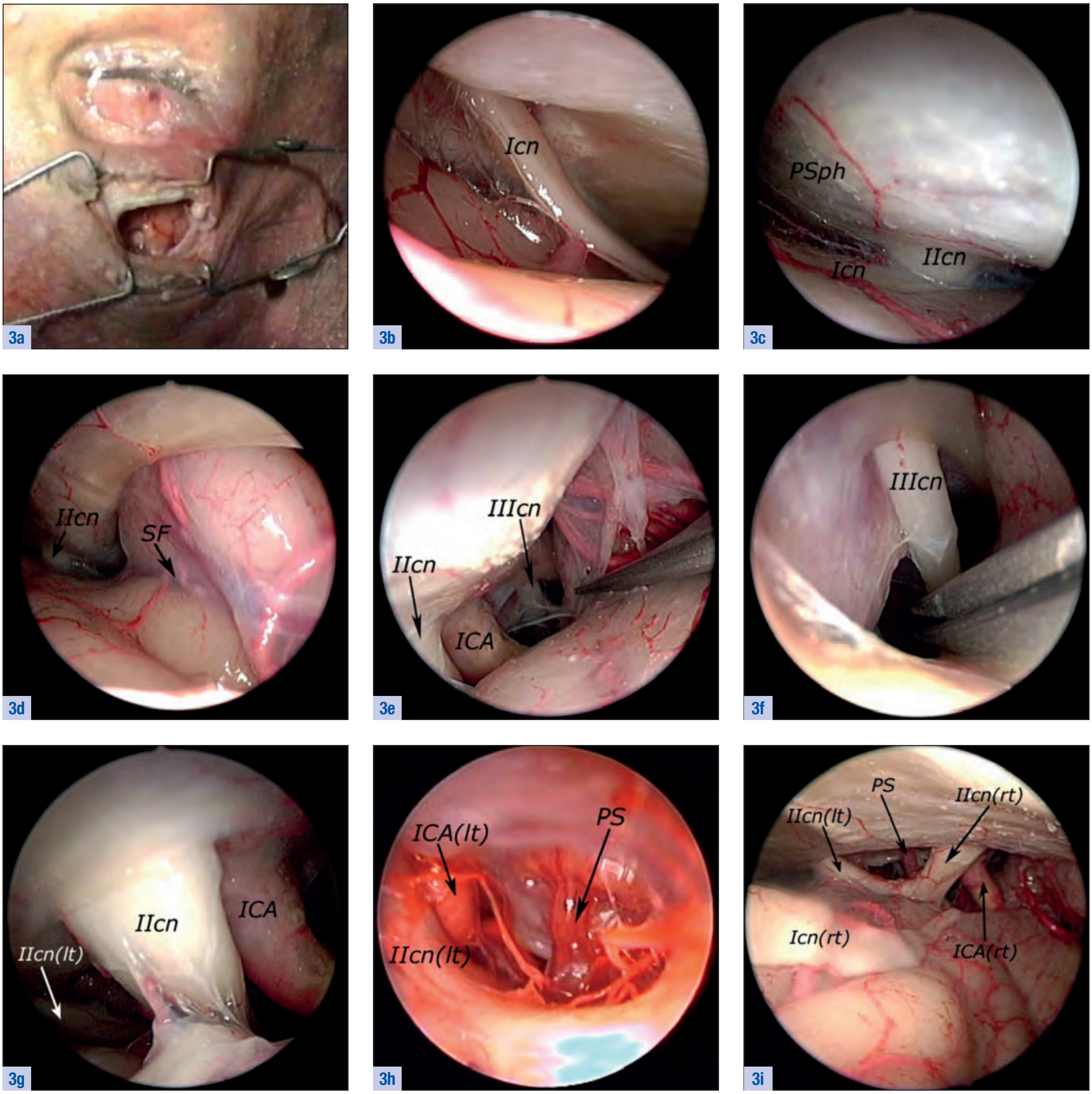

Figs. 3a–u
Endoscopic exploration using the right supraorbital approach.

further, and to separate from the temporal lobe, which exposes the proximal tract of the intradural internal carotid artery (ICA) and the distal part of the 3rd cranial nerve (IIIcn), in turn allowing the superior wall of the cavernous sinus to be entered (**Fig. 3e**); the arachnoid surrounding the 3rd cranial nerve is sectioned (**Fig. 3f**); likewise, the arachnoidal plane around the optic nerve and the carotid siphon is bluntly dissected (**Fig. 3g**); the prechiasmatic cistern is opened to visualize the contralateral optic nerve, along with the proximal-most portion of the opposite intradural ICA underneath and the pituitary stalk (PS) (**Fig. 3h**); once dissection of the arachnoid of the frontobasal region is complete, a wide panoramic view of the anterior basal structures is provided (**Fig. 3i**); at this point, the 0°-scope is replaced by a 30° forward-oblique endoscope (28162 BOA); there are at least three different surgical corridors for passing the scope through: between the optic nerve and the internal carotid artery, between the internal carotid artery and the 3rd cranial nerve, and lateral to the 3rd cranial nerve (**Figs. 3j, k**).

Key to Acronyms (Figs. 3a–i):

I cn	olfactory nerve
II cn	optic nerve
III cn	oculomotor nerve
ICA	internal carotid artery
PS	pituitary stalk
PSph	planum sphenoidale
SF	Sylvian fissure
(lt)	left
(rt)	right

The corridor between optic nerve and ICA is usually narrow and occupied by several perforators coming from the posterior wall of the carotid artery (**Fig. 3l**); advancing the endoscope through the corridor located lateral to the 3rd cranial, which is the narrowest pathway, places the nerve at risk of iatrogenic injury evoked by undue traction or mechanical trauma: this corridor may be further enlarged by sectioning the most proximal portion of the edge of the tentorial notch (TE) (**Fig. 3m**); the compartment of the corridor situated between the optic nerve and the ICA is normally the widest and therefore best suited for surgical maneuvers (**Figs. 3n, o**); Once dissection of the arachnoid of Liliequist's membrane (Lm) is complete, the following anatomical structures come into view: pre-mesencephalic cisterns; the posterior communicating artery (PCoA); the inferolateral aspect of the pituitary stalk located just anterior to the posterior clinoidal process (PCP); the origins of the posterior cerebral artery (PCA) and of the superior cerebellar artery (SCA), with the 3rd cranial nerve between them (**Fig. 3p**); advancing the endoscope downward, the midbasilar artery can be visualized, along with the origin of the anterior inferior cerebellar arteries (AICA) (**Figs. 3q, r**); the large number of perforators (Perf) and the thalamostriate arteries (ThS) can be explored posterior to the basilar bifurcation (**Fig. 3s**); the basilar artery bifurcation shows considerable interindividual variability (**Fig. 3t**) and occasionally an aneurysm can be found (**Fig. 3u**).

Key to Acronyms (Figs. 3j–u):

II cn	optic nerve	**PCoA**	posterior communicating artery
III cn	oculomotor nerve	**Pcp**	posterior clinoid process
AICA	anterior inferior cerebellar artery	**Perf**	perforators
BA	basilar artery	**PS**	pituitary stalk
ICA	internal carotid artery	**SCA**	superior cerebellar artery
Lm	Liliequist's membrane	**TE**	edge of the tentorial notch
P1	precommunicating tract of PCA	**ThS**	thalamostriate artery
P2	postcommunicating tract of PCA	**(lt)**	left
PCA	posterior cerebral artery	**(rt)**	right

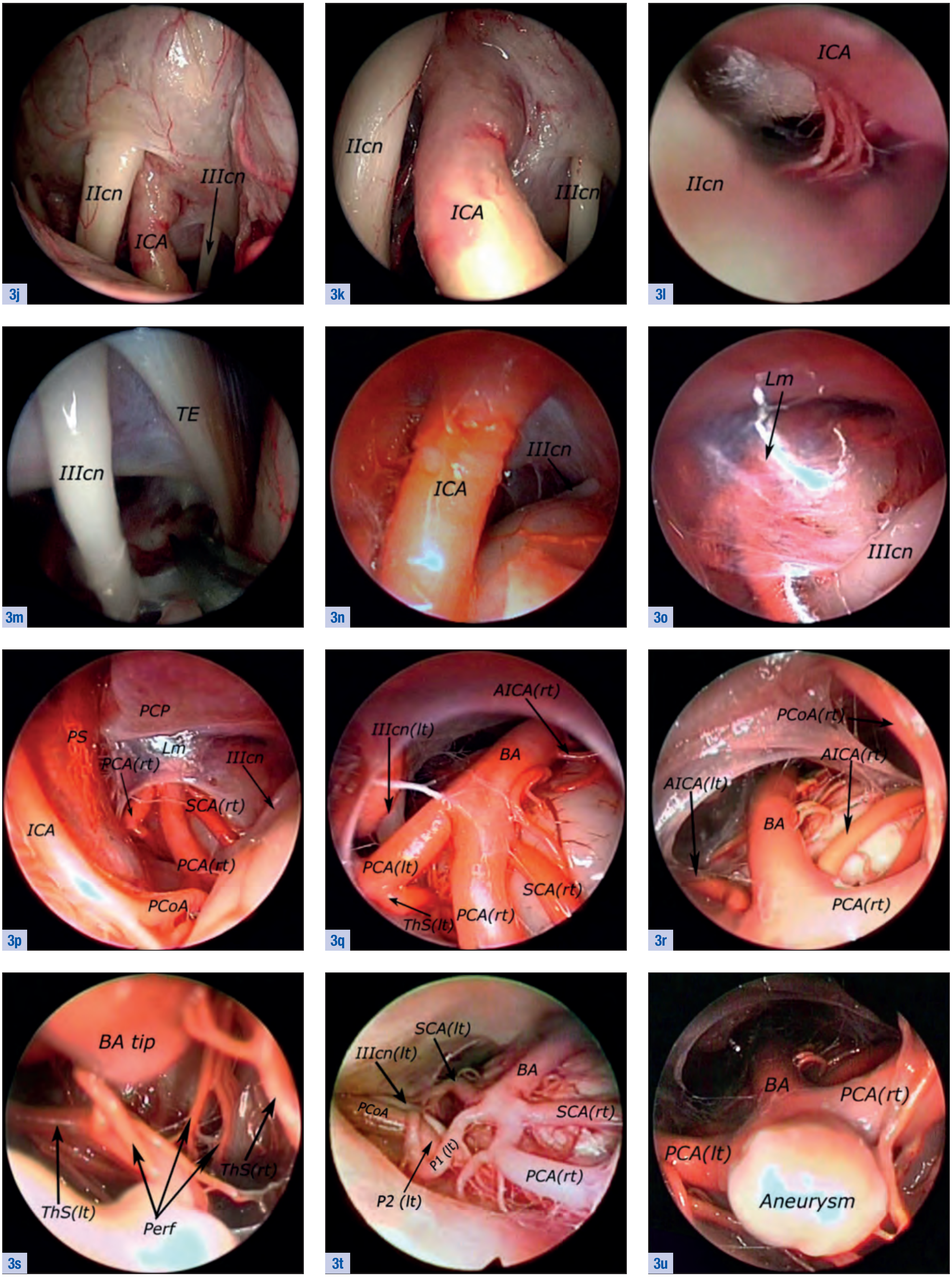

Figs. 3a–u
Endoscopic exploration using the right supraorbital approach.

2.2 Endoscopic Inspection of the Cisterns of the Posterior Cranial Fossa Using the Retrosigmoid Approach

The cisterns of the cerebello-pontine angle cover a region that lends itself well to the use of a combined endoscope-assisted microsurgical approach, particularly to the treatment of neurovascular conflicts and of extra-axial expansive or cystic lesions.

Once a small right retrosigmoid craniotomy has been performed, the cerebellar hemisphere descends, revealing the region of the cerebello-pontine angle (**Fig. 4a**); a 0°-scope with straight-ahead view (28162 AUA) is introduced to visualize the arachnoid of the cerebello-pontine angle cistern overlying the lower cranial nerves (LCNs) and the complex of the 7^{th} and 8^{th} cranial nerves (VII–VIII cns), the proximal portion of which is covered by the flocculus (Flo); subsequently, the internal acoustic meatus (IACpw) (**Fig. 4b**) is entered; the endoscope is advanced downward, guided above the VII–VIII cns and the arachnoid is opened under the vein of Dandy (DV), localizing the fifth (Vcn) cranial nerves and the postmeatal portion of the anterior inferior cerebellar artery (AICA) (**Fig. 4c**); moving the scope further downward, the entrance site of the trigeminal nerve (Vcn) in the brainstem (BrS), the anterior inferior cerebellar artery (AICA), at the level of its parameatal loop, overlying the complex of the 7^{th} and 8^{th} cranial nerves (VII–VIII cns) are visualized (**Fig. 4d**); a different inclination of the scope also allows vision of the 6^{th} cranial nerve (VIcn) and improves exposure of the AICA located between the 7^{th} (VIIcn) and the 8^{th} (VIIIcn) cranial nerves (**Fig. 4e**); the scope is advanced below the Vcn, presenting a distal branch of the superior cerebellar artery (SCAdb), the entrance of the VIcn into the dura overlying Dorello's canal, and an artery that comes from the basilar artery (BA) and enters the clival dura on the left side, anastomosing with a persistent trigeminal artery (PTA) (**Fig. 4f**); the scope is directed downwards and the BA, the proximal course of the AICA underneath the VIIcn and the entire course of the VIcn from its origin in the BrS come into view (**Fig. 4g**); moving the scope upwards, it is possible to visualize the pituitary stalk (Ps), the optic nerves (ONs), the superior cerebellar artery (SCA) and the right 3^{rd} cranial nerve (IIIcn): mention must be made, that all these structures are located in the ambient cistern (**Fig. 4h**); at higher magnification, the Ps above the infundibulum (Inf), the left ON, the origin of the SCA arising from the BA can be visualized most clearly, and the left internal carotid artery (ICA) comes into view (**Fig. 4i**); the scope is retracted to obtain a panoramic view of the distal course of the AICA, VIIIcn, Vcn and labyrinthine artery (LA) (**Fig. 4j**); the scope is moved, presenting the inferior surface of the tentorium (Te) and the entrance of the Vcn into the posterior wall of the cavernous sinus (CSpw) (**Fig. 4k**); moving the scope downwards and using the scissors to create an opening in the arachnoid between the VIIIcn and the roots of the 9^{th} and 10^{th} cranial nerves (IX–Xcns), the proximal course of the AICA arising from the BA comes into view while the right vertebral artery (VA) can be identified below the IX–Xcns (covered by arachnoid) (**Fig. 4l**).

Key to Acronyms (Figs. 4a–l):

AICA	anterior inferior cerebellar artery	**ON**	optic nerve
Ab	arachnoid bridge	**PICA**	posterior inferior cerebellar artery
BA	basilar artery	**Ps**	pituitary stalk
BrS	brainstem	**PTA**	persistent trigeminal artery
CSpw	cavernous sinus, posterior wall	**Sc**	scissors
Dv	Dandy's vein	**SCAdb**	distal branch of the superior cerebellar artery
Flo	flocculus	**Te**	cerebellar tentorium
IAC	internal auditory canal	**VA**	vertebral artery
IACpw	internal auditory canal, posterior wall	**Vcn**	trigeminal nerve
ICA	internal carotid artery	**VIcn**	abducens nerve
Inf	infundibulum	**VIIcn**	facial nerve
IIIcn	oculomotor nerve	**VIIIcn**	acoustic nerve
IX–Xcns	glossopharyngeal and vagus nerves	**(posme)**	postmeatal
LA	labyrinthine artery	**(preme)**	premeatal
LCNs	lower cranial nerves	**db**	distal branch

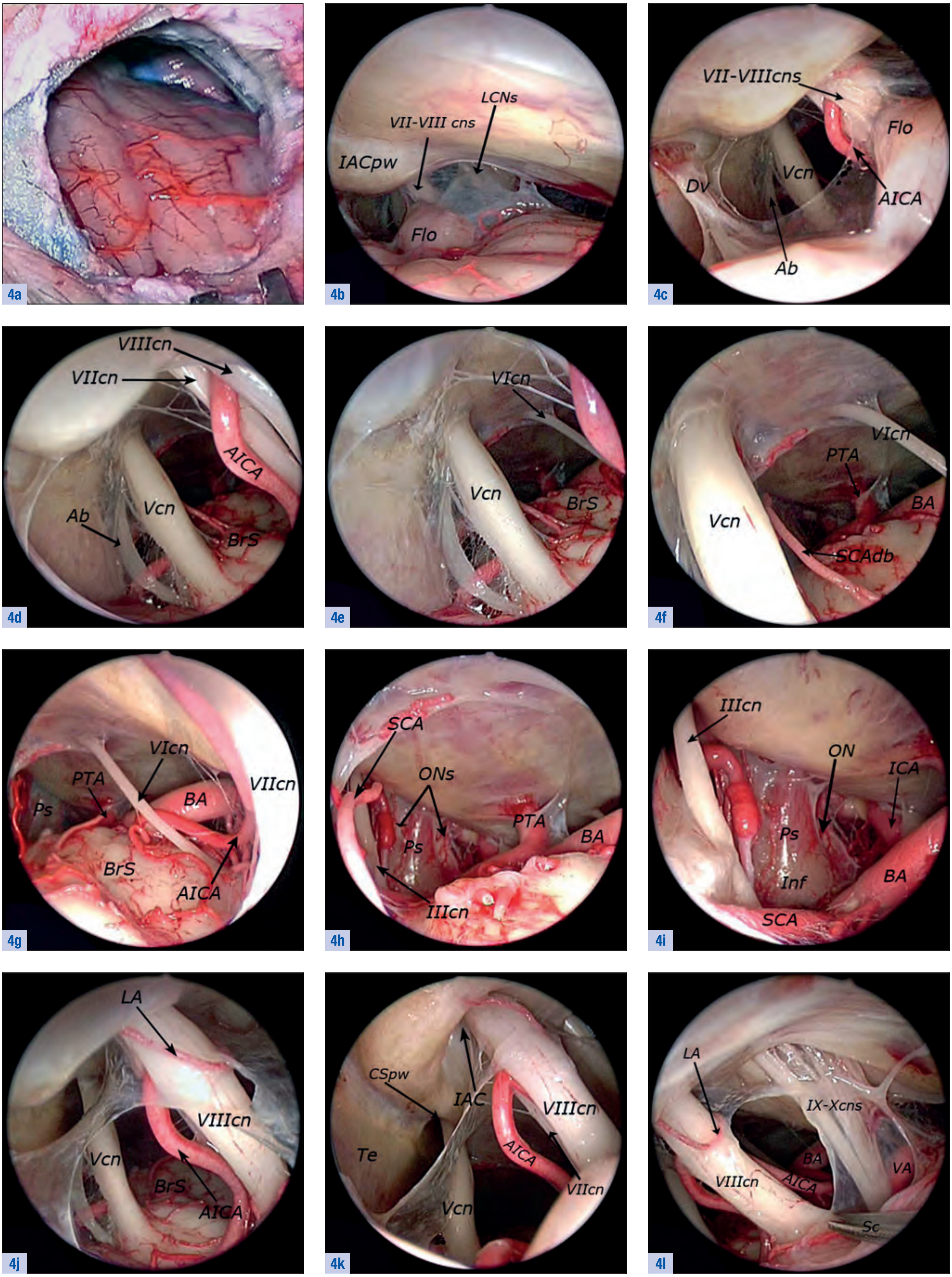

Figs. 4a–l
Endoscopic exploration using the retrosigmoid approach (image sequence continued overleaf).

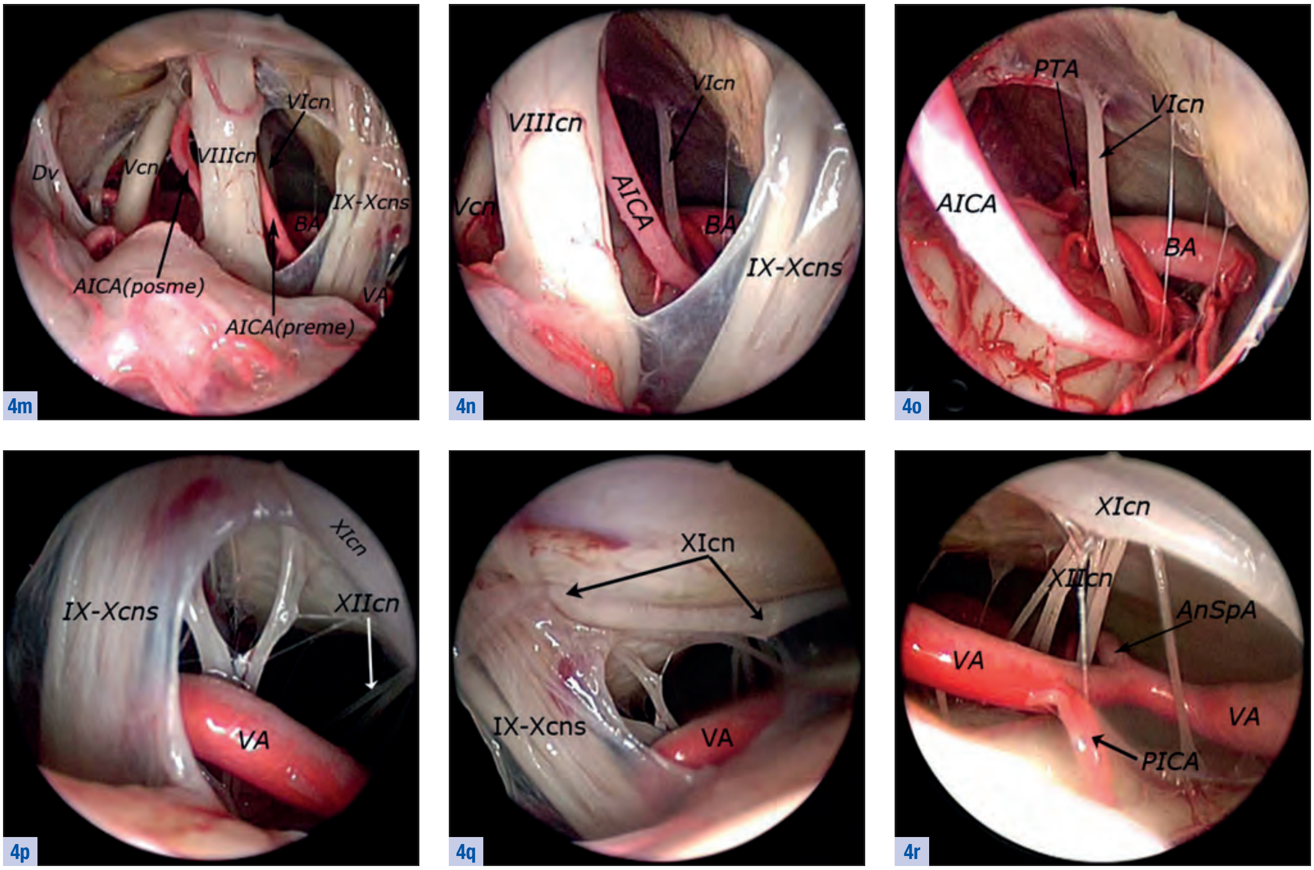

Figs. 4m–r
Endoscopic exploration using the retrosigmoid approach.

Key to Acronyms (Figs. 4m–r):

AICA	anterior inferior cerebellar artery
AnSpA	anterior spinal artery
BA	basilar artery
Dv	Dandy's vein
IVcn	trochlear nerve
IX–Xcns	glossopharyngeal and vagus nerves
PICA	posterior inferior cerebellar artery
PTA	primitive trigeminal artery
VA	vertebral artery
Vcn	trigeminal nerve
VIcn	abducens nerve
VIIcn	facial nerve
VIIIcn	acoustic nerve
XIcn	spinal accessory nerve
XIIcn	hypoglossal nerve
(posme)	postmeatal
(preme)	premeatal

The scope is retracted allowing the relationships of the premeatal portion of the AICA (premeAICA) and the postmeatal portion of the AICA (posmeAICA) with the VIIIcn to be visualized (**Fig. 4m**); moving the scope into the space between VIIIcn and IX–Xcns, the origin of the AICA arising from the BA and the VIcn is shown from below (**Fig. 4n**); at higher magnification, the course of the proximal portion of the AICA and the VIcn can be demonstrated more clearly (**Fig. 4o**); by moving the scope downwards and creating an opening in the arachnoid overlying the VA, the roots of the IX–Xcns, the spinal accessory nerve (XIcn) and the rootlets of the twelfth cranial nerve (XIIcn) come into view (**Fig. 4p**); the scope is advanced downwards to unveil the course of the XIcn (**Fig. 4q**); once again, the scope is moved downwards to present the course of the rootlets of the XIIcn and the intradural VA, which gives rise to the right posterior inferior cerebellar artery (PICA) and the anterior spinal artery (AnSpA) (**Fig. 4r**).

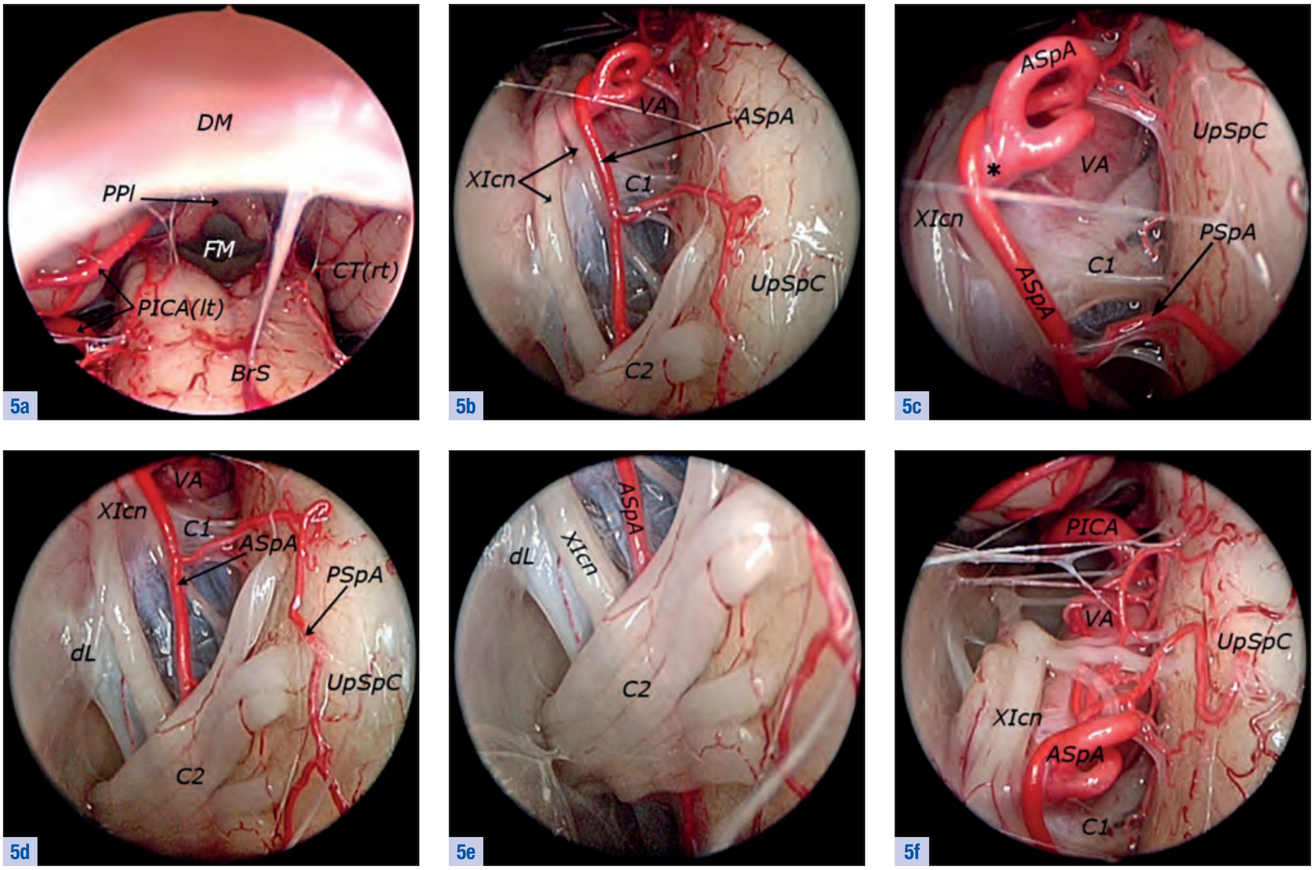

Figs. 5g–u
Endoscopic exploration of the perimedullary and cerebello-medullary cisterns using the suboccipital approach (image sequence continued overleaf).

2.3 Endoscopic Inspection of the Perimedullary and Cerebello-Medullary Cisterns Using the Suboccipital Approach

Expansive and cystic lesions can infiltrate the perimedullary and the cerebello-medullary cisterns. These lesions may be approached via the suboccipital (median or monolateral) or the far lateral approach. Endoscope-assisted microneurosurgery is particularly useful in this context as it can reduce the risk of iatrogenic trauma. The endoscopic vision of structures located in the perimedullary and cerebello-medullary cisterns is more or less the same whether the latter or the former approach is used. Accordingly, we limit our description to the view of the left-sided cisterns, obtained via a median suboccipital approach using a 30° forward-oblique endoscope (28162 BOA).

The scope is introduced through a median suboccipital craniotomy after creation of an opening in the dura mater (DM). The endoscope's panoramic view first allows identification of the following reference structures: the dorsal brainstem (BrS), the foramen of Magendie (FM), the choroid plexuses (ChPl) inside the fourth ventricle and the cerebellar tonsils (CT) with the overlying loop of the posterior inferior cerebellar artery (PICA) (**Fig. 5a**); the scope is moved downwards and guided toward the left perimedullary cistern to visualize the dorsal aspect of the upper spinal cord (UpSpc), the intradural course of the vertebral artery (VA) that gives rise to the anterior spinal artery (ASpA) with a redundant loop, the ascending roots of the eleventh cranial nerve (XIcn), the roots of C1 and the dorsal roots of C2 (**Fig. 5b**). At higher magnification, a more detailed view is given of the loop-shaped origin of the ASpA, which in this case gives rise to an abberrant branch (✱) (presumably a proatlantal artery) passing below the XIcn and to the posterior spinal artery (PSpA), and the roots of C1 passing above the VA and below the ASpA and XIcn (**Fig. 5c**). Directing the scope inferiorly allows visualization of the dorsal roots of C2 traversing above the ASpA, the XIcn and the denticulate ligament (dL) (**Fig. 5d**). Moving the scope, the exit foramen of the roots of C2 is better visualized (**Fig. 5e**). The scope is directed upwards visualizing the origin of the PICA arising from the VA (**Fig. 5f**).

Key to Acronyms (Figs. 5a–f):

ASpa	anterior spinal artery
BrS	brainstem
C1	first cervical root
C2	second cervical root
ChPl	choroid plexus
CT	cerebellar tonsil
dL	denticulate ligament
DM	dura mater
FM	foramen of Magendie
PICA	posterior inferior cerebellar artery
PSpA	posterior spinal artery
UpSpC	upper spinal cord
VA	vertebral artery
XIcn	spinal accessory nerve
(rt)	right

Key to Acronyms (Figs. 5g–u):

BrS	brainstem
ChPl	choroid plexus
CT	cerebellar tonsil
Hc	hypoglossal canal
IAC	internal auditory canal
IX–Xcns	glossopharyngeal and vagus nerves
JF	jugular foramen
JT	jugular tubercle
la	labyrinthine artery
PetB	petrous bone
PICA	posterior inferior cerebellar artery
PPl	plexus papillaris
VA	vertebral artery
Vcn	trigeminal nerve
VIcn	abducens nerve
VII–VIIIcns	facial and acoustic nerves
XIcn	spinal accessory nerve
XIIcn	hypoglossal nerve
(db)	distal branch
(di)	distal
(lt)	left
(pr)	proximal
(rt)	right

Moving the scope allows visualization of the site where the proximal (pr) portion of the PICA enters the vertebro-medullary cistern (✳), located between the brainstem (BrS) and the left cerebellar tonsil (CT), with the distal (di) portion of the PICA coursing above the CT (**Fig. 5g**). The scope is moved proximal to the PICA(pr) which allows identification of the roots of the hypoglossal nerve (XIIcn) emerging from the BrS and running towards the hypoglossal canal (Hc), located below the dura covering the bony salience of the jugular tubercle (JT), medial to the course of the XIcn traversing toward the jugular foramen (**Fig. 5h**). At higher magnification, the distal roots of the XII cn entering the hypoglossal canal can be identified more clearly (**Fig. 5i**). Turning somewhat laterally and moving the scope downward, it is possible to see the XIcn and the distal portion of the roots of the 9th and 10th cranial nerves (IX–Xcns) entering the jugular foramen (JF) (**Fig. 5j**). Passing the scope below and lateral to the proximal portion of the PICA allows visualization of the 6th cranial nerve (VIcn) penetrating the dura mater overlying Dorello's canal (Dc) in the petrous bone (PetB) and the 5th cranial nerve (Vcn) (**Fig. 5k**). Directing the scope laterally, the complex of the 7th and 8th cranial nerves (VII–VIIIcns) is demonstrated entering the internal auditory canal (IAC) accompanied by their corresponding arterial branches emerging from the anterior inferior cerebellar artery (AICA) (**Fig. 5l**). Moving the scope towards the IAC, the complex of the VII–VIII cranial nerves located proximal to the Vcn, (and the spinal accessory nerve (XIcn) can be distinctly identified with the labyrinthine artery (la) (**Fig. 5m**). The scope is guided downwards, below the JT, the entrance of the roots of the XIIcn in the hypoglossal canal (Hc) is clearly visible (**Fig. 5n**). The scope is retracted and again directed towards the space between the cerebellar tonsil (CT) and the brainstem (BrS) where the choroid plexus (ChPl) of the foramen of Luschka is visualized lateral to the first (proximal) loop of the PICA and to the roots of the XIIcn (**Fig. 5o**). At higher magnification, the origin (✳) of the roots of the XIIcn arising from the BrS comes into view (**Fig. 5p**). Moving the scope medially allows to visualize the proximal portion of the PICA and the VII–VIIIcns, while the lower cranial nerves, which enter the jugular foramen (JF), are masked by the XIIcn (**Fig. 5q**). The scope is again guided medially to the PICA it is possible to view the VII–VIIIcns running to the internal acoustic meatus, covered by the dura mater (✳), and the course of the Vcn (**Fig. 5r**). Guiding the scope downward, the anatomical relationship of the VII–VIII cranial nerve complex to the AICA and the labyrinthine artery can be viewed (**Fig. 5s**). Again advancing the scope demonstrates the Vcn most clearly. It has to be noted that all these structures are contained in the cisterns of the cerebellopontine angle (**Fig. 5t, u**).

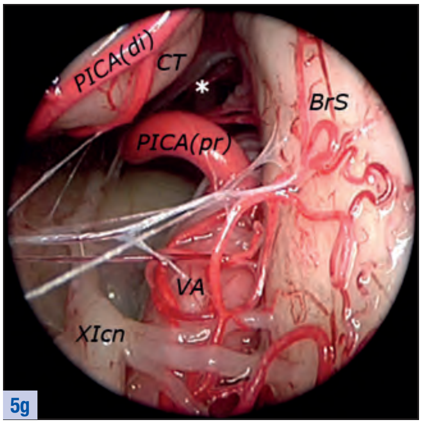

5g

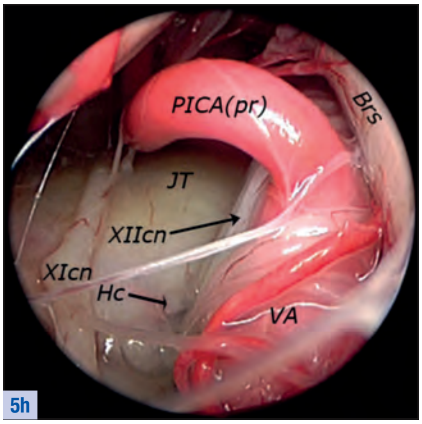

5h

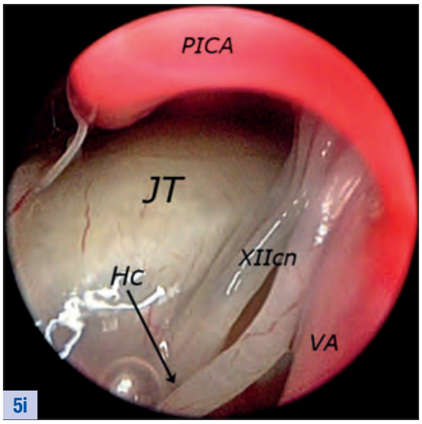

5i

Figs. 5g–u
Endoscopic exploration of the perimedullary and cerebello-medullary cisterns using the suboccipital approach.

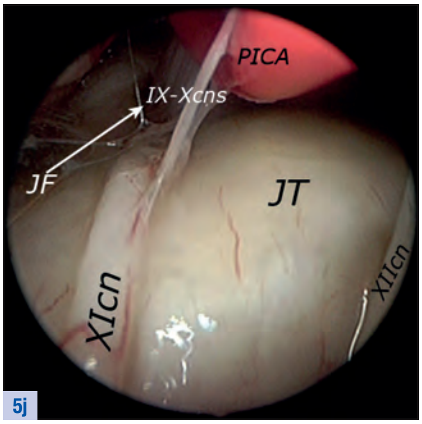
PICA
IX-Xcns
JF
JT
XIcn
XIIcn
5j

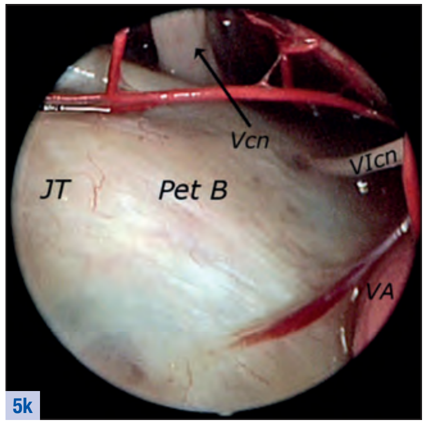
Vcn
VIcn
JT
Pet B
VA
5k

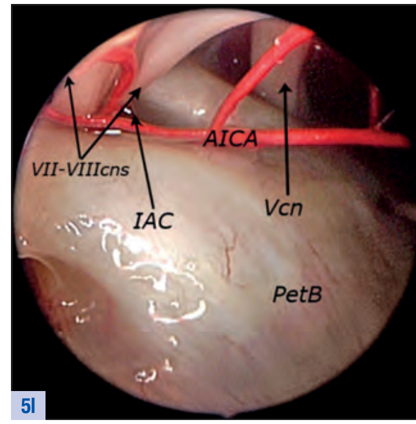
AICA
VII-VIIIcns
IAC
Vcn
PetB
5l

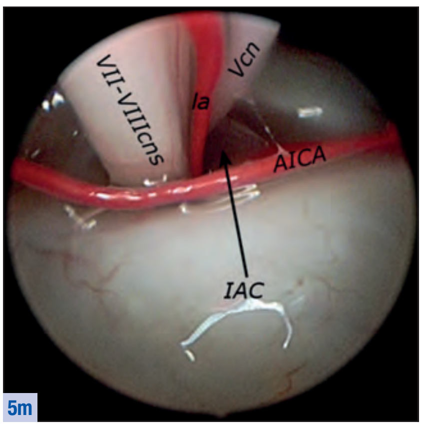
VII-VIIIcns
Vcn
la
AICA
IAC
5m

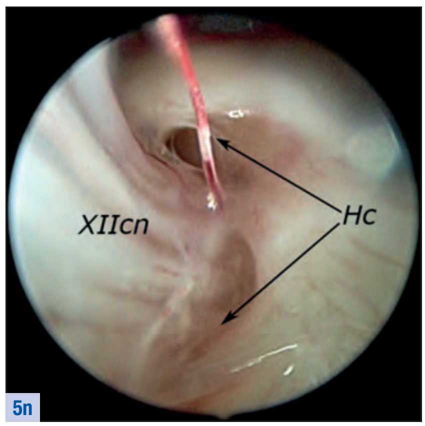
XIIcn
Hc
5n

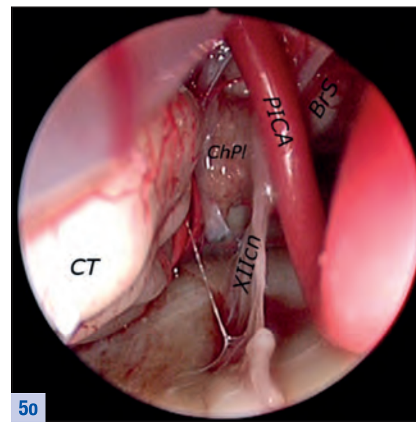
PICA
BrS
ChPl
CT
XIIcn
5o

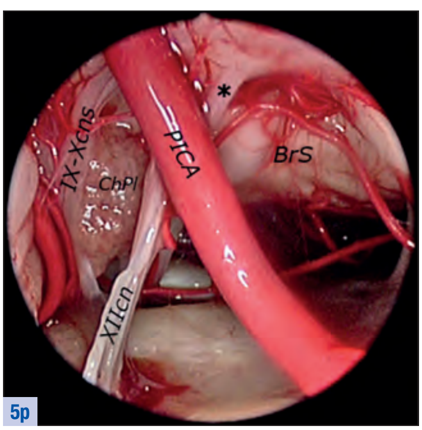
*
IX-Xcns
ChPl
PICA
BrS
XIIcn
5p

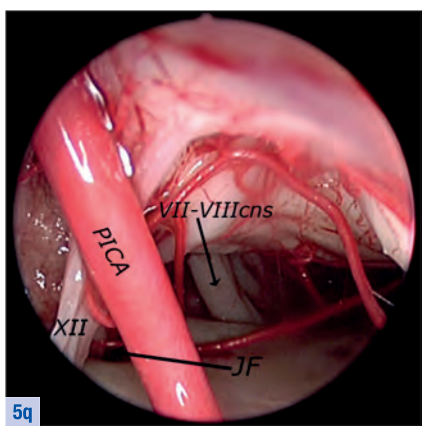
VII-VIIIcns
PICA
XII
JF
5q

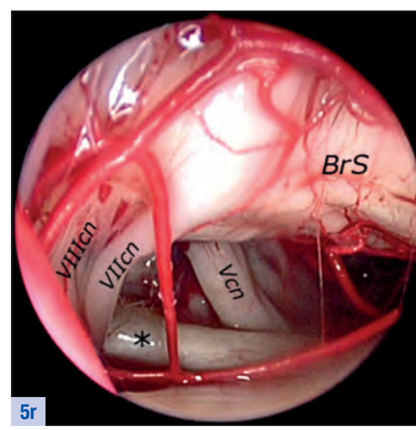
BrS
VIIIcn
VIIcn
Vcn
*
5r

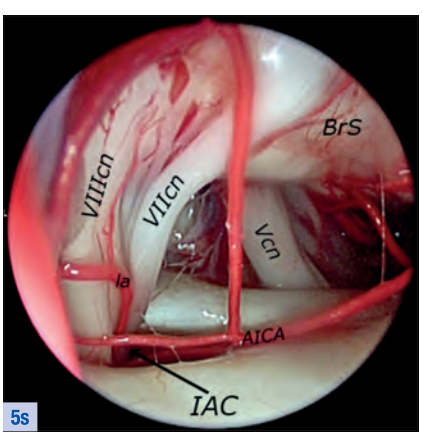
BrS
VIIIcn
VIIcn
Vcn
la
AICA
IAC
5s

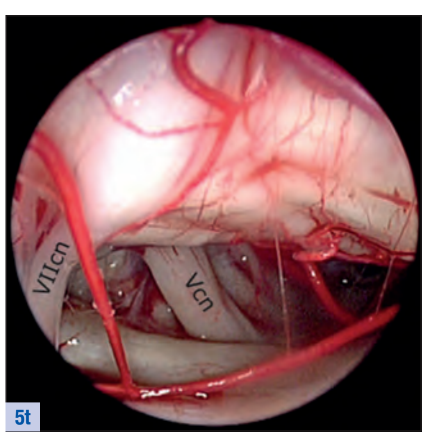
VIIcn
Vcn
5t

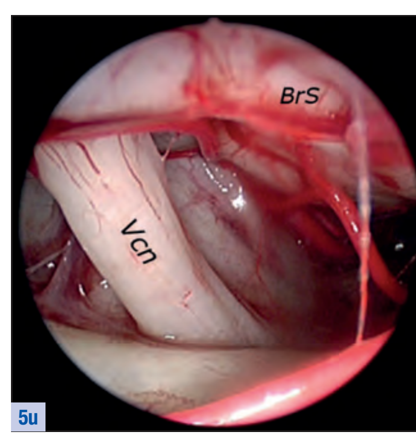
BrS
Vcn
5u

2.4 Endoscopic Inspection of the Spaces of the Fourth Ventricle Using the Suboccipital Approach

As already discussed, a fully endoscopic neurosurgical approach is the most effective way to treat small cystic and tumoral lesions located in the lateral and 3rd ventricular cavities and has also been shown to be useful in the collection of biopsy samples from large expansive lesions lodged inside the same area, while endoscope-assisted microneurosurgery has proven particular useful in the treatment of neoplastic lesions located in the fourth ventricle.

A median 3 cm suboccipital incision is performed to skeletonize the inferior-most aspect of the occipital bone at the level of the foramen magnum (FoM) and the lamina of the 1st cervical vertebra (C1 pa). After removing the atlanto-occipital membrane and opening the dura mater, the arachnoid (arach) of the cisterna magna is incised to allow insertion of a 30° forward-oblique endoscope (28162 BOA, KARL STORZ Tuttlingen, Germany) (**Fig. 6a**). The dorsal brainstem (BrS), the cerebellar tonsils (CT) with the inferior loop of the posterior inferior cerebellar arteries (PICA) and the foramen of Magendie (FM) can be visualized through the endoscope (**Fig. 6b**); the scope is guided further downwards allowing the floor of the 4th ventricle to be examined and to clearly identify the medullary striae of the 4th ventricle (MStr), separated by the median sulcus (ms). Next, the distal opening of the aqueduct of Sylvius (AS do) and the right choroid plexus (ChPl) come into view (**Fig. 6c**). The endoscope is passed through the foramen of Magendie, and the distal opening of the aqueduct of Sylvius is presented more clearly, while at the site of the floor of the 4th ventricle the medial eminence (me) and the facial colliculus (FColl) can be identified (**Fig. 6d**). Further advancing the scope provides a clear view of the aqueduct, with the overlying superior medullary velum (SMV), including its proximal opening (AS po) (**Fig. 6e**). The scope is again advanced to expose the superior medullary velum (SMV) and the lateral walls (LW) of the intraventricular space (**Fig. 6f**). Slight rotation of the scope to the right demonstrates that the lateral wall is made up of the inner part of the superior (supCP) and inferior (infCP) cerebellar peduncles (**Fig. 6g**). Rotating the scope to the left offers a more distinct identification of the demarcation between the superior and inferior cerebellar peduncles in the left lateral wall of the ventricular space (**Fig. 6h**). Next, the scope is moved to expose the lateral recess (LR) (**Fig. 6i**). It should be kept in mind, that anatomy of the posterior fossa is subject to extreme inter-individual variability (**Figs. 6j–l**).

Key to Acronyms (Figs. 6a–l):

arach	arachnoid	**FoM**	foramen magnum
AS (do)	distal opening of the aqueduct of Sylvius	**LR**	lateral recess
AS (po)	proximal opening of the aqueduct of Sylvius	**LW**	lateral wall
BrS	brainstem	**me**	medial eminance
BrS (ls)	lateral surface of the brainstem	**ms**	median sulcus
C1 pa	posterior arch of C1	**me**	medial eminance
ChPl	choroid plexus	**MStr**	medullary striae of the fourth ventricle
cn	cranial nerve	**PICA**	posterior inferior cerebellar artery
CT	cerebellar tonsil	**SMV**	superior medullary velum
FColl	facial colliculus	**(lt)**	left
FM	foramen of Magendie	**(rt)**	right

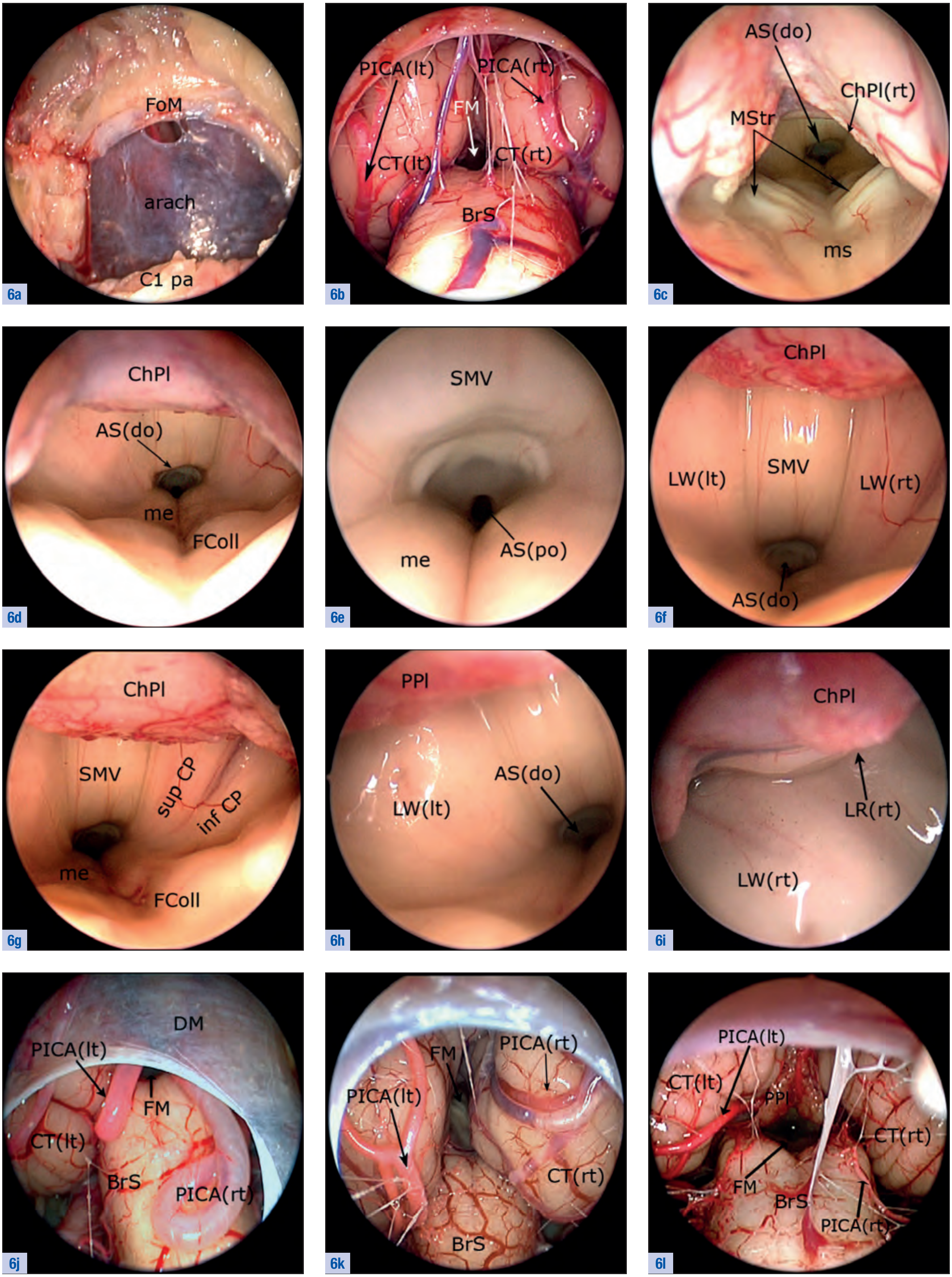

Figs. 6a–l
Endoscopic inspection of the spaces of the 4th ventricle using the suboccipital approach.

3.0 Methodology of Endoscope-Assisted Microneurosurgery

In order to maintain adequate control over the operative field during endoscope-assisted microneurosurgical procedures, the surgeon must simultaneously integrate the visual information provided by the microscope and the endoscope. This can be accomplished by placing the endoscopic monitor in front of the microscope. With this set-up, the surgeon is allowed to maintain simultaneous visual control by switching from the microscopic view to the endoscopic image on the video screen, and vice versa (**Fig. 7**). A small endoscopic video monitor can be mounted directly on the body of the microscope, above and behind the binoculars, so that only minimal ergonomic eye movements are needed to obtain simultaneous visual information[36] (**Fig. 8**).

State-of-the-art operating microscopes allow the user to superimpose the endoscopic video image directly into the binoculars. For this purpose, however, the endoscopic video signals are digitally processed resulting in an unacceptably blurred image, which in turn requires that the surgeon cannot avoid switching repeatedly between video monitors, one connected to the microscope and the other to the endoscope. Accordingly, in our opinion, also with these modern microscopes, we recommend that the surgeon uses a dedicated video monitor for the endoscopic video image in addition to the operating microscope. Special head-mounted LCD screens have also been proposed to coordinate and harmonize display modes when video signals are received from the microscope and the endoscope[37–39]. We used such screens for a trial period, found them uncomfortable and abandoned their use. In our operating room, we have four monitors, one in each corner, where microscopic and/or endoscopic video images are displayed. If required, the picture-in-picture mode is used to allow any member of the operative and anesthesiological teams to follow the operation in real-time.

Endoscope-assisted microneurosurgical procedures are performed, as any other microneurosurgical procedure, after an accurate preoperative planning. The approach is tailored according to the particular pathology and to the individual anatomical features of each single patient; neuronavigation is used, if required.

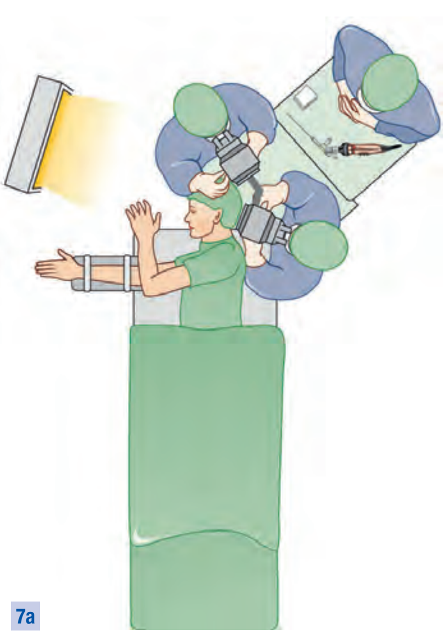

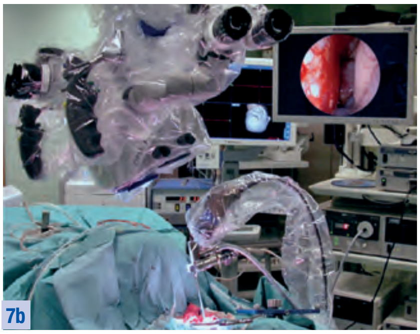

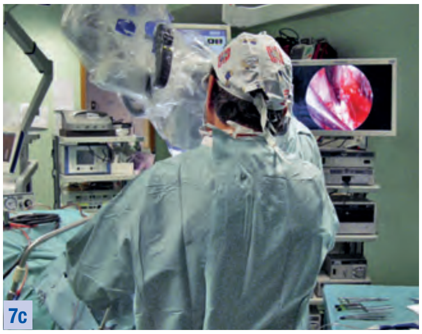

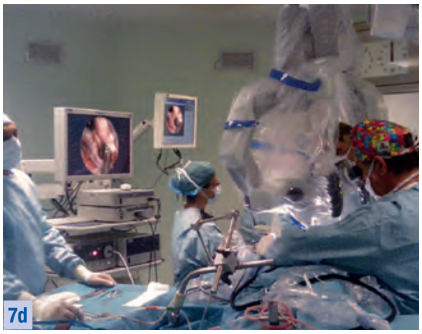

Schematic drawing (**7a**) and photographs (**7b–d**) illustrating the ideal position of the endoscopic monitor, placed in front of the surgeon, during an endoscope-assisted microsurgical operation.

The endoscopic monitor is mounted directly above the microscope in front of the binoculars (**8a, b**) allowing the surgeon to maintain simultaneous control of the microscopic and endoscopic views by minimal ergonomic eye movements (**8c, d**).

For intracranial EAM procedures, the patient is subjected to general anesthesia with orotracheal intubation. The operative field is established under microscopic vision to provide for a controlled insertion of the endoscopes. At this point, endoscopic assistance to microsurgical maneuvers comprises a sequence of three operative steps:

- Initial inspection
- Operating time required to perform the key surgical maneuvers
- Final inspection.

The initial inspection should enable the neurosurgeon to first collect the necessary visual information about the patient's individual endoscopic anatomy of lesional and perilesional areas. This information must be integrated with the microsurgical anatomy of the same region. Initial inspection is always performed with the handheld 0°-scope first to perform endoscopic identification and assessment of those structures located beyond and behind the uppermost sectors of the operative field. During this phase, insertion of the endoscope is conducted under direct microscopic control. When the use of a 30°-endoscope is planned during the key surgical maneuvers, this is again preceded by endoscopic exploration, which is performed with the free-hand technique.

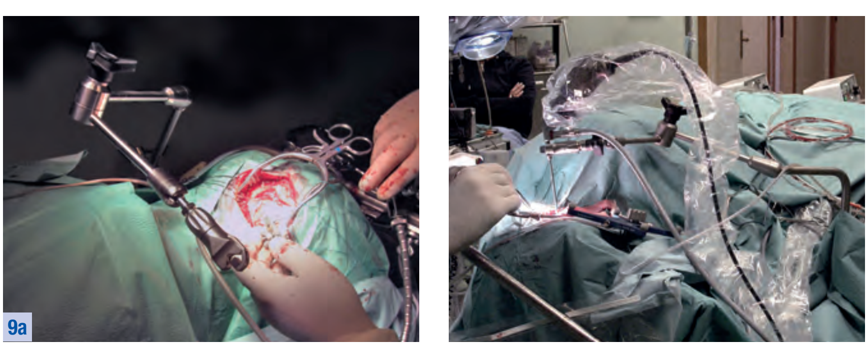

Mechanical holders are better suited to secure the scope in the operative field as compared to pneumatic holders, because the former allow for delicate and precise repositioning of the scope without producing a dangerous rebound effect.

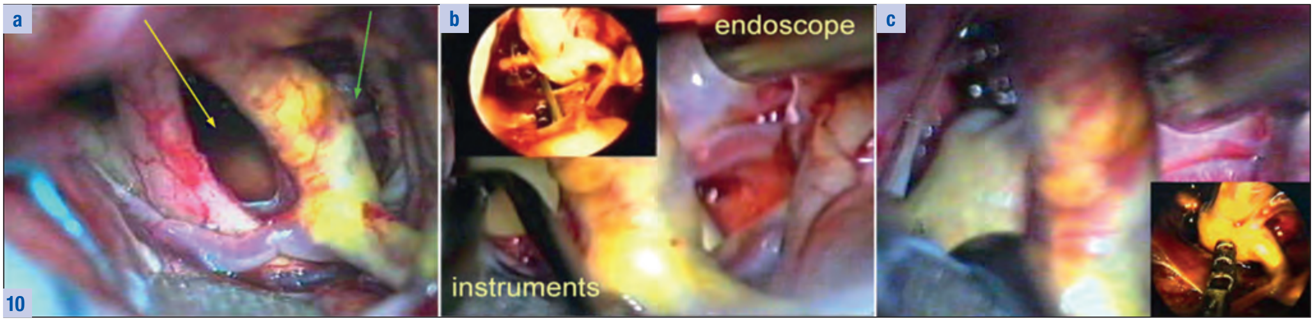

Initially, the scope is secured in the operative field in a position not interfering with surgical maneuvers. In the course of the surgical procedure, the scope is advanced through a corridor different from the one used for surgical maneuvers and, as shown in the case above, enters the space between the internal carotid artery and the third cranial nerve (**green arrow**), while microsurgical instruments are inserted in the space between the internal carotid artery and the optic nerve (**yellow arrow**).

The use of the endoscopes during the key surgical maneuvers allows the microsurgical steps to be performed under visual control, which considerably helps to minimize the risk of iatrogenic trauma. At this point of the procedure, the endoscope can be used free-hand in a step-by-step fashion, mainly to "*look behind the corner*" and to determine the immediate outcome of surgical maneuvers on the spot: this modality is particularly useful when dealing with expansive and cystic lesions in narrow spaces, but it can also be used effectively in the treatment of neurovascular conflicts. However, in most instances, it is necessary to fix the endoscope with a holding device, once the proper intracranial position in the operative field has been reached. Positioning and fixation of the scope is accomplished by use of mechanical holders that are mounted to the operating table or to the headrest (**Fig. 9**).

The scope is fixed in a position that does not interfere with the operating trajectories used for microsurgical maneuvers, taking into account that various anatomical corridors are employed during the operation (**Fig. 10**). During aneurysm surgery, it is mandatory that the scope be secured by a holding device, because the microsurgical maneuvers involved in the procedure must be conducted only under constant endoscopic assistance: if a perforator or any other vital neurovascular structure becomes wedged during clip application, the iatrogenic damage will be allowed to go unnoticed until detected during the subsequent endoscopic control; however, by the time of delayed clip removal, the incidence has already induced irreversible effects. Using the endoscope as an additional optical device during microscope-based procedures not only allows control of microsurgical maneuvers but also permits, after an adequate training, the performance of surgical maneuvers under pure direct endoscopic control. During endoscope-assisted microneurosurgical maneuvers, the light of the endoscope is always kept at low intensity, because illumination of the operative field provided by the microscope is normally reflected also in the depth, giving the possibility of adequate endoscopic vision. Using the endoscope with a high-power light beam can even result in burned out highlights (overexposure). In our experience, the standard illumination intensity of the endoscopic cold light source is 5 – 20% of its maximum power. In many instances, it is also possible to get satisfactory endoscopic images using only the light provided by the microscope when surgical maneuvers are performed under direct endoscopic control. This eliminates, among others, the risk of potential thermal injury to critical neurovascular structures.

Once the key surgical maneuvers are finished, the procedure is usually completed with pure microsurgical techniques (i.e. control of the hemostasis), but a final free-hand endoscopic inspection is needed to control the definitive results: when an expansive lesion has been resected it is mandatory to visually check for the presence of tumor residuals in hidden corners. A final endoscopic control is, however, also recommended after the treatment of neurovascular conflicts and of aneurysms, in order to localize unidentified deep-seated sources of bleeding or clots and to inspect the situation of the clip(s) after the artery has reassumed its definitive position.

4.0 Clinical Applications of Endoscope-Assisted Microneurosurgery

As already discussed, endoscopic vision is only possible in pre-existing anatomical spaces; accordingly, endoscopic assistance can be provided effectively only in microsurgical procedures that are performed to treat intracranial lesions deeply located in the cisternal spaces or in the ventricular system (mainly in the cavity of the fourth ventricle). Endoscope-assisted microsurgical procedures are also performed effectively for the treatment of sellar and parasellar lesions via the transsphenoidal route (even though a few recent reports have suggested the use of the fully endoscopic transsphenoidal approach for this purpose).

From April 1997 to April 2009 the senior author of this booklet (*RJ Galzio*) has performed 542 endoscope-assisted microneurosurgical procedures consisting of 445 intracranial and 97 transnasal transsphenoidal procedures. EAM procedures represent about 19% of all intracranial procedures carried out by the author in the same period (excluding surgeries for trauma); it should be noted that the percentage of procedures performed by endoscope-assisted microneurosurgery was elevated during inital stages, because specific indications began to emerge more clearly only after an adequate number of procedures, and also because the author had used extended indications during the training period. In the last 4 years, the rate of EAM procedures leveled out at less than 11% of all intracranial procedures.

4.1 Expansive and Cystic Intracranial Lesions

238 EAM procedures for intracranial expansive and cystic lesions have been performed.

Endoscope-assisted microsurgery has shown to be particularly useful in the treatment of expansive lesions located in the anterolateral cisterns of the skull base and in the cerebello-pontine cisterns, as described in the literature[6,8,40–47]. EAM provides visualization of critical deep-seated neurovascular structures, allowing them to be dissected at an increased level of safety and preventing the superficial sectors from being exposed to inadvertent manipulation (**Fig. 11, Case 1**).

Case 1 (Figs. 11a–b, continued overleaf)
Meningioma of the Left Tentorial Notch

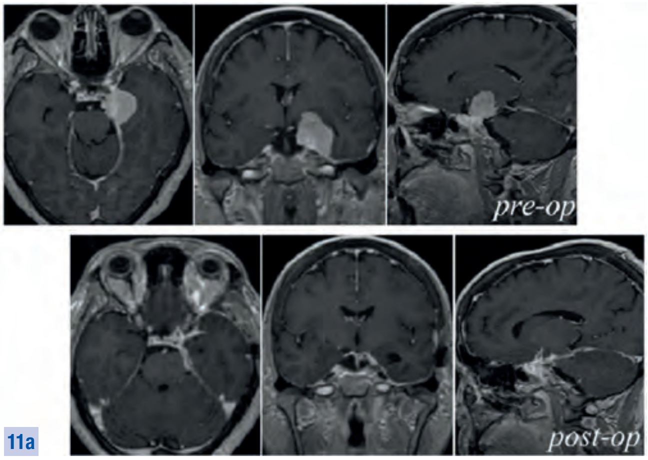

11a

Pre- and post-operative MR scans of the lesion.

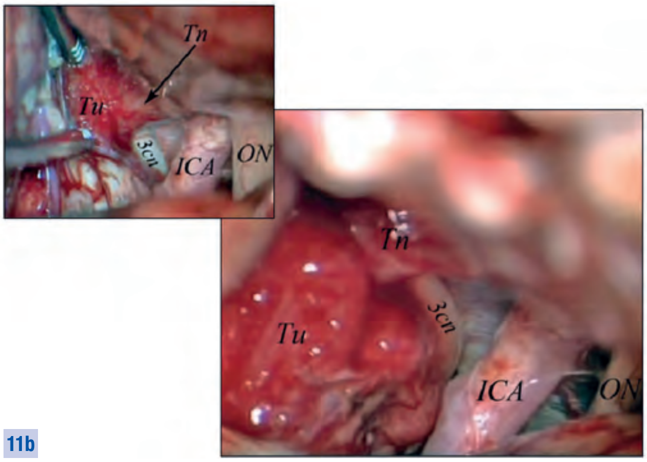

11b

Through a left pterional approach, under microscopic vision, the Sylvian fissure was widely opened to expose the tentorial notch and the antero-medial portion of the tumor, with the 3rd cranial nerve located in the deep medial border of the meningioma.

Key to Acronyms (Figs. 11a–h):

3 cn	oculomotor nerve	**pre-op**	pre-operative
ICA	internal carotid artery	**Tu**	tumor
ON	optic nerve	**Tn**	tentorial notch
post-op	post-operative		

Case 1 (Figs. 11c–h) continued from page 23

Meningioma of the Left Tentorial Notch

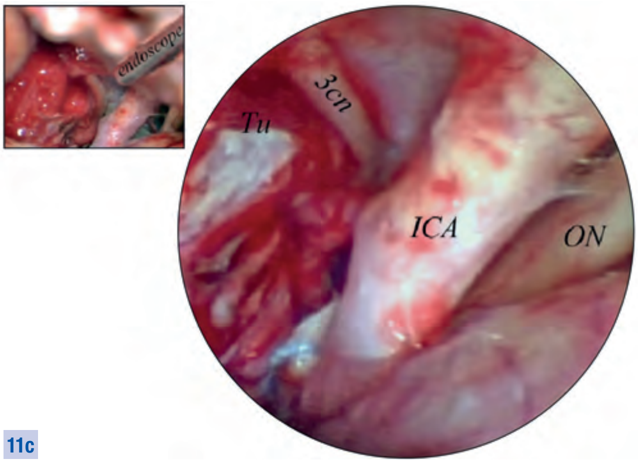

11c

The 0°-scope with straight-ahead view (28162 AUA) was introduced free hand to expose the 3rd cranial nerve located in the depth of the situs.

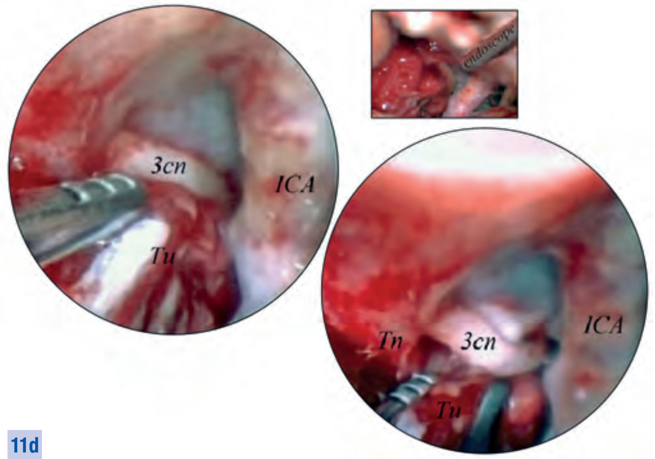

11d

The 3rd cranial nerve was dissected free from the tumor under direct endoscopic control (**d, e**), with the scope fixed to a Point Setter® pneumatic holder until its proximal portion, passing between the SCA and the P1 tract of the PCA (**f**).

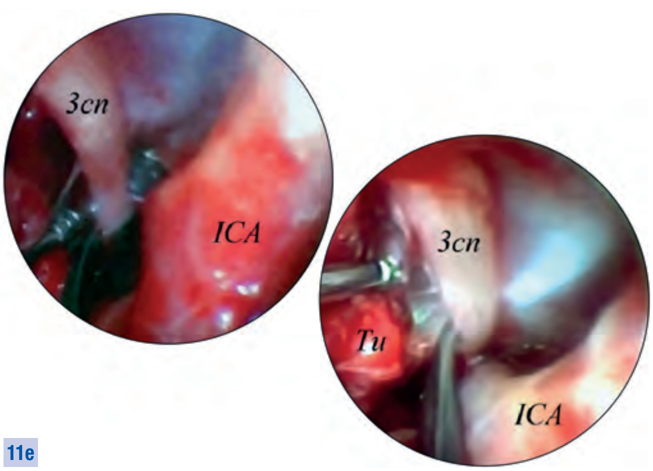

11e

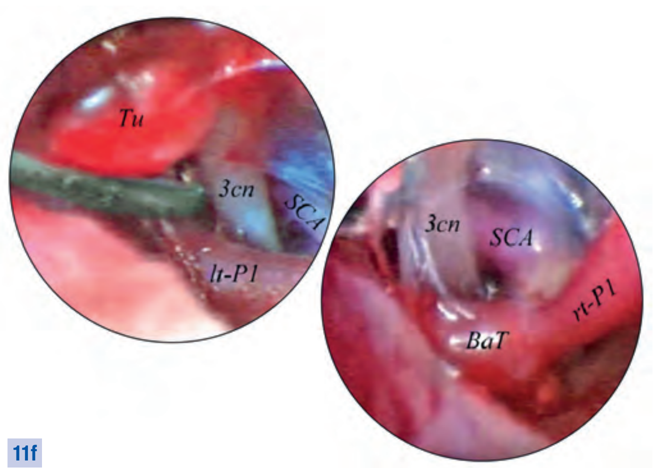

11f

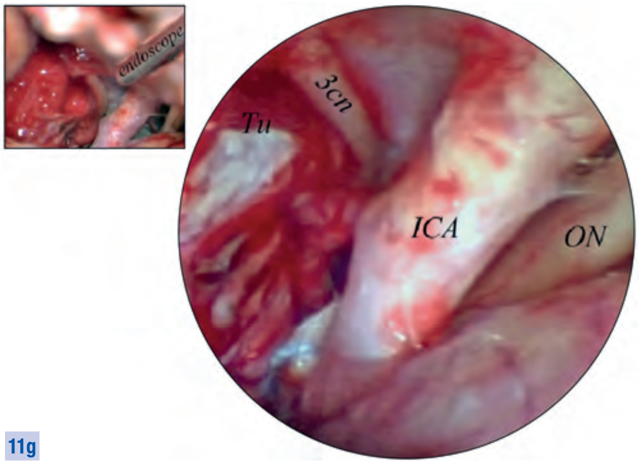

11g

Consecutively, the tumor was dissected free and excised applying mainly the microsurgical technique, however meticulous step-by-step control was employed with the endoscope, which was used free-hand, when surgical maneuvers were directed into the depth of the situs to improve visual recognition and thus preserve the integrity of vital structures, hidden "just behind the corner" (3rd cn).

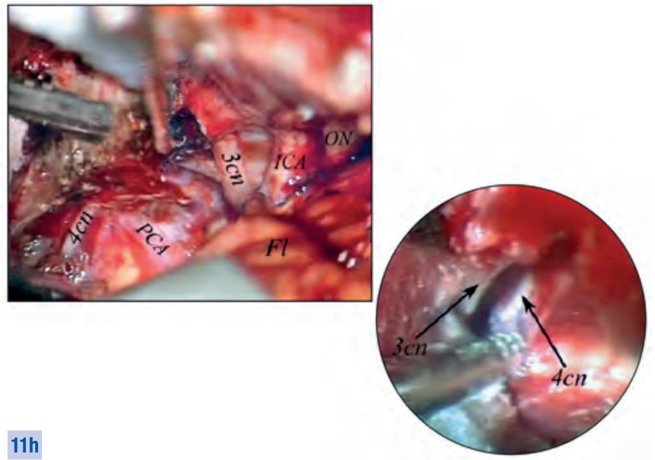

11h

After complete resection of the tumor and coagulation of the supero-lateral wall of the cavernous sinus to which the lesion was attached, integrity of deep-seated structures (3rd and 4th cranial nerves entering the oculomotor triangle of the cavernous sinus) was confirmed by a final endoscopic inspection.

Key to Acronyms (Figs. 11a–h):

3 cn	oculomotor nerve	**PCA**	posterior cerebral artery
4 cn	trochlear nerve	**post-op**	post-operative
BaT	top of the basilar artery	**pre-op**	pre-operative
Fl	frontal lobe	**rt**	right
ICA	internal carotid artery	**SCA**	superior cerebellar artery
lt	left	**Tu**	tumor
ON	optic nerve	**Tn**	tentorial notch
P1	pre-communicating segment of the posterior cerebral artery		

Comment to Case 1

EAM allowed visualization and safer manipulation of the 3rd cranial nerve through a limited pterional approach.

In some instances, surgical maneuvers are performed under pure direct endoscopic control, preserving anatomy and function (**Fig. 12, Case 2**).

Furthermore, the use of the endoscope as an adjunctive optical device during microsurgical procedures allows for less extensive approaches (**Fig. 13, Case 3**).

In the treatment of vestibular schwannomas, endoscopic assistance makes it easier to spare the facial nerve and greatly facilitates its early localization at the level of its emergence from the brainstem and along its course in the internal auditory canal (IAC). Moreover, the use of the endoscope can reveal the presence of tumor remnants in the IAC; extirpation of remnants can be performed under direct endoscopic control eliminating the need for drilling and reducing the risk of iatrogenic damage to labyrinthine and neurovascular structures (**Figs. 14, 15 Cases 4, 5**).

From our standpoint, EAM may also be used effectively in the treatment of other tumors located in the cerebello-pontine angle (petroclival meningiomas, dermoids, lower cranial nerve schwannomas, etc.) allowing visualization of critical neurovascular structures obscured by the lesion itself (**Fig. 16, Case 6**).

EAM is, in our opinion, of limited benefit in the treatment of tumoral lesions located within the lateral and 3rd ventricles, despite the fact that other authors report the contrary[48]. Most of these lesions, indeed, can be resected effectively in a straight-forward way using pure microsurgical techniques. "*Operative neuroendoscopy*" (in which fully endoscopic maneuvers are performed with instruments inserted through the working channels of the sheath of an "*operative*" neuroendoscope) is currently considered the gold standard in the treatment of colloid cysts of the 3rd ventricle. "*Operative neuroendoscopy*" may also be employed for biopsy sampling or cytoreductive procedures for small solid tumors and evacuation of cystic lesions, such as arachnoidal cysts of the ventricular cavities[12, 49–53].

Endoscope-assisted microsurgical manoeuvres are best-suited for visualizing anatomical structures concealed "*behind the corner*" in case of lesions located in the antero-inferior part of the 3rd ventricular cavity, exposed via the anterior basal approach which provides enough space to insert the scope in a step-by-step fashion (**Fig. 17, Case 7**).

Tumoral lesions involving the 4th ventricle are treated effectively by using endoscopic assistance. In effect, the endoscope allows exploration of the entire cavity of the 4th ventricle without any inadvertent manipulation of the superficial neurovascular structures, obviating the need for sectioning the vermis and/or excessive retraction of the cerebellar tonsils. Control of the distal end of surgical instruments inside the ventricular space is facilitated under direct endoscopic vision and has shown to be particularly useful in providing an accurate hemostasis by use of bipolar forceps (**Figs. 18, 19, Cases 8, 9**).

The treatment of cystic lesions of supratentorial and posterior-fossa compartments is considered to be performed more safely under endoscopic assistance[50, 54, 55]. Actually, the adjunctive use of an endoscope during microsurgical treatment of intracranial cysts, namely arachnoid, allows a more adequate control of instruments in the depth of the operative site and allows for less extensive approaches (**Figs. 20, 21, Cases 10, 11**).

Care should be taken to ensure, that the default setting for illumination intensity used in the endoscopic light source is adjusted to a very low output rate (never exceeding 20% of maximum power). This is feasible because the endoscopic light conditions are, in any case, enhanced by the light beam of the microscope, which illuminates the operative field also in deeply located sectors; in some instances, especially when the 0°-scope is used, clear endoscopic images can only be obtained by switching off the endoscopic light and/or reducing the intensity of the microscopic lighting beam.

Case 2 (Figs. 12a–h)

Infra-chiasmatic Cystic Craniopharyngioma

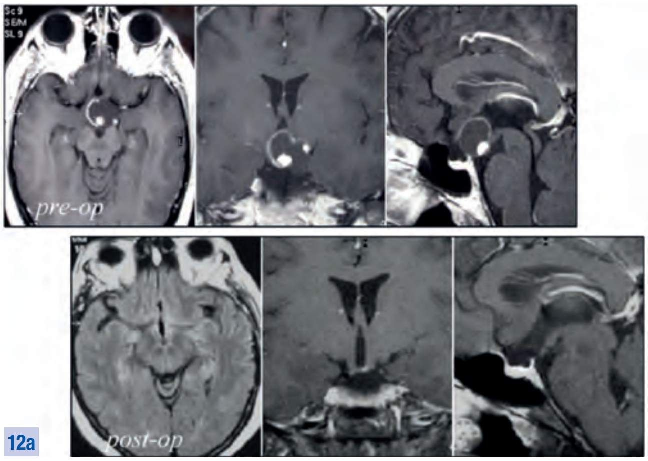

12a

Pre- and post-operative MR scans of the infra-chiasmatic lesion presenting two mural nodules and a cystic component expanding mainly toward the left.

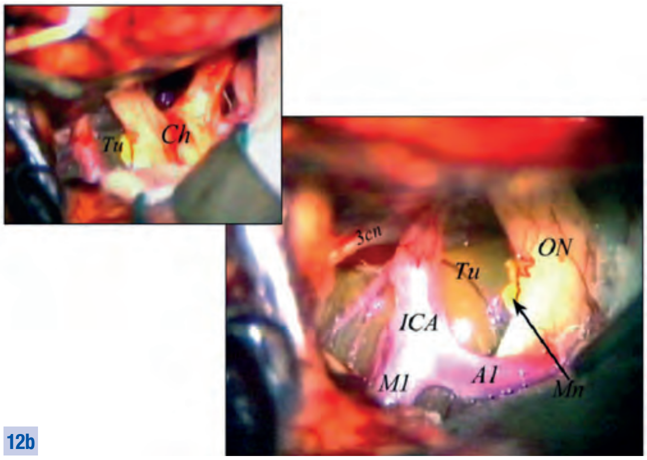

12b

A left pterional approach was used to expose the cystic tumor which was located behind the left ICA and elevated the chiasm. The most superficial mural nodule was interposed between the left optic nerve and tract.

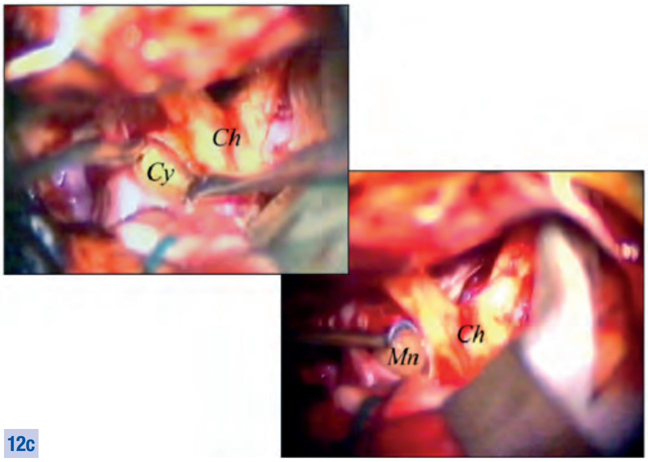

12c

The cystic component was evacuated and the superficial nodule was removed using microsurgical technique.

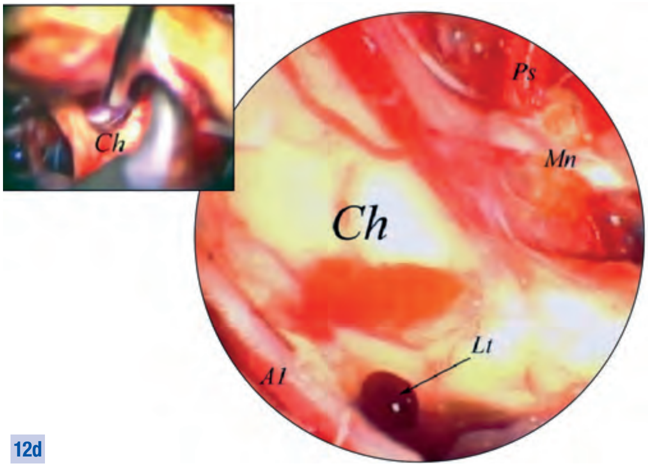

12d

Directing the 30° forward-oblique scope (28162 BOA) upward and advancing medially toward the left ON presented the deepest solid nodule, emerging like an iceberg from the right infundibulum.

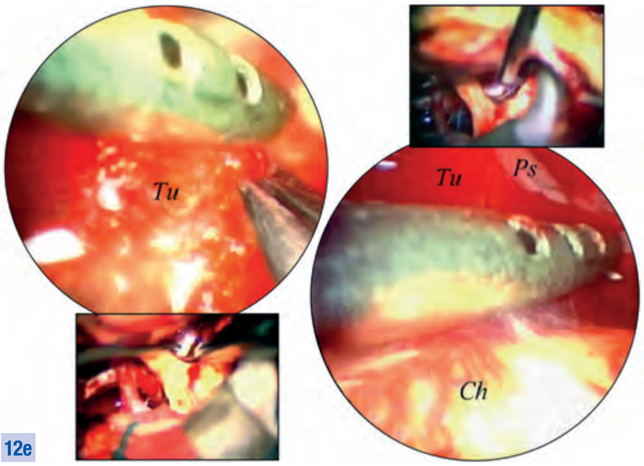

12e

The nodule was mobilized from the infundibulum and shifted toward the cystic cavity.

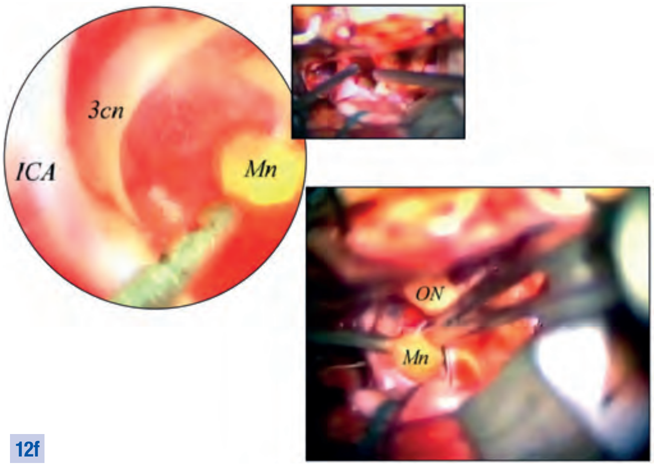

12f

The scope was inserted between the left ICA and the left ON into the cystic cavity to visualize the mural nodule, which thereafter was extracted without any manipulation of the optic nerve pathways.

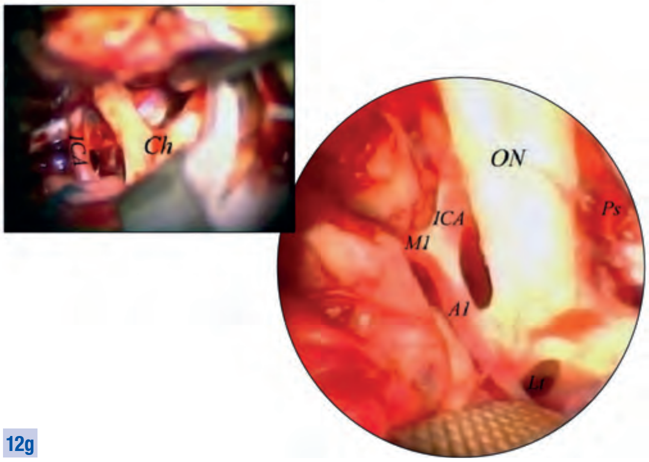

12g

At the end of the procedure the scope was used to obtain a panoramic view of the operative field.

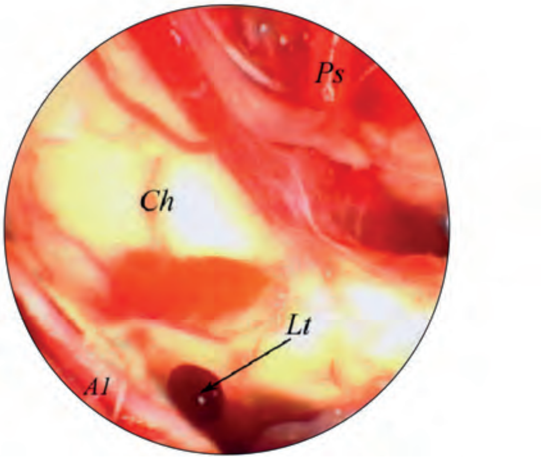

12h

Again inserting the scope medially to the left ON, in front of the chiasm, laterally to the infundibulum and to the pituitary stalk, revealed no evidence of residual tumor at the level of the right infundibular region.

Key to Acronyms (Figs. 12a–h):

3 cn	oculomotor nerve
A1	pre-communicating segment of the anterior cerebral artery
Ch	chiasm
Cy	cystic cavity
ICA	internal carotid artery
Lt	lamina terminalis
M1	proximal segment of the middle cerebral artery
Mn	mural nodule
ON	optic nerve
post-op	post-operative
pre-op	pre-operative
Ps	pituitary stalk
Tu	tumor

Comment to Case 2

EAM allowed resection of the infra-chiasmatic tumor with only minimal trauma to the optic nerve pathways.

Case 3 (Figs. 13a–b), continued overleaf

Small Right Clinoidal Meningioma

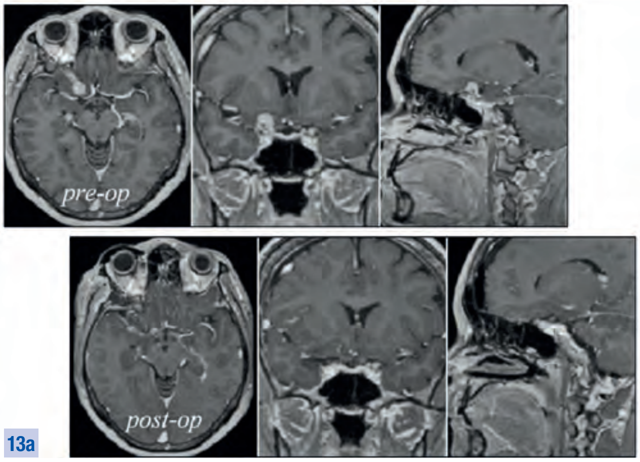

13a

Pre- and post-operative MR scans of the lesion …

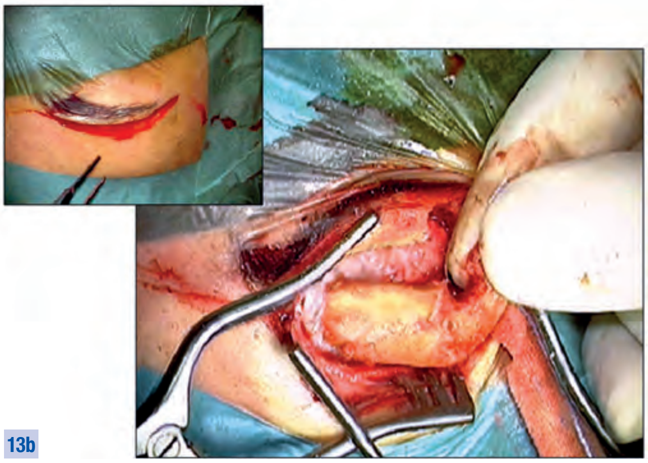

13b

… which was exposed through a right supraorbital eyebrow approach.

Case 3 (Figs. 13c–h) continued from page 27
Small Right Clinoidal Meningioma

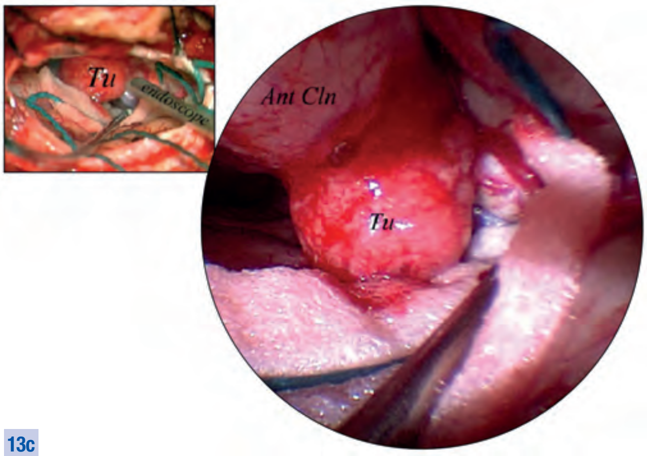

13c

Following elevation of the frontal lobe, the small tumor was dissected and exposed using a 0° scope with straight-ahead view (28162 AUA).

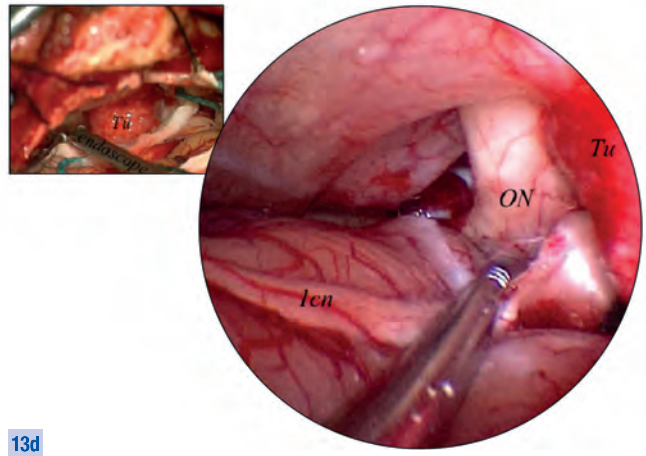

13d

The scope allowed clear vision of the right ON, obscured by the medial aspect of the lesion, and thereafter presented …

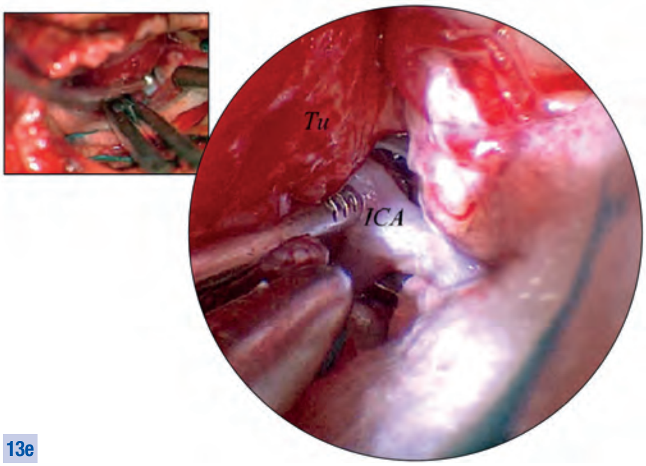

13e

… the right ICA at the level of the bifurcation, concealed by the lateral aspect of the lesion.

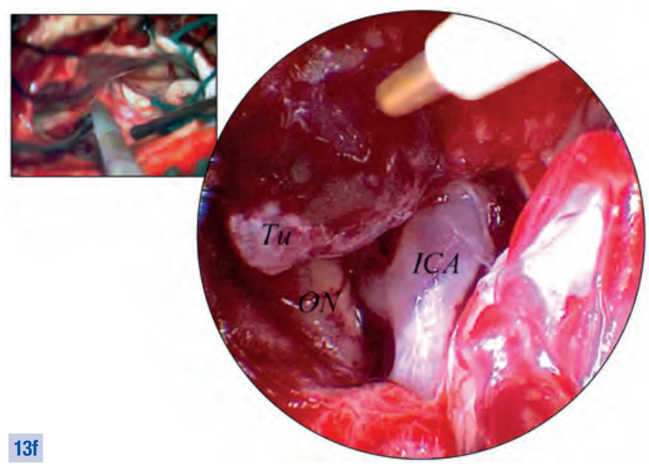

13f

Tumor debulking by use of an ultrasonic aspirator was performed under endoscopic vision, with the scope attached to a mechanical holding system (28272 RKB, KARL STORZ Germany) for improved control of the instrument.

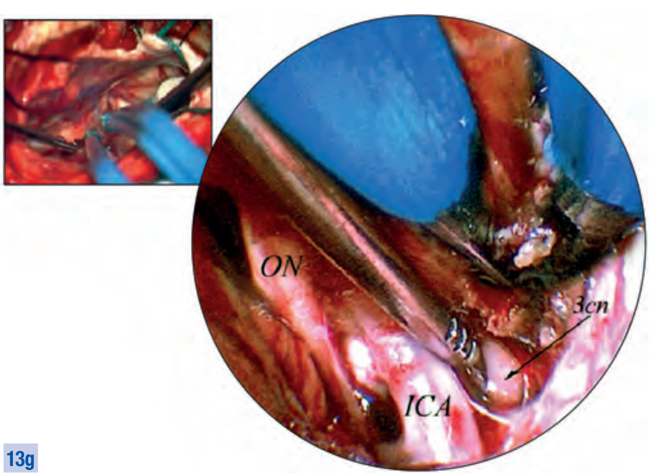

13g

The dural implant base of the tumor was resected and coagulated: the …

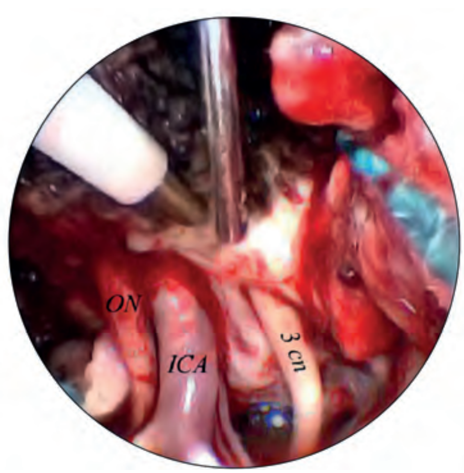

13h

… scope allowed for perfect control of surgical instruments in the depth of the operative site.

Key to Acronyms (Figs. 13a–h):

1 cn	olphactory nerve	**ON**	optic nerve
3 cn	oculomotor nerve	**post-op**	post-operative
Ant Cln	anterior clinoid process	**pre-op**	pre-operative
ICA	internal carotid artery	**Tu**	tumor

Comment to Case 3

EAM allowed complete resection of the lesion and of its implant base through a minimally invasive "key-hole" approach.

Case 4 (Figs. 14a–d), continued overleaf
Grade II Right Vestibular Schwannoma

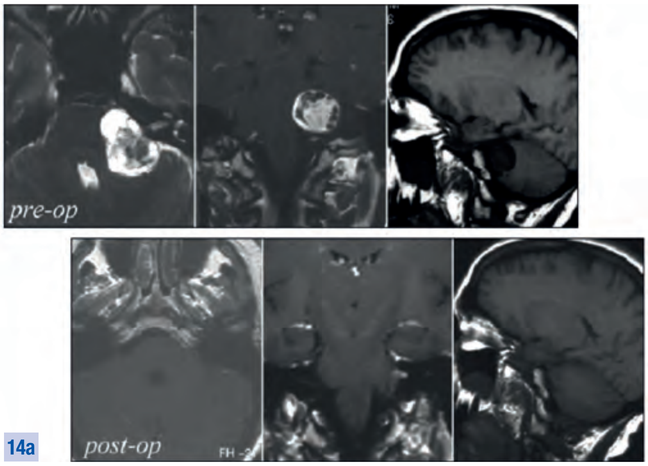

14a

Pre- and post-operative MR scans of the lesion.

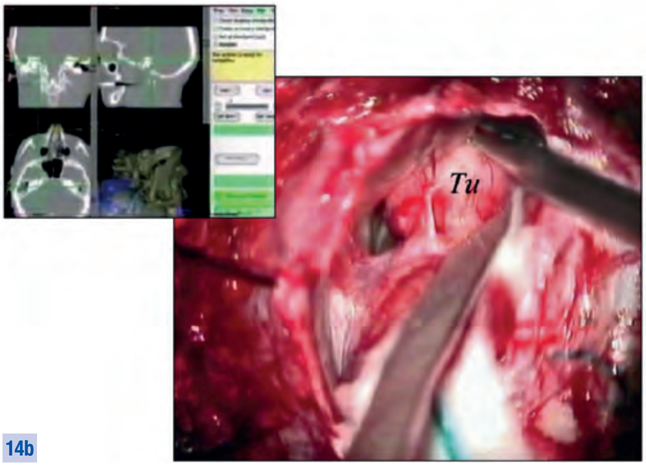

14b

The patient was placed in lateral decubitus position, and the tumor exposed through a right retrosigmoid approach by use of neuronavigation.

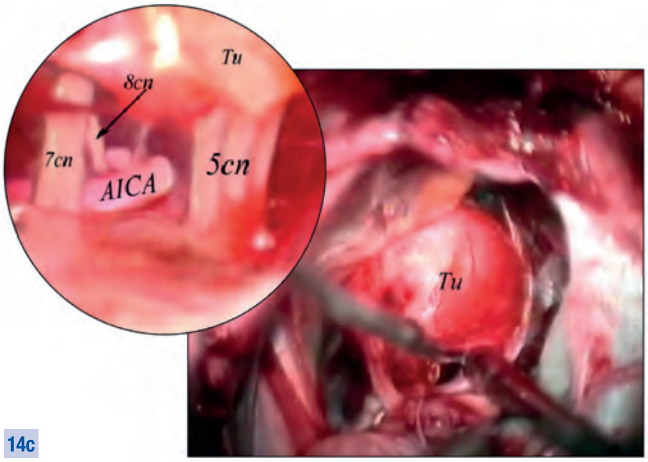

14c

After dissection of the posterior surface of the lesion, a 0°-scope (28162 AUA, KARL STORZ Germany) with straight ahead view was inserted, presenting the most proximal portions of the 5th cranial nerve and of the 7th–8th cranial nerve complex, with a loop of the AICA passing between them, at the level of the medial surface of the tumor.

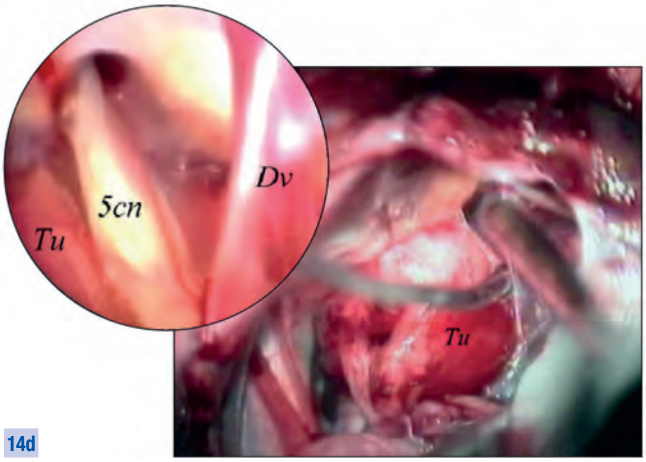

14d

Subsequently, the scope was advanced toward the supero-lateral superficial aspect of the tumor to visualize the distal portion of the main branch of the 5th cranial nerve located below the vein of Dandy.

Key to Acronyms (Figs. 14a–d):

5 cn	trigeminal nerve	**post-op**	post-operative
7–8 cns	complex of the 7th–8th cranial nerves	**pre-op**	pre-operative
AICA	anterior inferior cerebellar artery	**Tu**	tumor
Dv	Dandy's vein		

Case 4 (Figs. 14e–h), continued from page 29

Grade II Right Vestibular Schwannoma

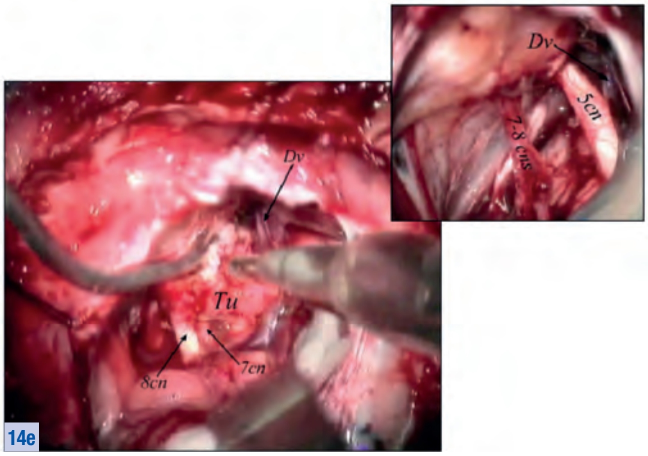

14e

The tumor was evacuated using the ultrasonic aspirator under microsurgical vision.

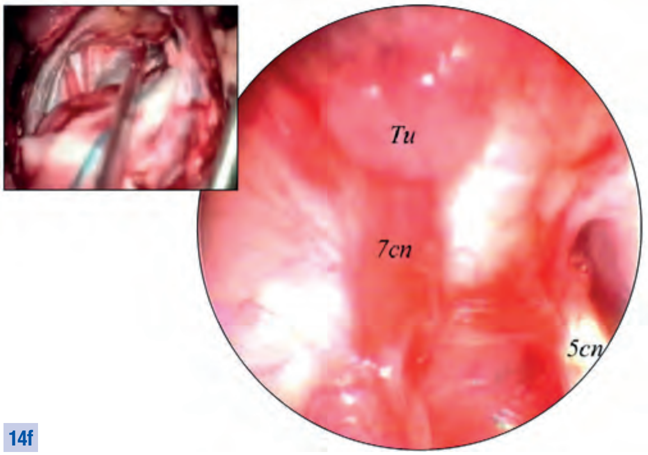

14f

Following extirpation of the main portion of the tumor developing in the cerebello-pontine angle – the vestibular and cochlear components of the 8th cranial nerve were resected because the patient was anacusic on the affected side – a 30°-scope with upward oriented vision (28162 BOA) allowed to visualize a small tumor remnant located anterior to the 7th cranial nerve and protruding into the internal auditory canal.

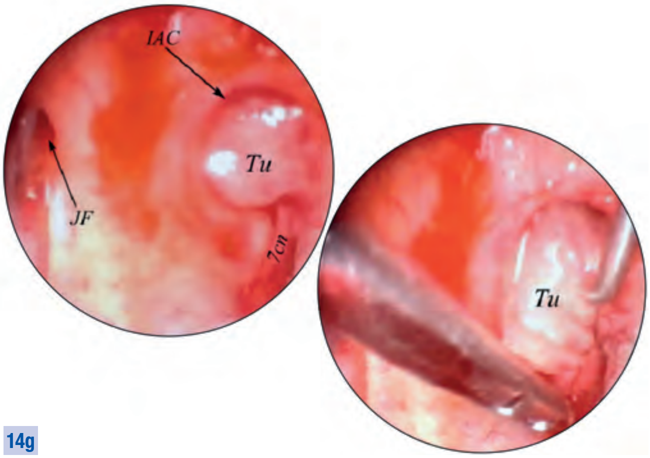

14g

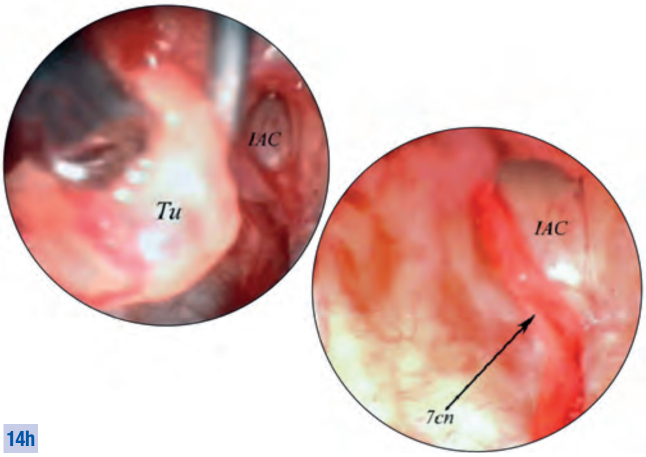

14h

The scope was attached to a mechanical holding system (28272 RKB, KARL STORZ Germany). Next, the residual tumor was resected under direct endoscopic control, without any need for drilling of the posterior rim of the IAC (**14g, h**).

Key to Acronyms (Figs. 14e–h and **15a–f):**

5 cn	trigeminal nerve	**JF**	jugular foramen
7–8 cns	complex of the 7th–8th cranial nerves	**post-op**	post-operative
8 cn	acoustic nerve	**pre-op**	pre-operative
AICA	anterior inferior cerebellar artery	**Tu**	tumor
Dv	Dandy's vein	**ves n**	vestibular nerve
IAC	internal auditory canal	**7cn**	facial nerve

Comment to Case 4

EAM allowed for early identification of the 7th cranial nerve at the level of its proximal portion near the brainstem, which, in turn, facilitated nerve preservation and permitted complete resection of the intracanalar portion of the tumor without any drilling of the IAC.

Case 5 (Figs. 15a–f)
Grade II Left Vestibular Schwannoma

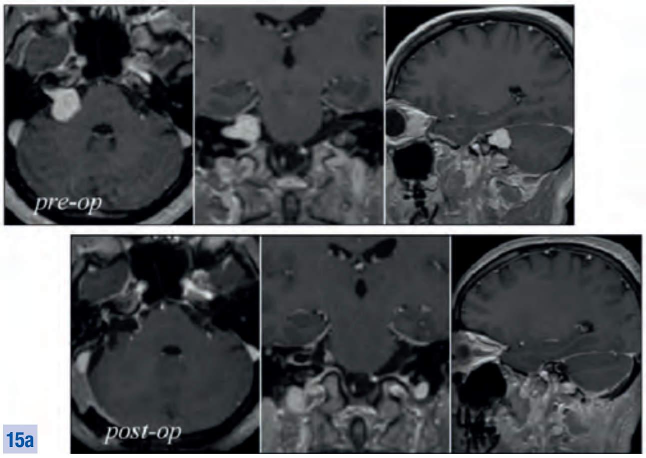

15a

Pre- and post-operative MR scans of the lesion.

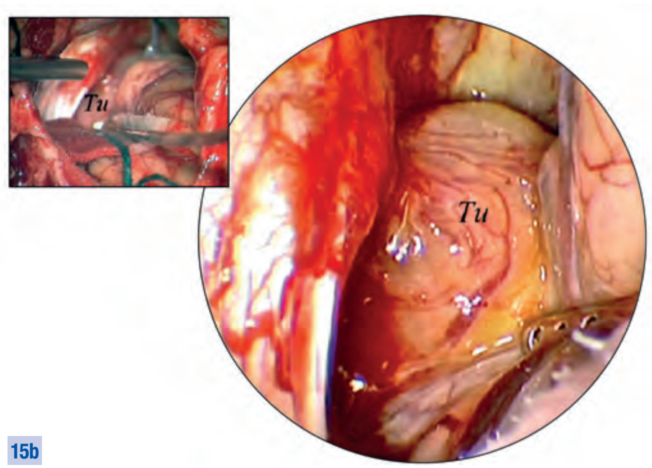

15b

The patient was placed in lateral decubitus position and the tumor exposed through a left retrosigmoid approach. After exposure of the posterior surface of the lesion, a 0° scope (28162 AUA) with straight ahead view was used free-hand for early inspection.

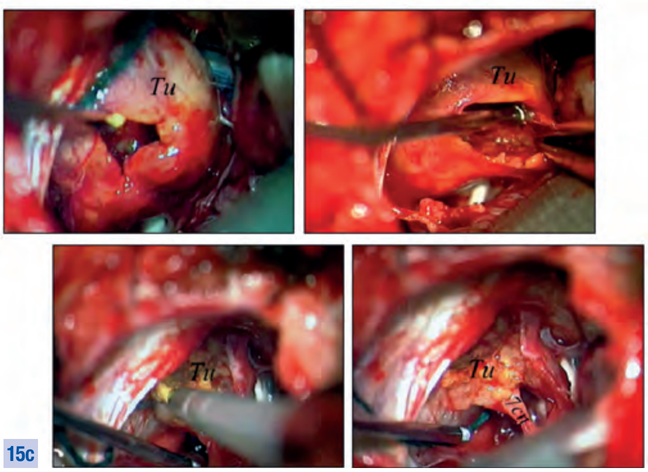

15c

After opening of the capsula, the tumor was debulked using the ultrasonic aspirator under microscopic vision, and leaving behind a residual portion at the level of the lateral pole of the lesion, adjoining the IAC.

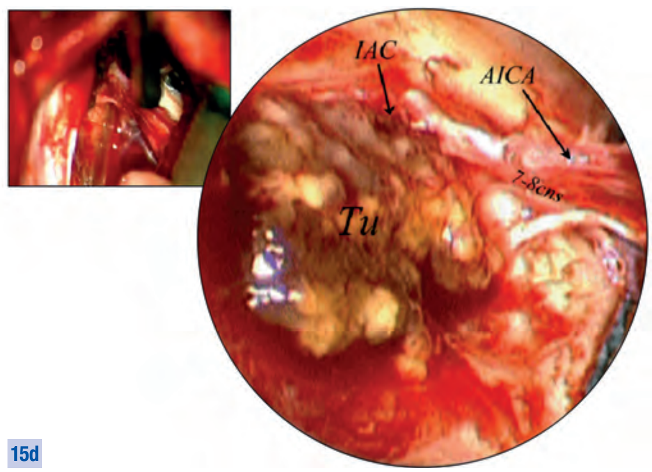

15d

A downward oriented 30°-scope (28162 BUA) was used to visualize the residual portion of the tumor and the cranial nerves entering the IAC.

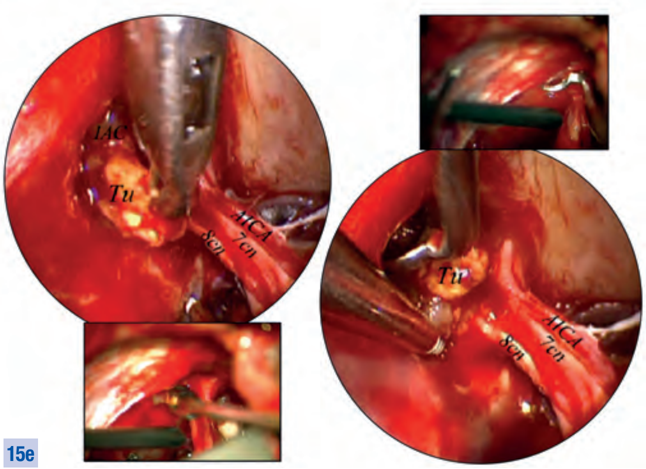

15e

The scope was attached to a mechanical holder allowing for direct control of instruments during resection of the tumor remnants (**15e–g**).

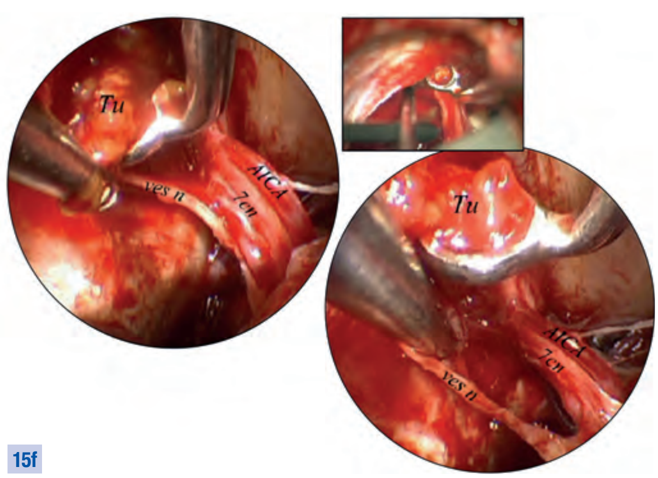

15f

Case 5 (Figs. 15g–h), continued from page 31
Grade II Left Vestibular Schwannoma

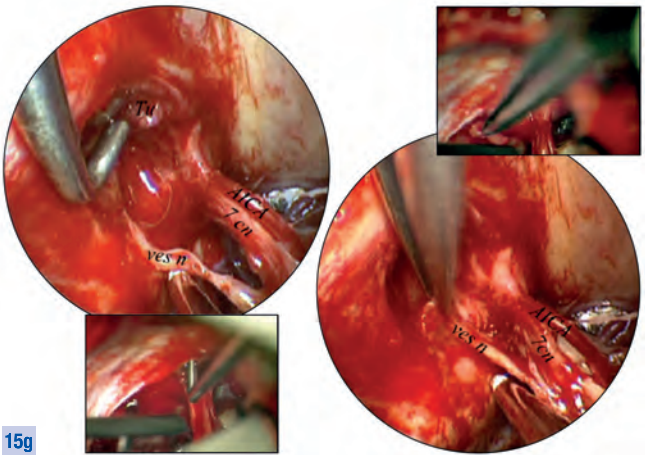

15g

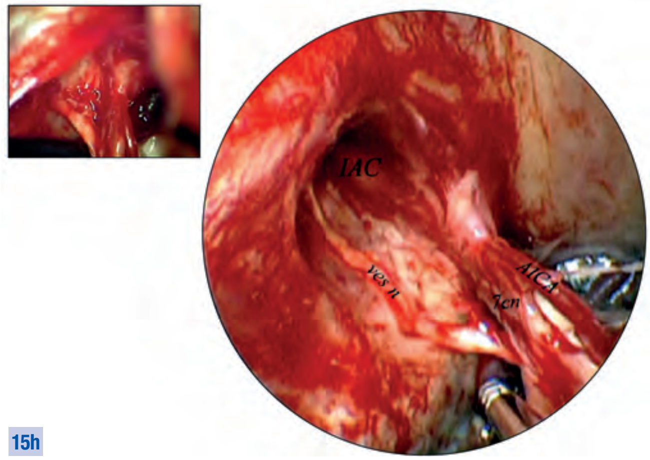

15h

Upon completion of the procedure, the final endoscopic inspection confirmed the complete extirpation of tumor remnants and preservation of the integrity of the following vital structures: the labyrinthine artery, the facial and acoustic nerves including one of the two vestibular nerves (only one of both had to be resected because the tumor originated from it).

Key to Acronyms (Figs. 15a–h):

7 cn	facial nerve	**IAC**	internal auditory canal
7–8 cns	complex of the 7th–8th cranial nerves	**Tu**	tumor
8 cn	acoustic nerve	**ves n**	vestibular nerve
AICA	anterior inferior cerebellar artery		

Comment to Case 5

EAM allowed for complete resection of the intracanalar tumor portion without any drilling of the IAC and with only minimal manipulation of the 7th and 8th cranial nerves.

Case 6 (Figs. 16a–f)
Recurrent Left PCA Dermoid

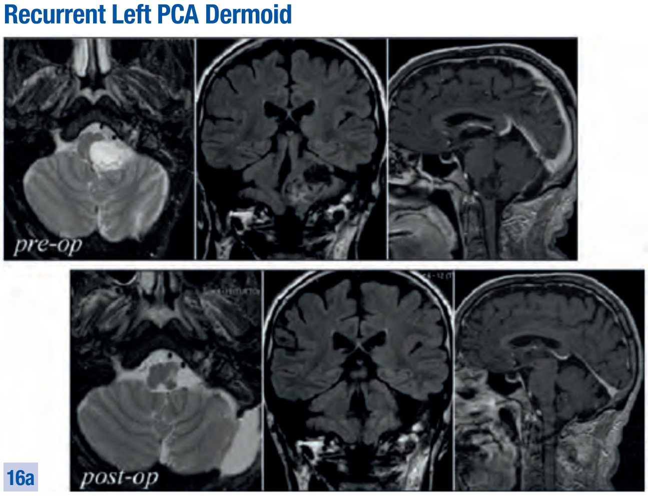

16a

Pre- and post-operative MR scans of the lesion.

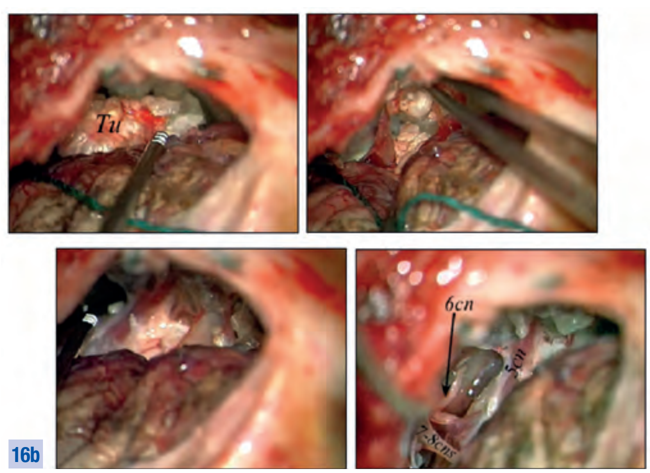

16b

The posterior and lateral portions of the tumor, mainly represented at this level by its pearly component, was removed using microsurgical techniques. The medial-most component of the matrix was left attached to the brainstem, at the site immediately overlying the emerging 5th cranial nerve.

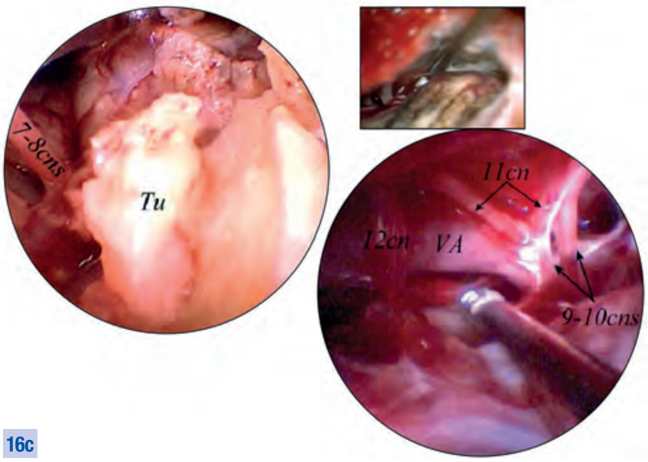

16c

A 30°-scope with upward oriented forward-oblique view (28162 BOA, KARL STORZ Germany) was used free-hand to explore the depth of the operative site, revealing small tumor remnants adherent to the emerging 7th–8th cranial nerve complex; moving the scope downwards, the intracranial course of the vertebral artery and lower cranial nerves came into view.

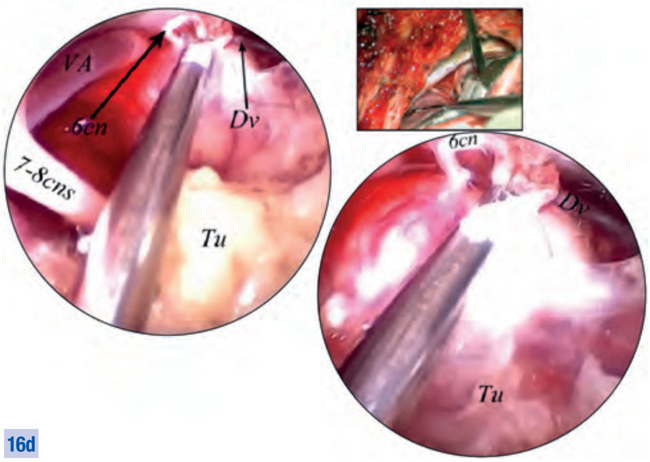

16d

The scope was used to inspect the medial-most and deep-seated areas of the brainstem and to visualize the complex of the 7th–8th cranial nerves, the vein of Dandy and the 6th cranial nerve.

Key to Acronyms (Figs. 16a–f):

5 cn	trigeminal nerve	**p. mes. v.**	pontomesencephalic vein
6 cn	abducent nerve	**post-op**	post-operative
7–8 cns	complex of 7th–8th cranial nerves	**pre-op**	pre-operative
9–10 cns	glossopharyngeal and vagus (cranial) nerves	**SCA**	superior cerebellar artery
11 cn	spinal accessory nerve	**Tu**	tumor
12 cn	hypoglossal nerve	**VA**	vertebral artery
Dv	Dandy's vein		

Comment to Case 6

EAM allowed for complete resection of the tumor without cerebellar retraction and only minimal manipulation of the critical neurovascular structures involved in the procedure.

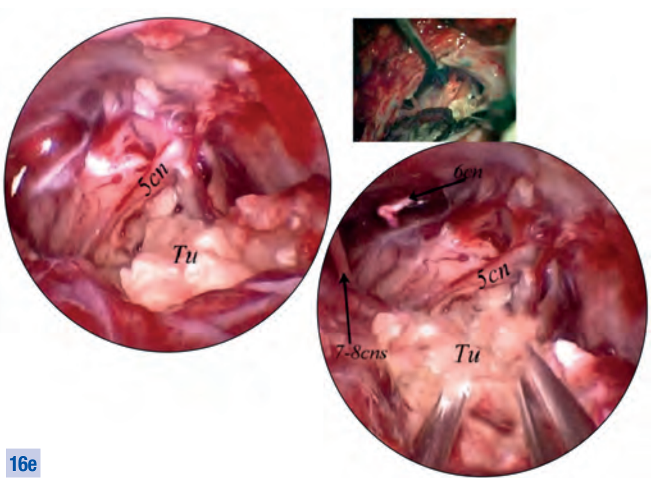

16e

The 30° scope was attached to a holder (28272 RKB) for enhanced control of the next surgical maneuvers involving extirpation of the tumor matrix.

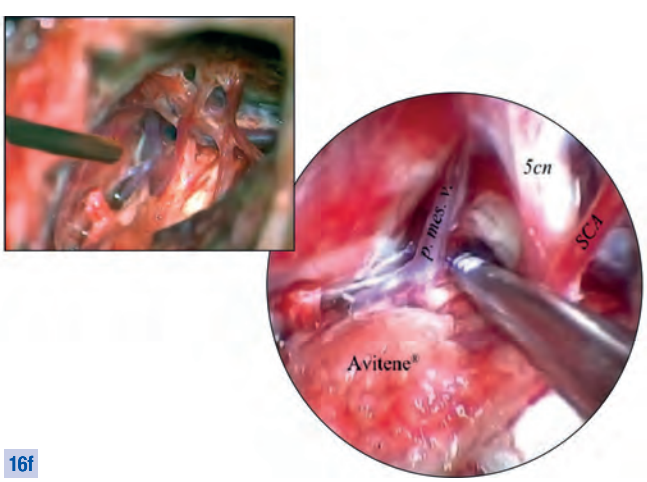

16f

At the end, without any retraction of the cerebellar hemisphere, the tumor was completely removed while sparing the pontomesencephalic vein and the 5th cranial nerve with its surrounding arteries; local hemostatic agents (Avitene®: Microfibrillar Collagen Hemostat, Davol Inc., Cranston, USA) were used to provide adequate hemostasis.

Case 7 (Figs. 17a–h)
Cystic Hypothalamic Glioma

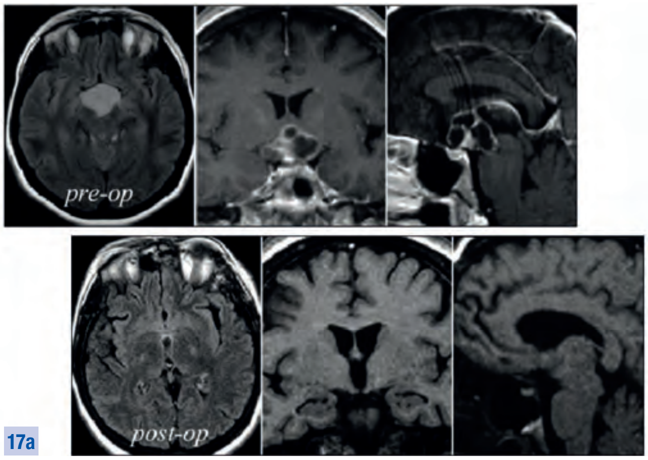

17a

The pre- and post-operative MR scans of the lesion, consisting in a heterogeneous mass with solid and cystic components.

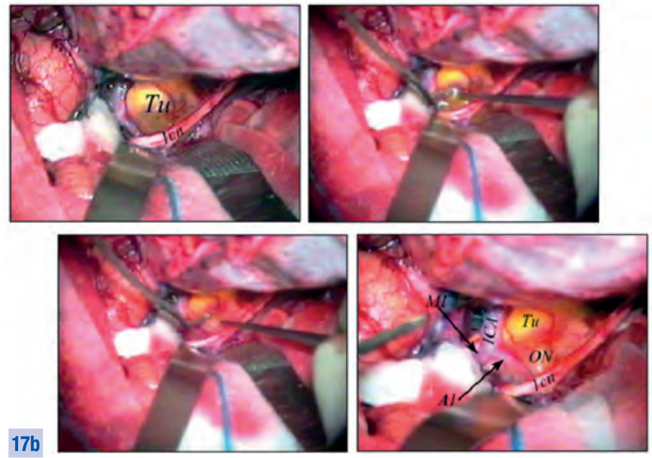

17b

The tumor was approached through a large left pterional approach, considering that extension of the solid component was more distinct on this side. Exposure of the lesion, which had displaced the left ICA and left A1 tract, required dissection and mobilization of the left olfactory nerve. The cyst, protruding laterally to the junction between the left optic nerve and tract, was thereafter evacuated microsurgically.

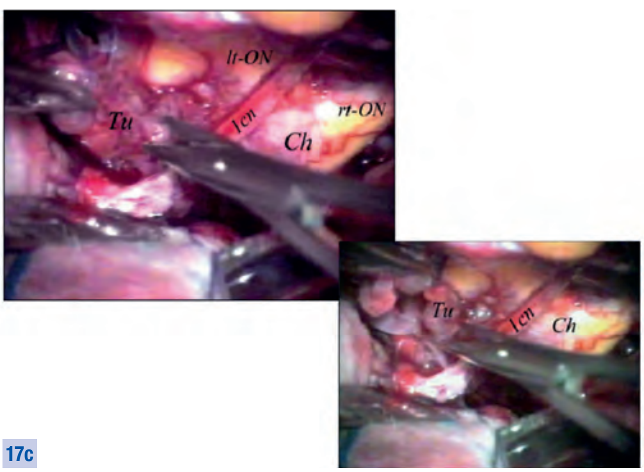

17c

Part of the solid component of the tumor was removed laterally to the olfactory nerve with the microsurgical technique.

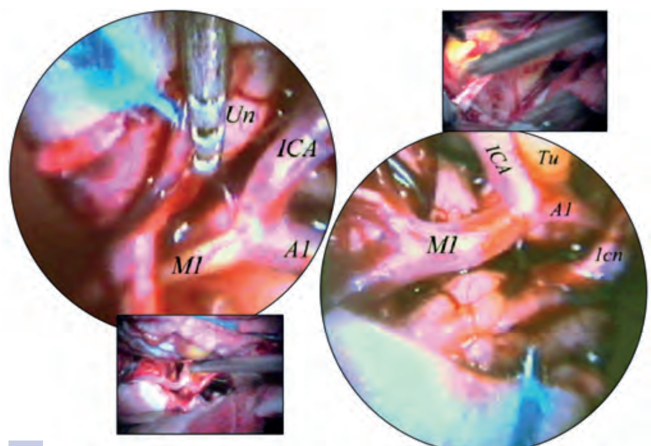

17d

A 30°-scope (28162 BOA) with upward oriented view was used free-hand to control the following situation: the relationships between the ICA siphon, the left middle cerebral artery (M1 tract) and the A1 tract.

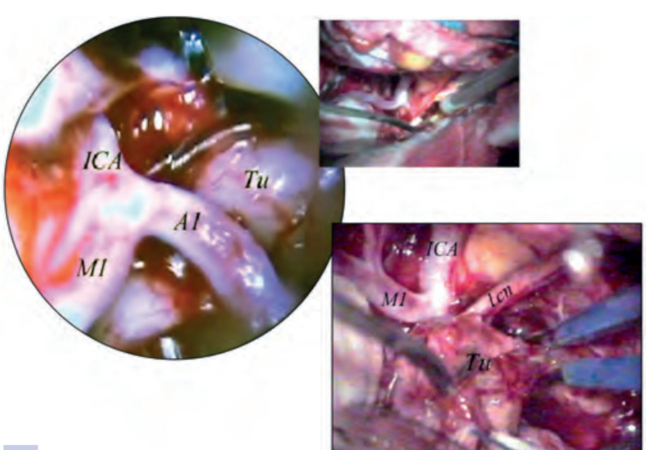

17e

The scope clearly demonstrated a residual tumor which protruded at the level of the lamina terminalis. The remnant was dissected medially to the olfactory nerve using the microsurgical technique.

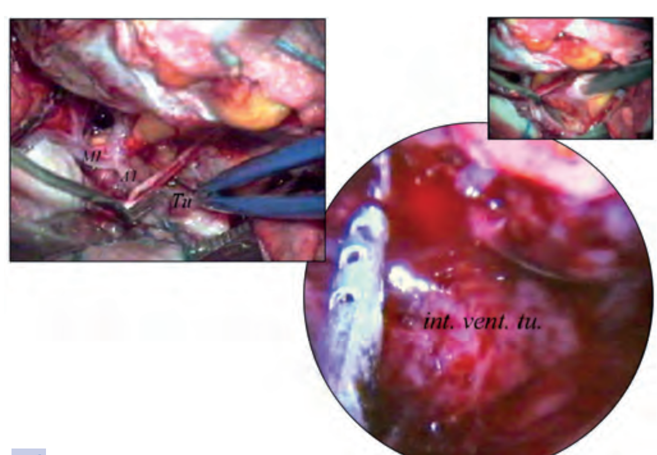

17f

After microsurgical fenestration of the lamina terminalis, the residual solid component of the tumor was removed from the anterior portion of the third ventricle, medially to the olfactory nerve. …

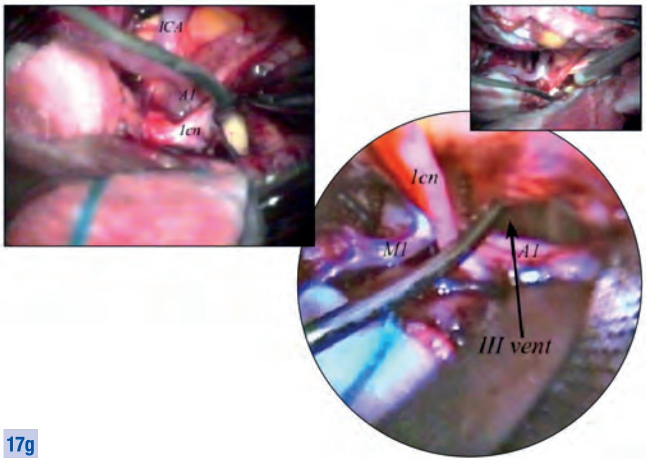

17g

… Again, the surgical field was meticulously inspected using the scope free-hand.

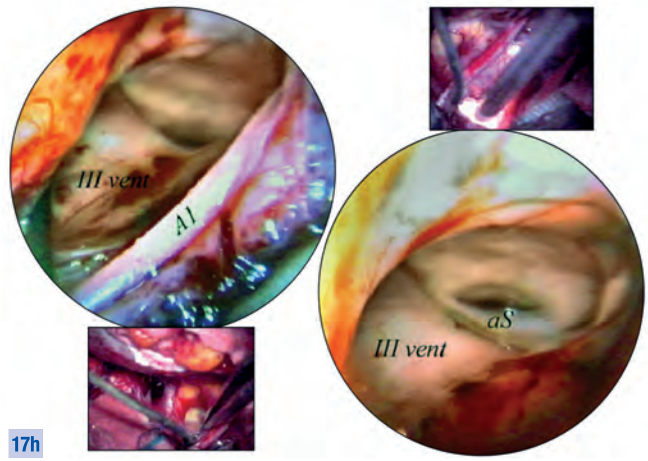

17h

After complete surgical excision, the third ventricular cavity, cleared from residuals, was explored using a 0°-scope (28162 AUA) with straight-ahead view demonstrating the proximal outlet of the Sylvian aqueduct.

Key to Acronyms (Figs. 17a–h):

A1	pre-communicating segment of the anterior cerebral artery	**M1**	proximal segment of the middle cerebral artery
aS	aqueduct of Sylvius	**ON**	optic nerve
Ch	chiasm	**post-op**	post-operative
ICA	internal carotid artery	**pre-op**	pre-operative
int. vent. tu.	intraventricular tumor portion	**rt**	right
lt	left	**Tu**	tumor
1cn	olphactory nerve	**Un**	uncus
III vent	3rd ventricle		

Comment to Case 7

The situation before and after microsurgical maneuvers was checked using the endoscope free-hand until complete surgical removal of the lesion was confirmed.

Case 8 (Figs. 18a–b), continued overleaf

Cystic Metastatic Lesion in the Latero-Inferior Wall of the Forth Ventricle

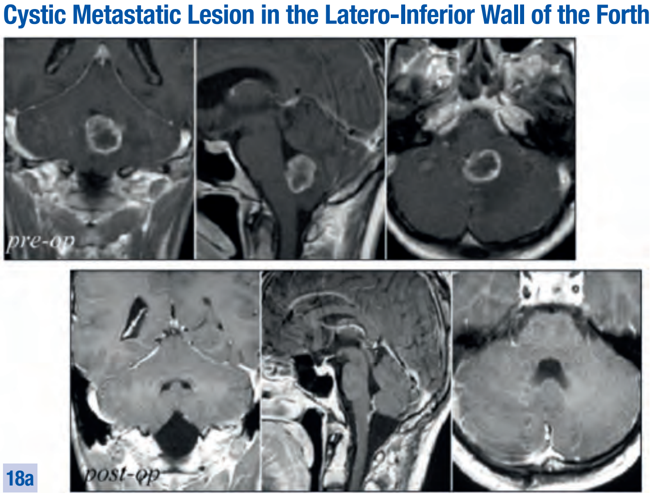

18a

Pre- and post-operative MR scans of the lesion.

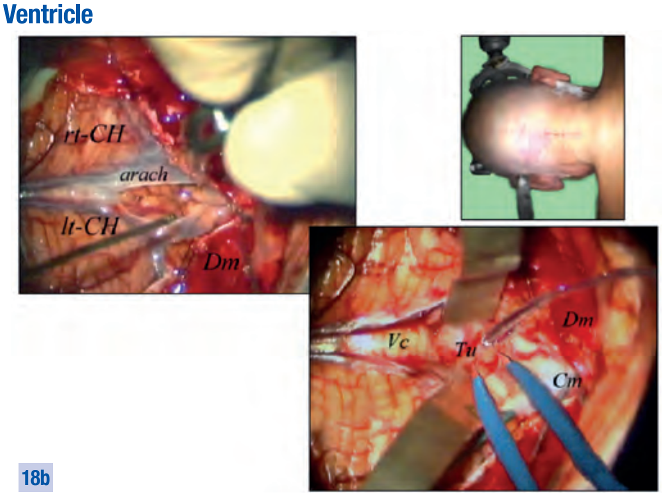

18b

The patient was placed in prone position, and the tumor exposed through a median suboccipital approach: opening of the arachnoidal wall of the cisterna magna provided exposure of the cerebellar tonsils and upper part of the dorsal medullary surface, with no evidence of tumor at this level. Only after retraction of the tonsils, the distal portion of the tumor appeared, emerging from the foramen of Magendie.

Case 8 (Figs. 18c–f) continued from page 35

Cystic Metastatic Lesion in the Latero-Inferior Wall of the Forth Ventricle

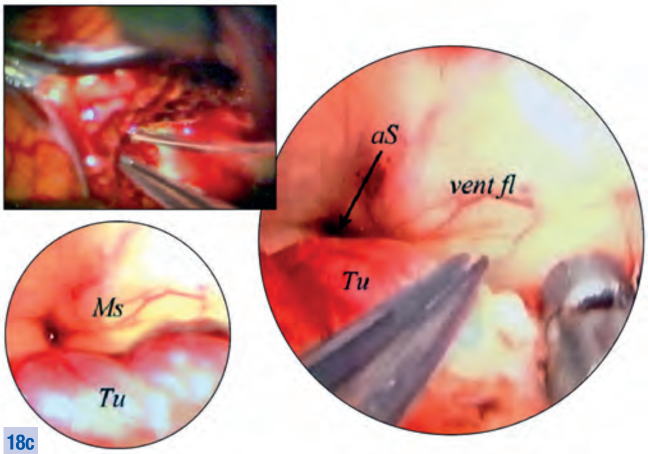

18c

A 0° scope (28162 AUA) with straight-ahead view was used to inspect the ventricular cavity, showing that the tumor was adherent to the left lateral ventricular wall while the floor of the distal portion of the 4th ventricle presented no signs of adherences with the lesion. An initial debulking of the tumor was performed under endoscopic control.

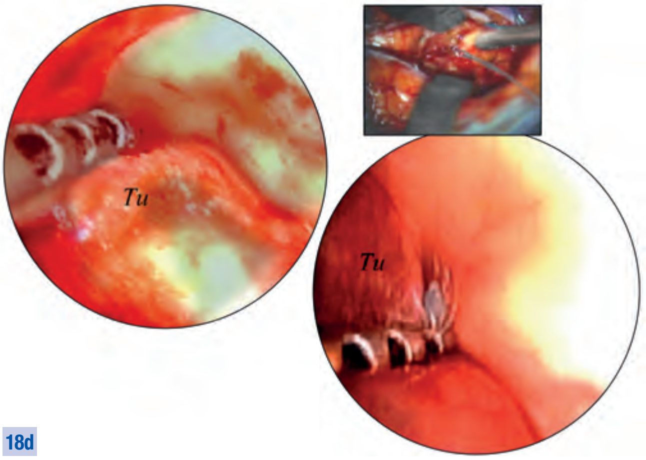

18d

With the scope attached to a holder (28272 RKB), debulking of the lesion was continued until complete removal of the lesion was achieved. The scope permitted good control of the distal end of microsurgical instruments, …

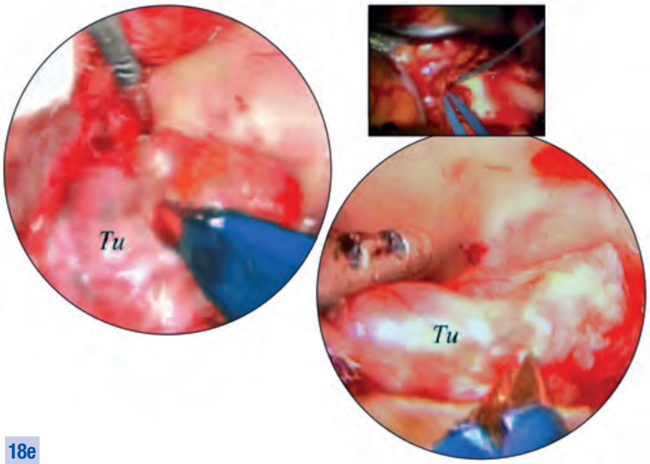

18e

… mainly aspirator and bipolar coagulator, which were deeply inserted in the ventricular space.

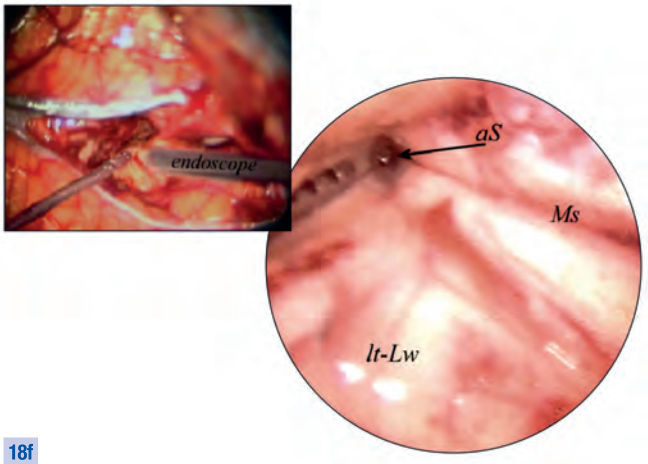

18f

At the end of the procedure, the ventricular cavity was shown to be cleared from residuals.

Comment to Case 8

EAM allowed for direct control of microsurgical instruments inside the cavity of the fourth ventricle, obviating the need for excessive cerebellar retraction and/or vermian splitting to expose the complete ventricular space as far as the distal outlet of the Sylvian aqueduct.

Key to Acronyms (Figs. 18a–f and 19a–f):

arach	arachnoid	**Ms**	median sulcus
aS	aqueduct of Sylvius	**PICA**	posterior inferior cerebellar artery
CH	cerebellar hemisphere	**post-op**	post-operative
Cm	cisterna magna	**pre-op**	pre-operative
Ct	cerebellar tonsil	**rt**	right
Dm	dura mater	**Tu**	tumor
lt	left	**Vc**	cerebellar vermis
Lw	lateral wall	**vent fl**	ventricular floor
Me	median eminence		

Case 9 (Figs. 19a–f, continued overleaf)
Partially Cystic Choroid Plexus Papilloma of the Fourth Ventricle

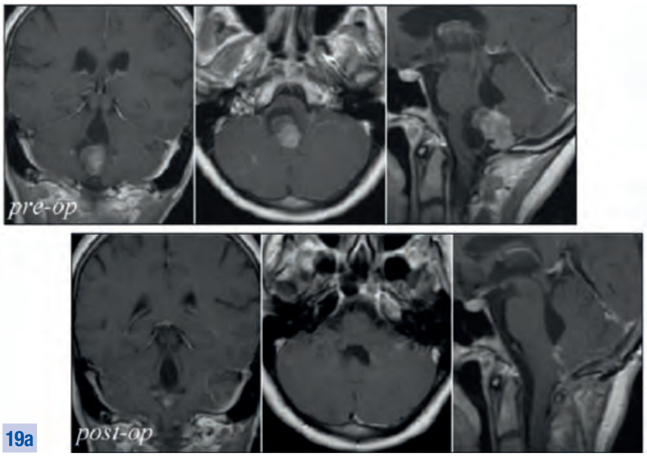

19a

Pre- and post-operative MR scans of the lesion.

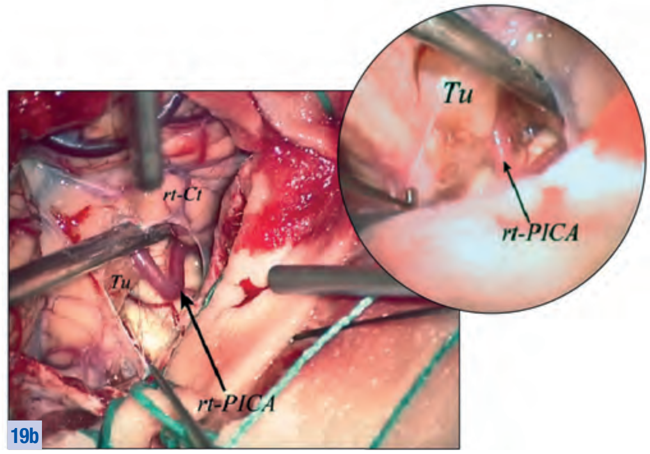

19b

The patient was placed in prone position and the tumor exposed through a median suboccipital approach: the tumor originated from the foramen of Magendie. A 0° scope (28162 AUA) with straight ahead view was used to evacuate the cystic component located in the ventricular floor.

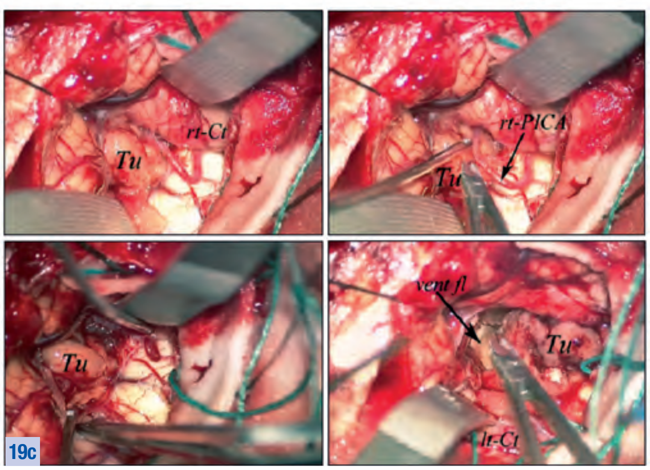

19c

Following tonsillar retraction, the inferior portion of the tumor was exposed, gradually dissected and debulked, leaving untouched the base of tumor implantation, at the level of the inferior part of the ventricular floor.

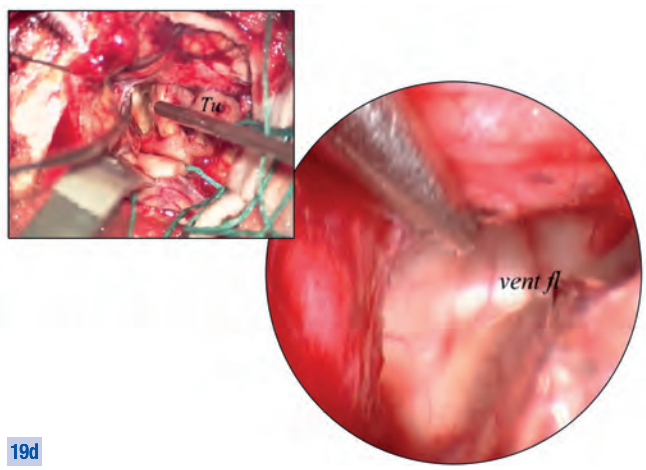

19d

The scope was used …

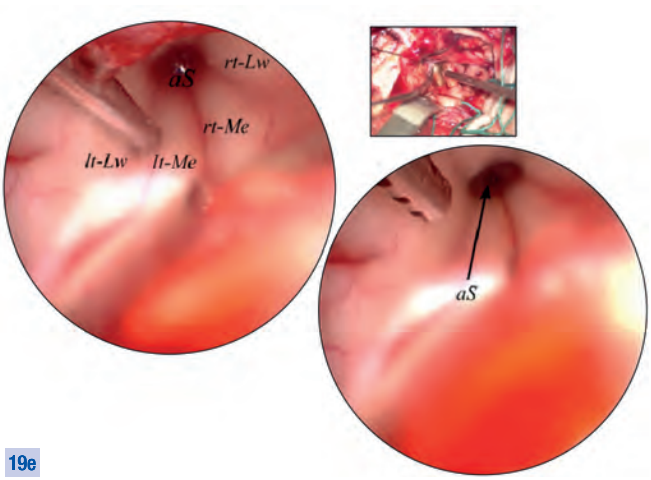

19e

… to inspect the ventricular cavity as far as the distal outlet of the Sylvian aqueduct.

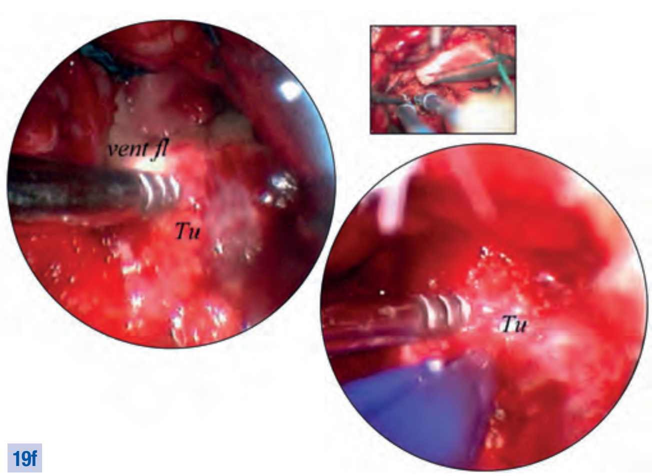

19f

The scope was attached to a holder (28272 RKB) and used to control the distal end of the surgical instruments during removal of the tumor component protruding from the distal portion of the ventricular floor.

Case 9 (Figs. 19g–h), continued from page 37
Partially Cystic Choroid Plexus Papilloma of the Fourth Ventricle

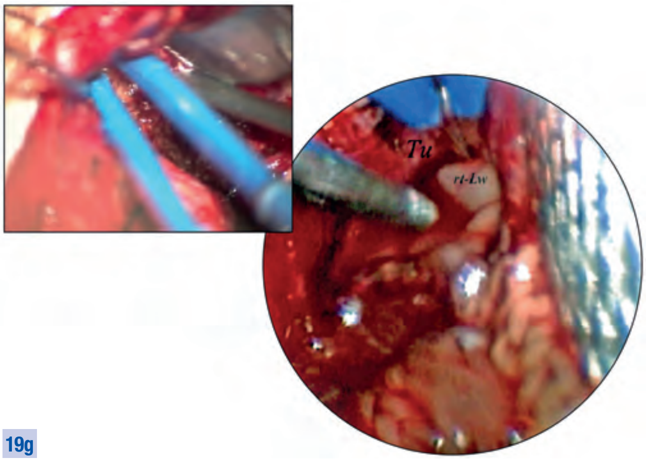

19g

Intraoperative control of the bipolar forceps was maintained by use of the scope during coagulation at the level of the roof of the ventricular cavity, where the microscope could not provide adequate view of the instruments' distal ends.

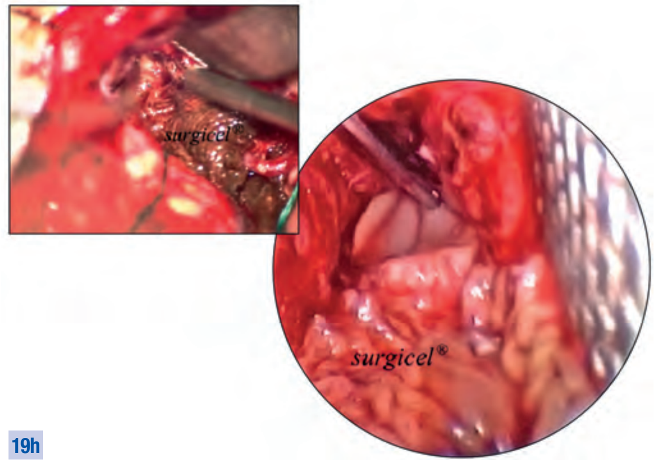

19h

At the end of the procedure, the floor of the ventricle was packed with a layer of Surgicel® (Surgicel®; Fibrillar Absorbable Hemostat, *Johnson & Johnson Medical Ltd, UK*). Finally, completeness of excision was assessed by using again the endoscope.

Comment to Case 9

EAM allowed for direct control of microsurgical instruments inside the cavity of the 4th ventricle, obviating the need for excessive retraction and/or vermian splitting to expose the complete ventricular space as far as the distal outlet of the Sylvian aqueduct.

Key to Acronyms (Figs. 19g–h):

(lt)	left	**(rt)**	right
Lw	lateral wall	**Tu**	tumor

Case 10 (Figs. 20a–f)
Sellar-Retrosellar Arachnoid Cyst

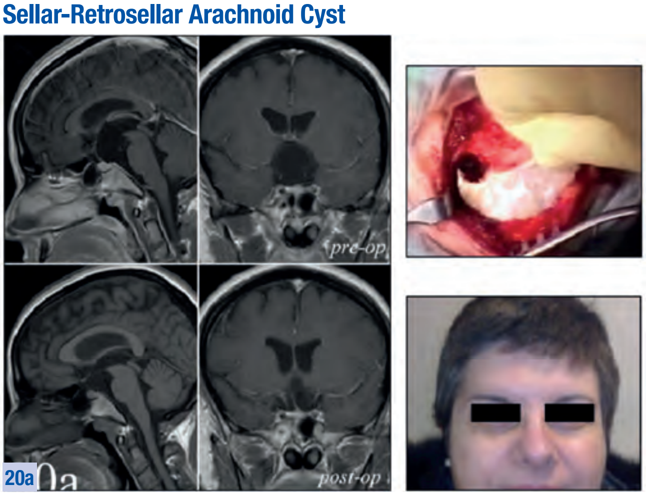

20a

Pre- and post-operative MR scans of a lesion, which was exposed through a right supraorbital eyebrow approach.

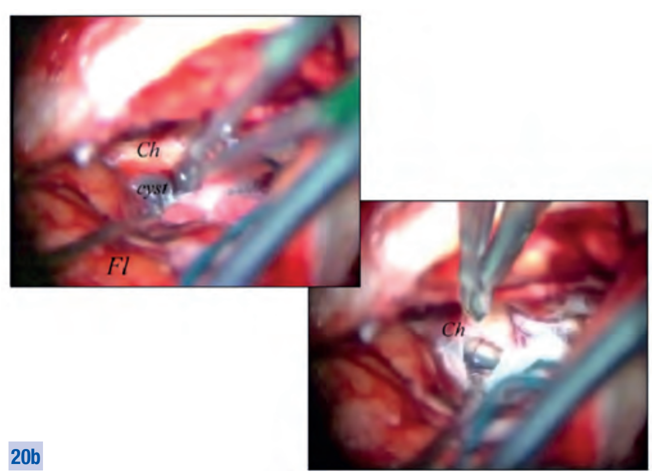

20b

Following elevation of the frontal lobe, the most external wall of the cyst was found to overlie a prefixed optic chiasm: this wall was resected using microsurgical technique.

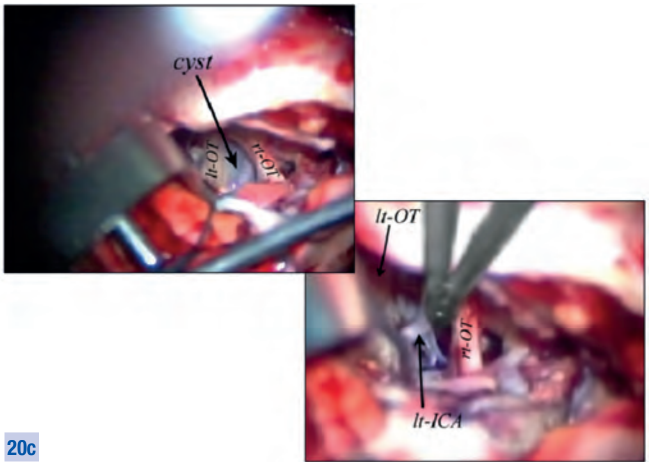

20c

The posterior cystic wall revealed to be interposed between the optic tracts which were driven apart by the lesion; the cyst wall was incised with microscissors.

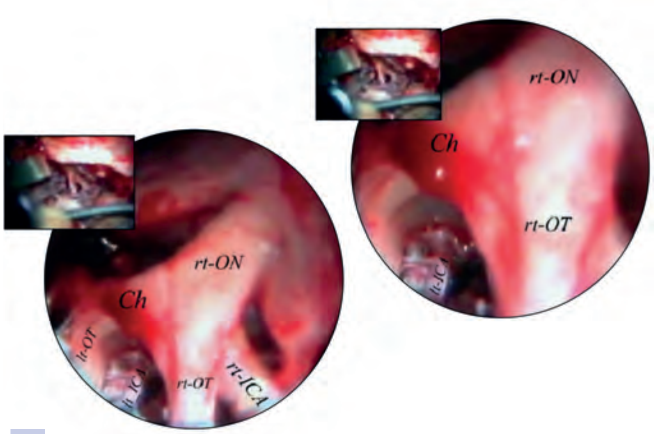

20d

Using the free-hand technique, a 30° scope (28162 BUA) with forward-oblique view was advanced between the optic tracts, …

Key to Acronyms (Figs. 20a–f):

Ba	basilar artery	**ON**	optic nerve
Ch	chiasm	**OT**	optic tract
Fl	frontal lobe	**post-op**	post-operative
ICA	internal carotid artery	**pre-op**	pre-operative
lt	left	**rt**	right

Comment to Case 10

EAM allowed for direct complete fenestration of a complex lesion through a minimally invasive "key-hole" approach.

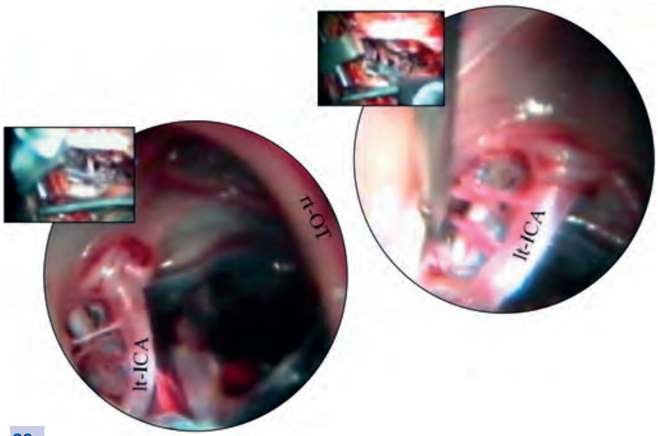

20e

… presenting a left hypoplastic, but functional ICA, which was found to be displaced below the left ON.

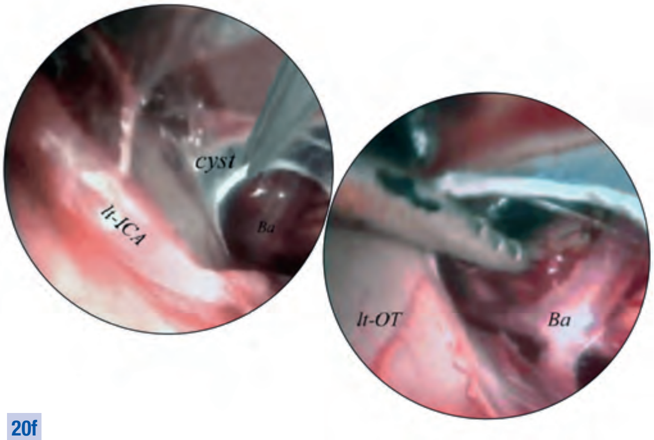

20f

Advancing the endoscope further into the depth (manually guided by the assistant surgeon), the posterior-most portion of the cystic wall was opened, revealing the tip of the basilar artery and creating a complete fenestration.

Case 11 (Figs. 21a–h) Multiloculated Arachnoid Cyst of the Posterior Fossa Involving the Cisterna Magna Region as far as the C2 Segment

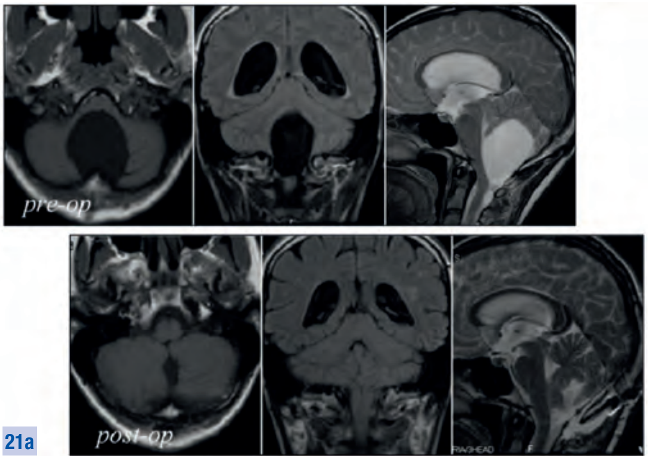

21a

The pre- and post-operative MR scans of the lesion.

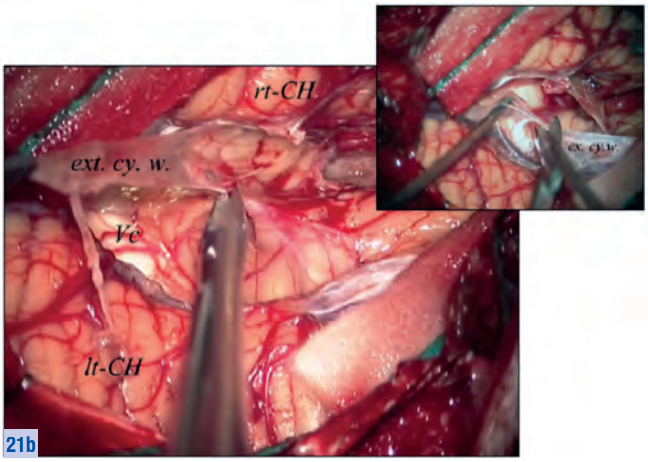

21b

The lesion was exposed through a median suboccipital approach. The most external wall of the multiloculated cystic lesion was overlying the inferior portion of the cerebellar vermis. At first, this wall was excised using the microsurgical technique.

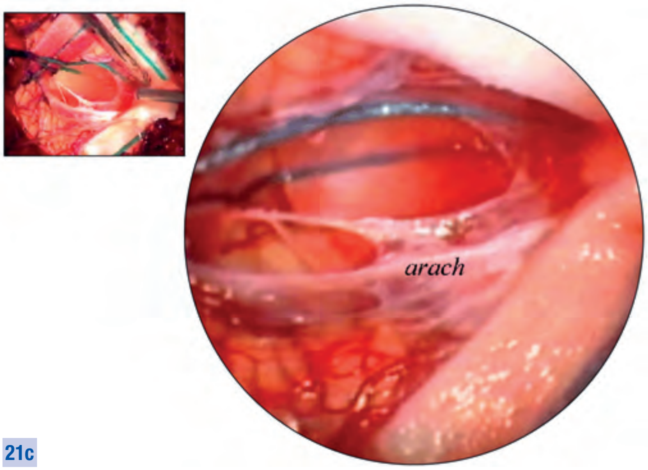

21c

A 0°-scope (28162 AUA) with straight ahead view was used for inspection of the cyst lumen and …

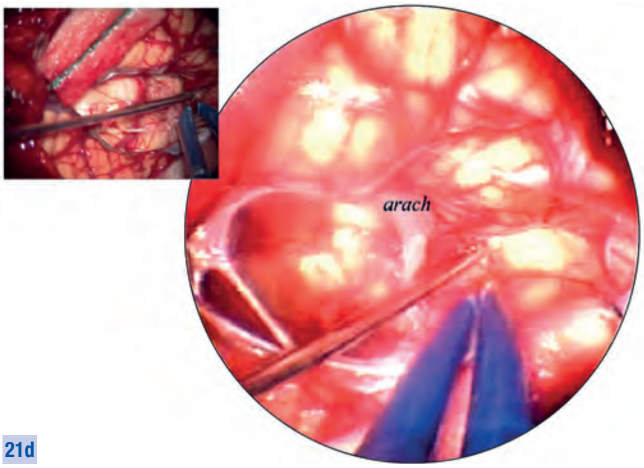

21d

… controlled removal of the inner arachnoid layers.

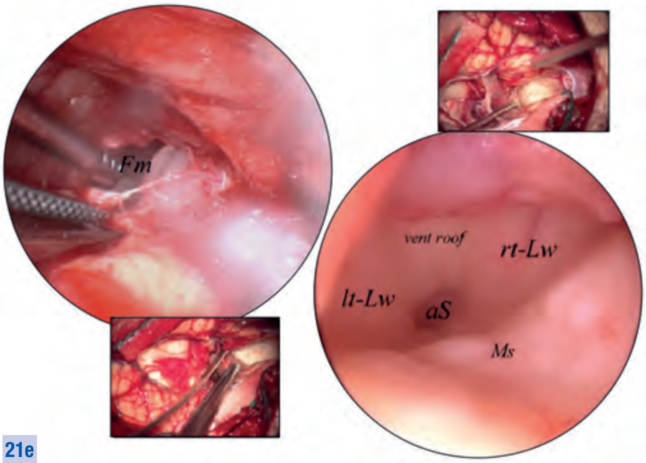

21e

The foramen of Magendie was partially occluded by an arachnoidal septum, which was opened under direct endoscopic vision (with the scope guided by the assistant surgeon). Upon endoscopic inspection (again using the free-hand technique), the cavity of the 4th ventricle was found to be free from arachnoid membranes.

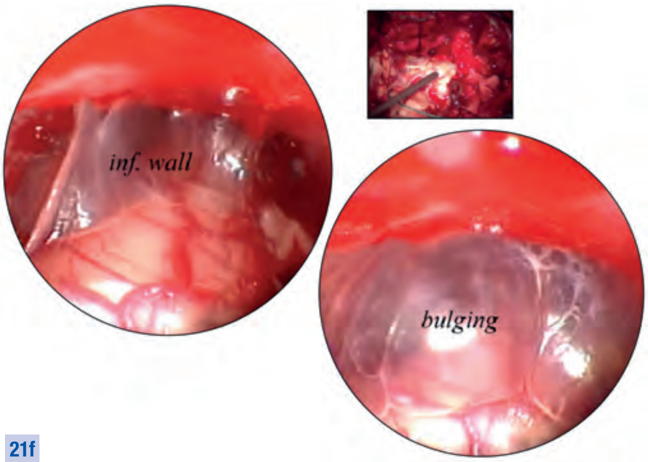

21f

Next, the scope was advanced toward the cervical region and attached to a mechanical holder (28272 RKB), revealing the presence of residual cystic loculations, synchronously bulging during inspiration.

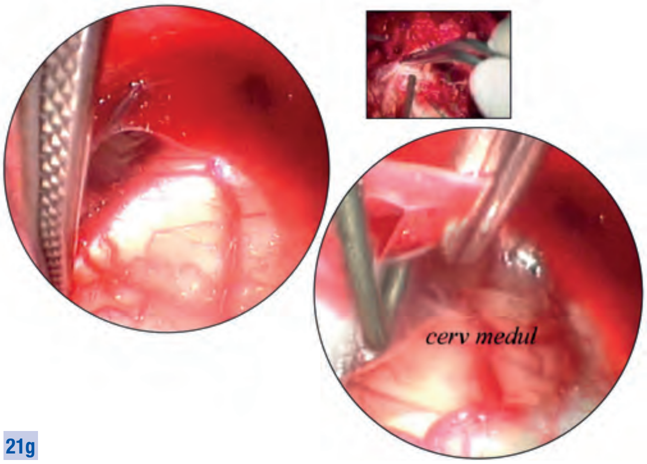

21g

The arachnoid septations were removed under direct endoscopic control.

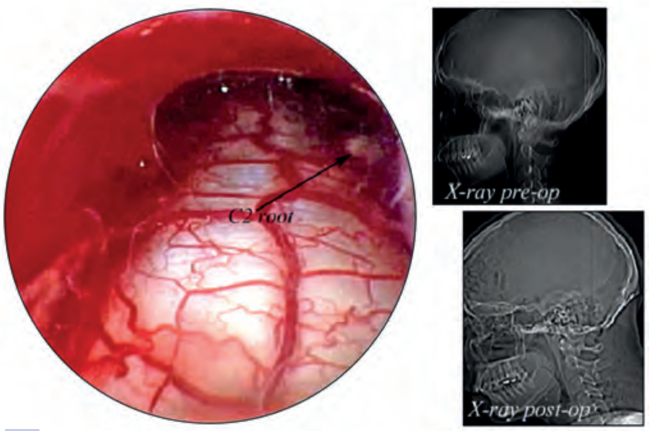

21h

At the end of the procedure, complete exposure of the dorsal aspect of the cervical medulla was obtained. Pre- and post-operative lateral plain radiographs of the skull and upper cervical segment confirmed the integrity of the posterior C1 arch.

Key to Acronyms (Figs. 21a–h):

arach	arachnoid	**Lw**	lateral wall
aS	aqueduct of Sylvius	**Ms**	median sulcus
cerv medul	cervical medulla	**(rt)**	right
CH	cerebellar hemisphere	**Vc**	cerebellar vermis
ex. cy. w.	external wall of the cyst	**vent roof**	ventricular roof
Fm	foramen of Magendie	**pre-op**	pre-operative
inf. wall	inferior wall of the cyst	**post-op**	post-operative
(lt)	left		

Comment to Case 11

EAM allowed for complete excision of the lesion with a limited approach. Even though the multiloculated cyst extended as far as C2 level, removal of the C1 arch was not required to expose and remove the lesion.

4.2 Neurovascular Conflicts

A number of reports emphasize the role of endoscopy as an helpful adjunct during procedures performed for microvascular decompression of cranial neuropathies in the posterior fossa[44, 45, 56–66]. There are also reports in the literature on the fully endoscopic decompression of neurovascular conflicts[67–69].

A total number of 41 EAM procedures for surgical management of neurovascular conflicts in the cerebello-pontine angle have been performed personally by the senior author (R.J.G.), comprising 25 cases of trigeminal neuralgia, seven cases of hemifacial spasm, six cases of disabling positional vertigo, two cases of glossopharyngeal neuralgia and one case of spasmodic torticollis. All procedures were performed via the retrosigmoid approach with the patient placed in the modified park-bench position. Neuronavigation was used in most instances, mainly for proper placement of the craniotomy in relation to the location of the transverse and sigmoid sinuses. Intraoperative neurophysiological monitoring was used only in cases of hemifacial spasm. In 23 cases, the endoscope was used free-hand, and in 18 cases the endoscope was fixed in the operative field allowing operative maneuvers to be performed under direct endoscopic control. All cases have been investigated by retrospective evaluation to assess the usefulness of endoscopic assistance in the treatment of neurovascular conflicts.

The endoscope allowed, in our opinion, a better comprehension of the local anatomy in all cases, and in 9 cases it gave an effective vision of the vascular conflict, also when it was not clearly visible under pure microscopic vision (in three cases revealing the vascular structure responsible for the conflict, and in six cases revealing additional vascular structures responsible for multiple conflict situations). Conclusively, EAM in all cases provided a clearer vision of all nervous and vascular structures in the operative field, opened up the possibility of manipulating these structures with minimal cerebellar retraction, and reduced the number of negative explorations, resulting in more effective treatment and smaller approaches (in no case, the use of spatulas was needed to retract the cerebellar hemispheres during the procedure and the diameter of the retrosigmoid craniotomy could be progressively reduced, during our experience, to 2 – 2.5 centimetres (**Figs. 22, 23, Cases 12, 13**). The potential risks of endoscope-related mechanical and thermal injuries to the cranial nerves and to other critical vascular and neural structures in the cerebello-pontine angle have been reported[69–70]. In reality, the scope provides vision only at its tip and its inability to look sideways and backwards when introduced into the operative field exposes adjacent structures to the risk of direct contact damage; this may be true if fully endoscopic vascular decompression technique is used, but any injury can be avoided if the scope is inserted under microscopic guidance, as is the case during EAM procedures; the use of mechanical holders allows, as previously stated, precise and atraumatic positioning of the scope. Moreover, the illumination intensity of the endoscopic light source is set, during procedures of microvascular decompression in the cerebello-pontine angle, at levels also inferior to those used for EAM procedures in case of expansive and cystic lesions deeply located in other anatomical sites, which virtually avoids any possibility of thermal injury.

Case 12 (Figs. 22a–f)
Left Trigeminal Neuralgia Secondary to Neurovascular Conflict

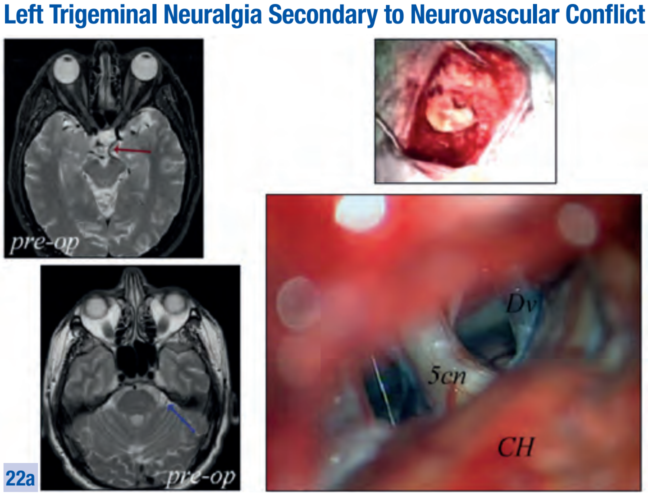

Preoperative MR scans showing a left persistent trigeminal artery (red arrow) in a patient with a neurovascular conflict at the level of the left 5th cranial nerve (blue arrow); the lesion was approached through a small left retrosigmoid craniotomy.

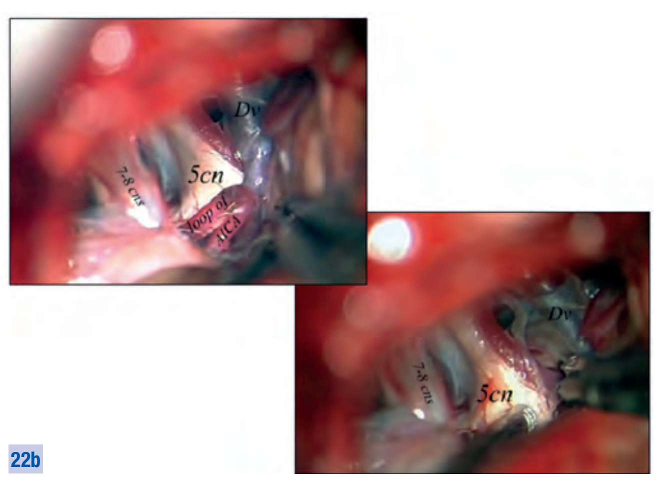

Microsurgical maneuvers allowed to expose the trigeminal nerve which was dissected until its point of emergence from the brainstem: the vein of Dandy obscured clear vision of the most proximal part of the nerve which appeared displaced by an arterial branch firmly adherent in its anterior and medial aspects.

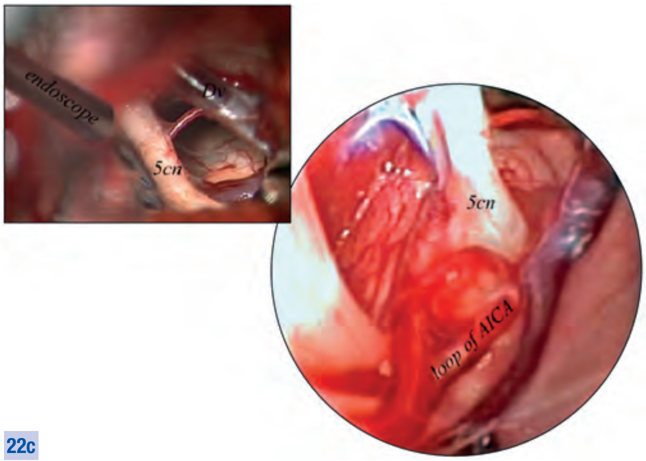

22c

Dissection was continued, and in the next step, the 0° scope (28162 AUA) was guided with the free hand to explore the region, when a loop of the AICA was found to be the source of a neurovascular conflict with the dorsal exit zone of the nerve.

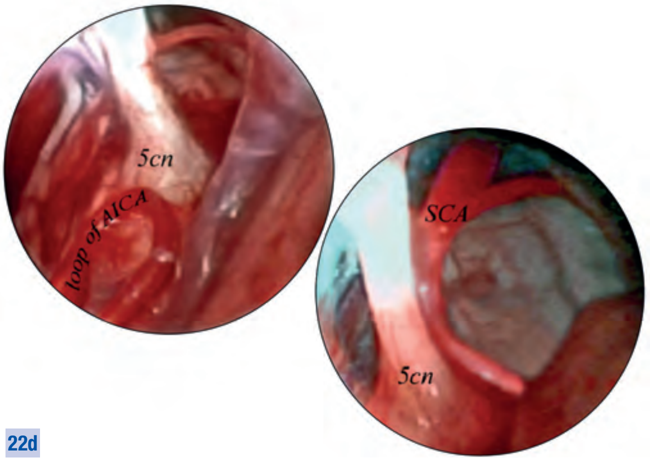

22d

A second artery was identified as the cause of a neurovascular conflict with the ventral portion of the nerve: it emerged from above and was shown to be the main branch of the SCA.

Key to Acronyms (Figs. 22a–f):

5 cn	trigeminal nerve	**Dv**	Dandy's vein
7–8 cns	complex of the 7th–8th cranial nerves	**pre-op**	pre-operative
AICA	anterior inferior cerebellar artery	**SCA**	superior cerebellar artery
CH	cerebellar hemisphere		

Comment to Case 12

EAM allowed to clearly localize multiple neurovascular conflicts and to perform surgical maneuvers suited for providing microvascular decompression without using any cerebellar retraction.

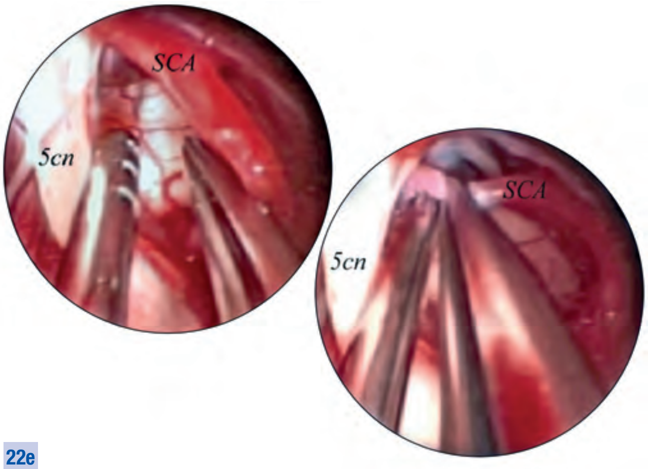

22e

The scope was attached to a holder, and the artery shown in (**d**) was mobilized from the nerve with some difficulty, because it gave off a small branch – passing anteriorly to the distal portion of the primary root of the 5th cranial nerve – which had to be dissected.

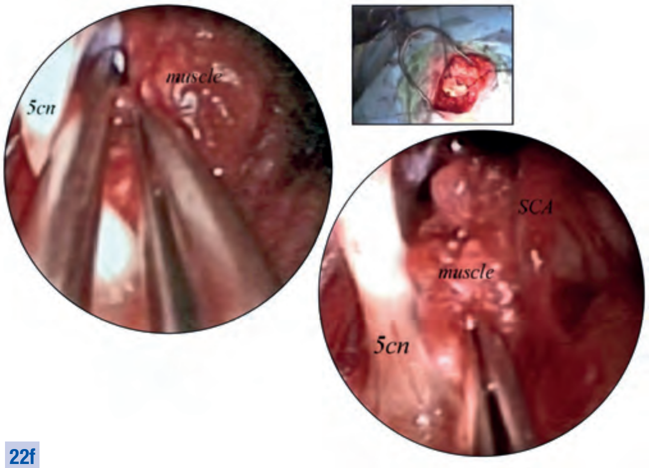

22f

A small piece of muscle was placed to keep the arterial branch apart from the junctional zone of the trigeminal nerve. At the end of the procedure, the osteoplastic flap was replaced.

Case 13 (Figs. 23a–f)

Left Hemifacial Spasm Secondary to Neurovascular Conflict

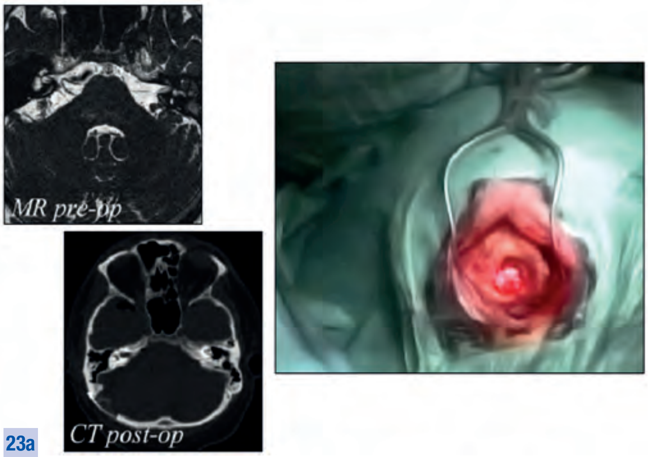

23a

Preoperative MR scan demonstrating left neurovascular conflict at the level of the 7th–8th cranial nerve complex in a patient with hemifacial spasm and disabling positional vertigo, with mild ipsilateral neuro-sensorial hypoacusia. The lesion was approached through a small left retrosigmoid craniectomy replaced with a titanium mesh at the end of the operation, as shown on the postoperative CT scan.

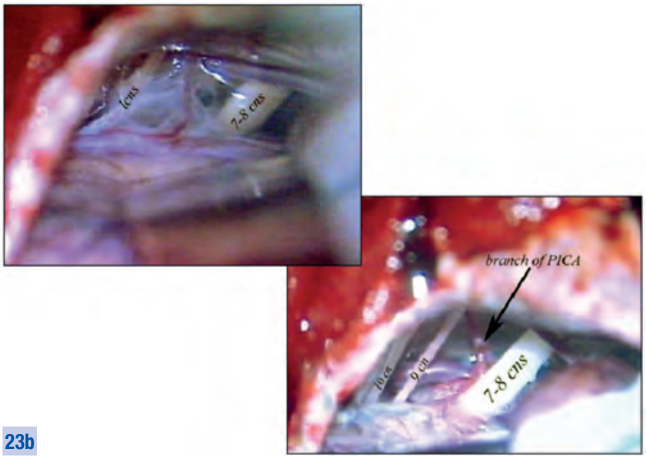

23b

Microsurgical dissection was performed from below because the offending artery had been diagnosed to be an ascending branch of the PICA. Dissection of dense arachnoid adhesions was necessary to expose the 7th–8th cranial nerve complex and the inferior cranial nerves.

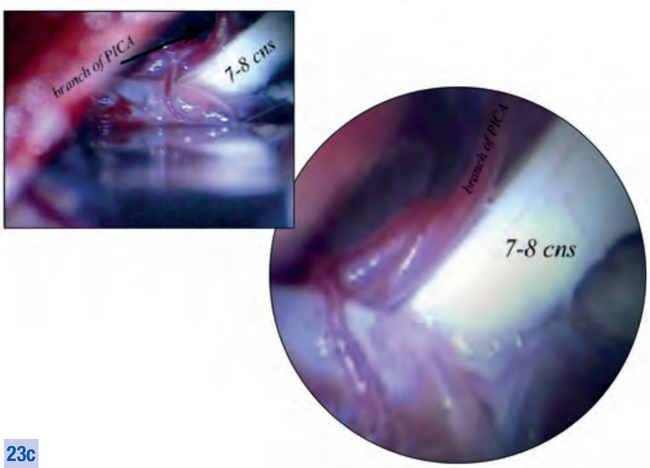

23c

Microscopic dissection required excessive cerebellar retraction to expose the junctional zone of the 7th cranial nerve. Next, an upward oriented 30°-scope (28162 BOA) was inserted to explore the region.

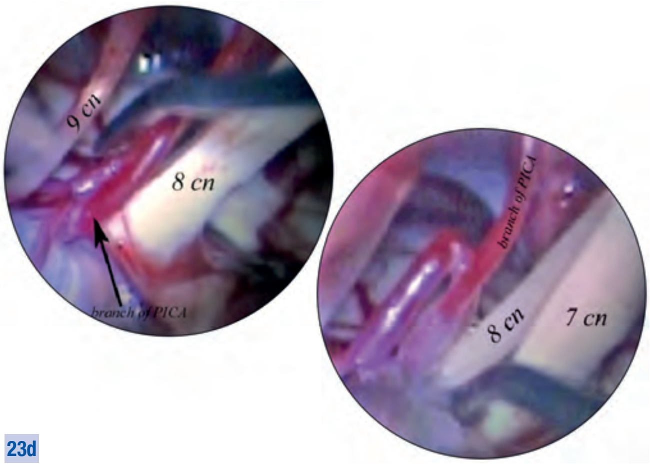

23d

The scope was fixed in place and the artery creating the apparent conflict was mobilized from the 7th cranial nerve which was dissected also from the 8th cranial nerve: at the beginning it was not clear the exact position of the labyrinthine artery, located between 7th and 8th cranial nerves.

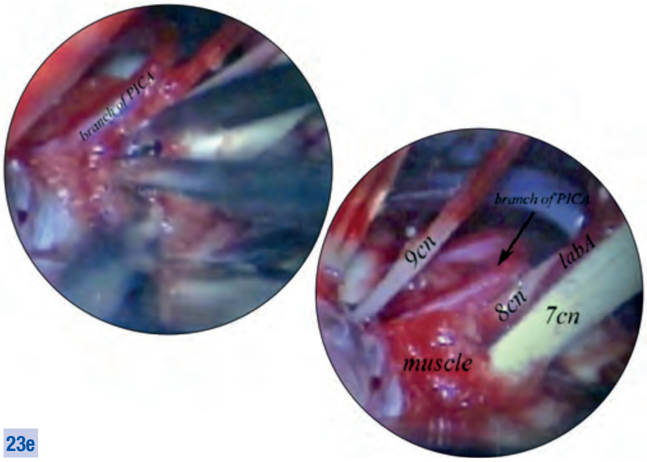

23e

Endoscopic control confirmed, that the labyrinthine artery was clearly separate from the branch of the PICA, which had caused the conflict. Repair was accomplished by placing a small piece of muscle between the offending artery and the junctional zone of the 7th–8th cranial nerve complex.

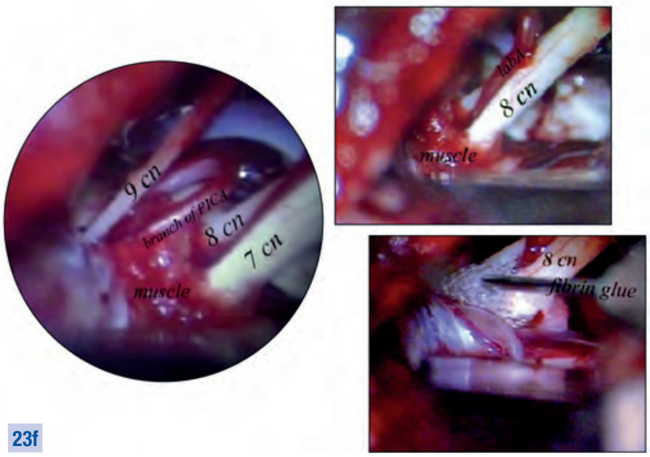

23f

The lower cranial nerves were clearly identified during surgical maneuvers. Final endoscopic inspection confirmed the definitive solution of the neurovascular conflict. At the end of the procedure, fibrin glue was administered under microscopic control.

Key to Acronyms (Figs. 23a–f):

7 cn	facial nerve	**labA**	labyrinthine artery
7–8 cns	complex of the 7th–8th cranial nerves	**lcns**	lower cranial nerves
8 cn	acoustic nerve	**PICA**	posterior inferior cerebellar artery
9 cn	glossopharyngeal nerve	**post-op**	post-operative
10 cn	vagus nerve	**pre-op**	pre-operative

Comment to Case 13

EAM allowed to resolve the neurovascular conflict while obviating the need for excessive cerebellar retraction which pure microsurgical maneuvers would have required.

Case 14 (Figs. 24a–d)
Right Hemifacial Spasm Secondary to Neurovascular Conflict

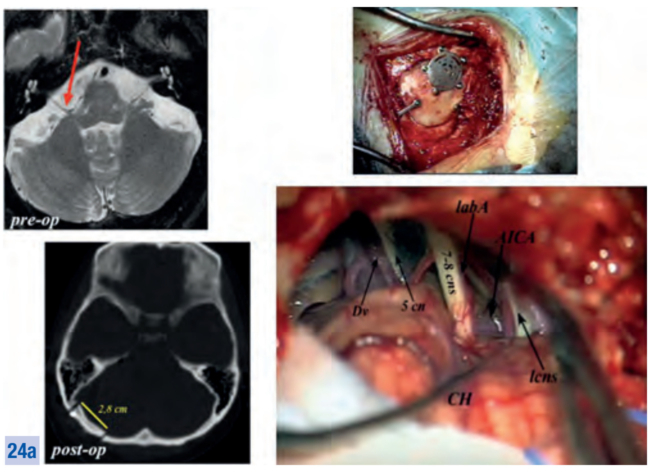

24a

Preoperative MR scan showing right neurovascular conflict between the 7th – 8th cranial nerve complex and the right anterior inferior cerebellar artery, in a patient with right hemifacial spasm. The lesion was approached through a small retrosigmoid craniotomy (the post-operative CT scan showed that the size of the craniotomy was 2.8 cm). After dural opening, the anatomy of the right cerebello-pontine angle was clearly exposed.

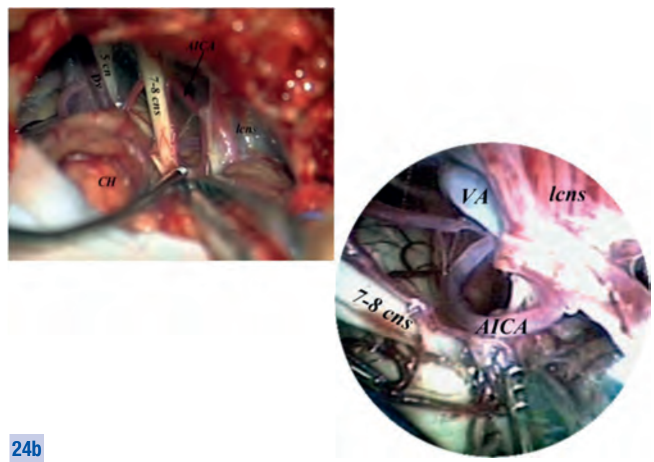

24b

The root entry zone of the 7th cranial nerve was exposed by micro-surgical dissection, but excessive cerebellar retraction was necessary to expose the conflict. Thereafter, a straight forward 0°-scope (28162 AUA) was introduced free-hand and the offending artery, the anterior inferior cerebellar artery, was clearly visualized.

Key to Acronyms (Figs. 24a–d):

5 cn	trigeminal nerve	**labA**	labyrinthine artery
6 cn	abducens nerve	**lcns**	lower cranial nerves
7-8 cns	complex of the 7th–8th cranial nerves	**post-op**	post-operative
AICA	anterior inferior cerebellar artery	**pre-op**	pre-operative
CH	cerebellar hemisphere	**VA**	vertebral artery
Dv	Dandy's vein		

Comment to Case 14

EAM allowed to identify the offending artery and to solve the conflict without excessive cerebellar retraction taking advantage of a minimally invasive approach.

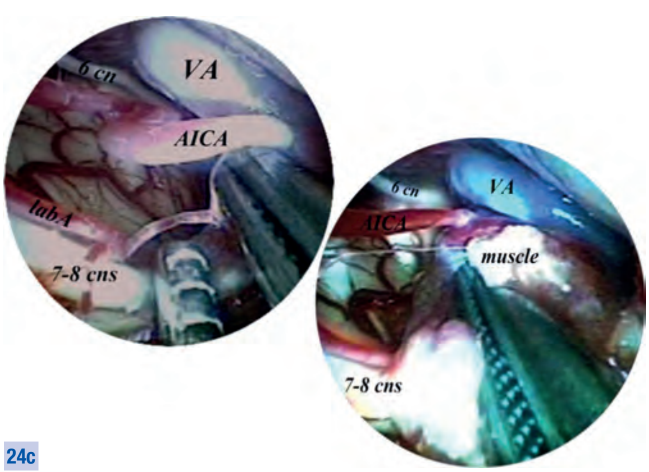

24c

The endoscope was fixed and the artery was mobilized from the nerve. A small piece of muscle was placed to keep apart the arterial branch from the root entry zone of the nerve.

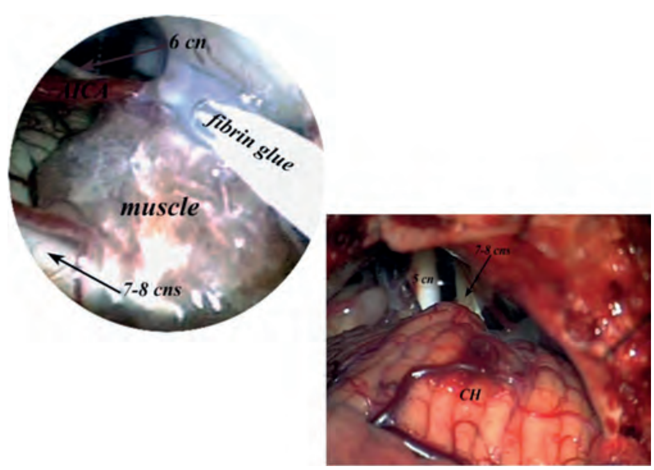

Following these maneuvers, fibrin glue was applied under endoscopic control. At the end of the procedure, microscopic vision revealed no signs of excessive retraction of the cerebellar hemisphere.

4.3 Intracranial Aneurysms

In our experience, the advantages of EAM are specially evident in the operative treatment of intracranial aneurysms, even though only a relatively small number of reports on this topic have been found in the literature[71–81]. The senior author performed 166 EAM procedures for the treatment of intracranial aneurysms in 157 patients harbouring 176 aneurysms. 141 procedures were performed to treat anterior circulation aneurysm(s) and 25 for posterior circulation aneurysm(s).

The first 108 procedures (April 1997–June 2004) were performed consecutively in all patients surgically treated during that period for aneurysm, irrespective of its location, to gather experience regarding the usefulness of EAM in the treatment of this kind of lesions. The results from a retrospective study on these cases suggest that EAM efficacy is only scarcely influenced by the preoperative clinical condition of the patient (Hunt-Hess grade), surgical timing, presence of blood in the cisterns (Fisher grade), hydrocephalus. The most important factors contributing to the efficacy of endoscope-assisted microsurgical treatment of aneurysms are determined by its location and size. For aneurysms located in the superficial sectors of the operative field (anterior wall of the internal carotid artery as in the case of carotid-ophthalmic aneurysms, middle cerebral artery, posterior inferior cerebellar artery) and for lesions essentially treated via skull base approaches (vertebro-basilar junction, middle basilar artery) endoscopic assistance did not provide any real advantage. Conversely, adjunctive visual information provided by an endoscope has shown to be particularly useful in the treatment of cerebral aneurysms deeply located in an arterial segment with numerous perforators, developing in cisternal regions offering enough space to introduce and guide the scope without risky microsurgical maneuvers. Lesions located in the posterior wall of the internal carotid artery (posterior communicating and anterior choroid artery aneurysms), aneurysms of the bifurcation of the internal carotid artery, aneurysms of the anterior communicating–anterior cerebral arteries complex and lesions located in the distal portion of the basilar artery can be treated effectively with the endoscope-assisted technique. The size of aneurysm proved to be a less important factor. In general terms, very large and giant aneurysms take less benefits from EAM than smaller ones of the same location, because the mass of the lesion can compromise insertion and fixation of the endoscope in the operative field and because these lesions are usually exposed through larger (or skull base) approaches. After the initial experience period, from July 2004 until April 2009, we have performed endoscope-assisted microneurosurgical procedures to treat aneurysmal lesions only in additional 58 selected cases.

To achieve satisfactory results, the methodological principles of EAM have to be strictly observed in the treatment of intracranial aneurysms, more than in any other field. First of all, it is mandatory, that endoscopic inspection be performed initially. Second, care must be taken that surgical maneuvers are conducted only with the scope firmly fixed into the operative field by use of a holding system, in a position not interfering with microsurgical instruments. Frequently, clip deployment is performed under direct endoscopic vision, to prevent the risk of iatrogenic damage to perforators and other neurovascular structures that are hidden in the depth and not clearly recognizable under microscopic vision. While performing maneuvers exclusively under endoscopic guidance, any manipulation, distortion and retraction of the afferent vessel itself and of any other adjacent arteries should be avoided, a precaution, which is particularly important in cases of advanced sclerotic changes. In case of aneurysms treated in the acute post-hemorrhagic phase, the use of the endoscope reduces the need for mobilizing the sac and the parental artery, thus minimizing the risk of intraoperative rupture. The presence of blood in the arachnoid spaces does not limit the use of the endoscope because, in any case, adequate vision will be provided after cisternal washing, performed during early microsurgical operative steps, and eventually after lamina terminalis opening. Minimally invasive “keyhole” approaches are essentially based on the use of the endoscope as an adjunctive optical device, that allows the surgeon to visually control the aneurysm implant base from various angles of view. Also during EAM procedures for intracranial aneurysms, any risk of mechanical and thermal injury to the critical perilesional neurovascular structures should be prevented by exercising great care while introducing the scope in the operative field under microscopic control, using mechanical holders and preadjusting the endoscopic light intensity to a low level. (**Figs. 25–30, Cases 15–20**).

Case 15 (Figs. 25a–d)
Aneurysm of the Posterior Wall of the right ICA at the Junction with the Posterior Communicating Artery

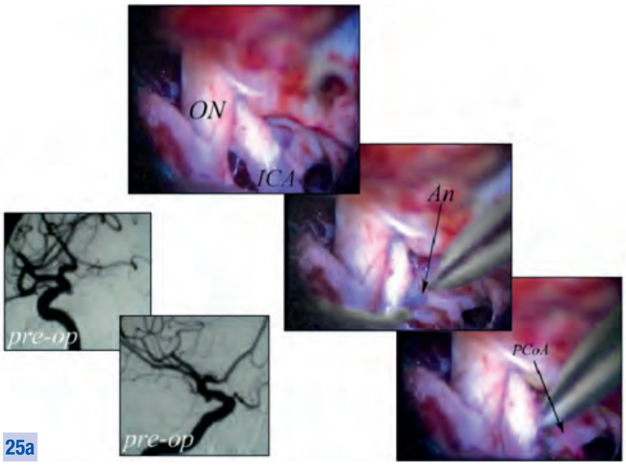

25a

Preoperative angiography showed a small aneurysm of the ICA siphon, which was approached via right pterional approach. Under microscopic vision, the implant base of this small lesion (3 mm in diameter), which had been bleeding 15 days before the operation, and its relationship to the small posterior communicating artery were not clearly visible.

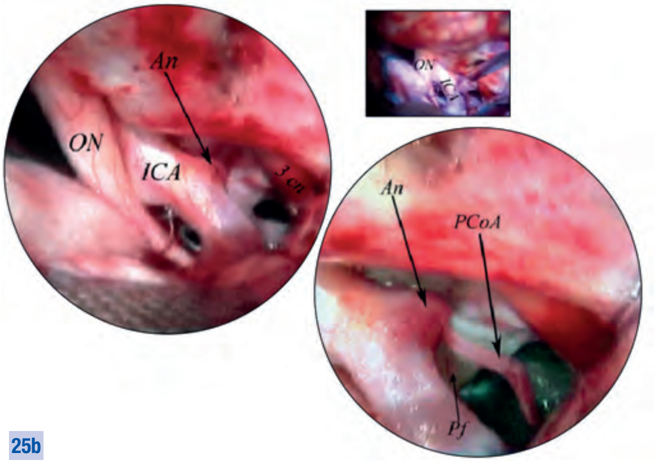

25b

A 0°-scope (28162 AUA) with straight ahead view was introduced showing the PCoA to arise, together with a small perforator, from the posterior wall of the ICA at the implant base of the aneurysm;…

Key to Acronyms (Figs. 25a–d):

3 cn	oculomotor nerve	**PCoA**	posterior communicating artery
An	aneurysm	**Pf**	perforator
ICA	internal carotid artery	**pre-op**	pre-operative
ON	optic nerve		

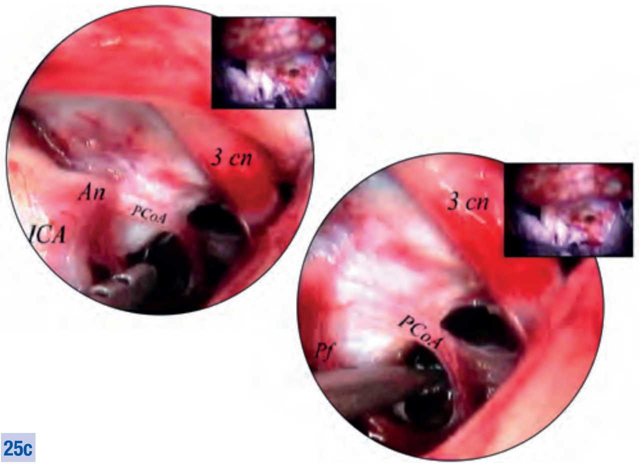

25c

… the PCoA appeared hypotrophic, but with several parent perforators arising along its course.

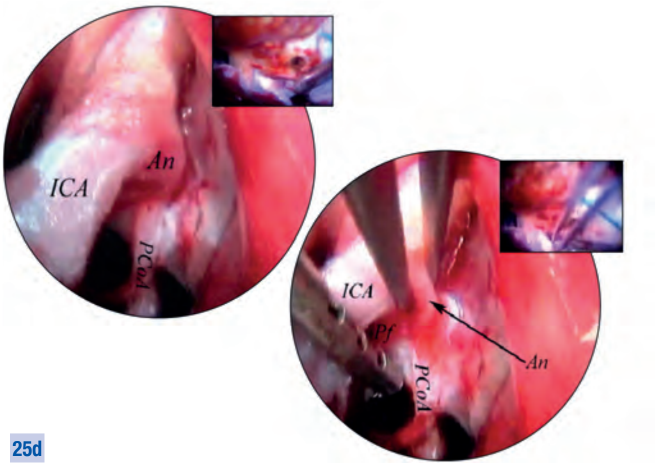

25d

The scope was fixed in place by use of a mechanical holder (28272 RKB). A forceps was used to explore the option of excluding the aneurysmal sac from circulation without compromising the integrity of neither the perforator nor the PCoA.

Case 15 (Figs. 25e–f) continued from page 47

Aneurysm of the Posterior Wall of the right ICA at the Junction with the Posterior Communicating Artery

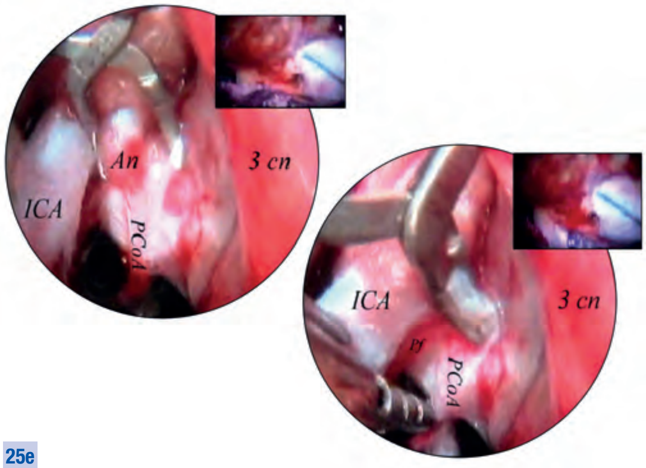

25e

The aneurysm was clipped under direct endoscopic vision while preserving the integrity of the perilesional vasculature.

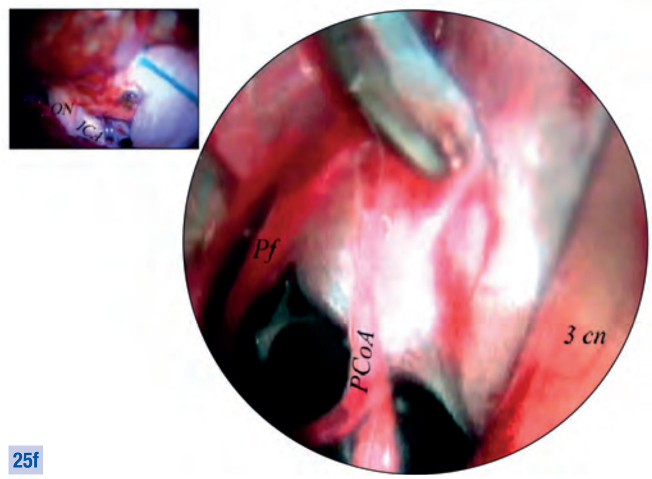

25f

By comparing endoscopic and microsurgical views, the clear superiority of the endoscopic control could be demonstrated in this particular case.

Comment to Case 15

EAM allowed definitive clipping of the lesion without compromising the integrity of a small perforator and hypoplastic, but functional PCoA, eliminating the need for any mobilization and manipulation of the parental ICA.

Key to Acronyms (Figs. 25e–f):

3 cn	oculomotor nerve	**ON**	optic nerve
An	aneurysm	**PCoA**	posterior communicating artery
ICA	internal carotid artery	**Pf**	perforator

Case 16 (Figs. 26a–f)

Aneurysm of the Posterior Wall of the right ICA at the Junction with the Anterior Choroidal Artery

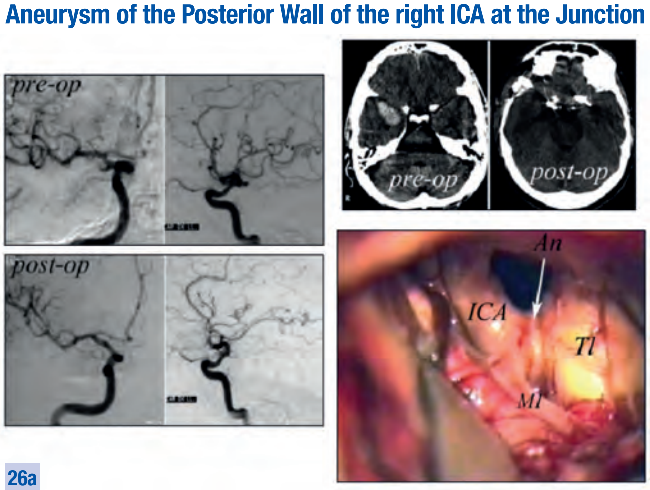

26a

Pre- and post-operative angiography and pre- and post-operative CT scans (not contrast-enhanced) of an aneurysm of the right carotid siphon at the level of the anterior choroidal artery, which had provoked a small intraparenchymal temporal hematoma, treated surgically at early stage: the lesion, approached through a pterional approach, appeared embedded into the temporal parenchyma.

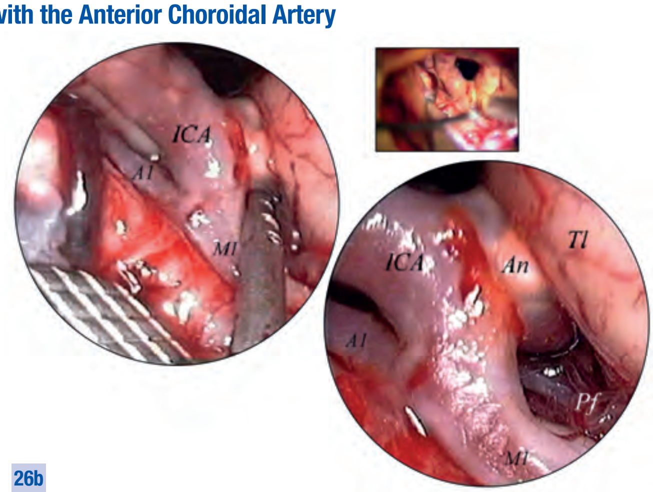

26b

A 0°-scope (28162 AUA) with straight ahead view was used free-hand, providing clear vision of the numerous perforators surrounding the lesion, without any need for mobilizing neither the ICA nor the parental artery.

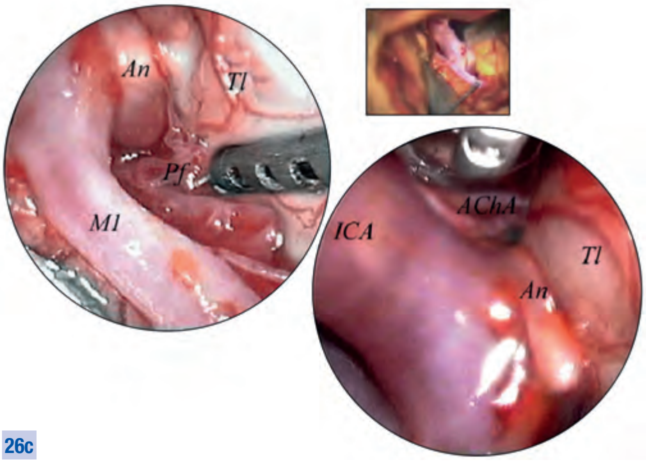

26c

Functional perforators were found both on superior and inferior aspects of the aneurysmal base.

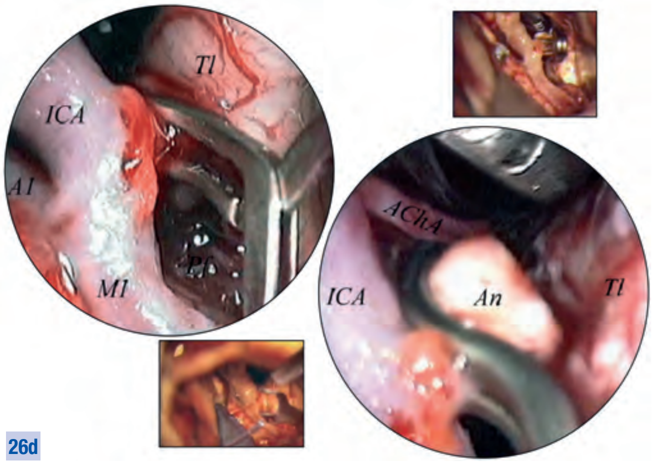

26d

The scope was attached to a mechanical holder (28272 RKB) and the aneurysm was clipped with an S-shaped clip applied under direct endoscopic control.

Key to Acronyms (Figs. 26a–f):

A1	pre-communicating segment of the anterior cerebral artery	**M1**	proximal segment of the middle cerebral artery
		Pf	perforator
AChA	anterior choroidal artery	**post-op**	post-operative
An	aneurysm	**pre-op**	pre-operative
ICA	internal carotid artery	**Tl**	temporal lobe

Comment to Case 16

EAM allowed for safe clipping of the lesion, treated surgically in the acute phase, without any mobilization of the parental vessel and of the lesion itself. In this way, the risk of intraoperative rupture was prevented without compromising the integrity of the anterior choroidal artery and other critical perforators adjacent to the lesion.

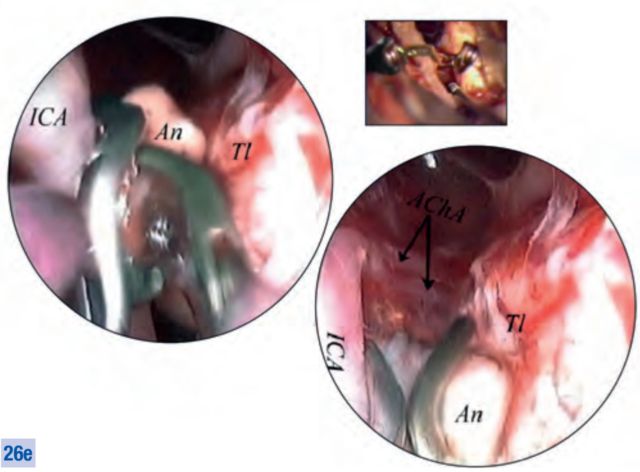

26e

The second clip was placed onto the other in a tandem fashion to achieve complete occlusion of the aneurysm neck without compromising the integrity of the anterior choroidal artery, arising below the implant base of the aneurysm and giving rise to two different branches immediately after its origin.

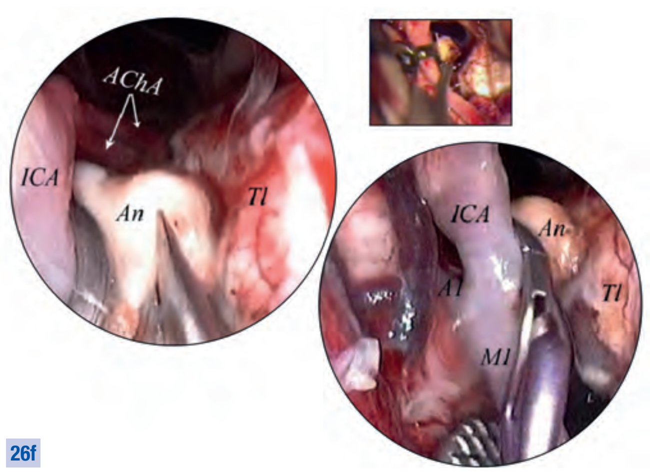

26f

Upon definitive clipping of the aneurysm, the sac was opened with microscissors and the lesion was mobilized from the parenchyma of the temporal lobe.

Case 17 (Figs. 27a–h), continued overleaf

continued overleaf

Multiple Aneurysms of the Left Anterior Circulation

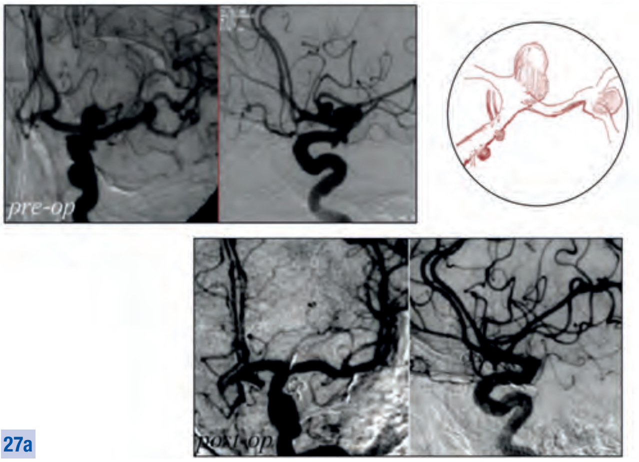

27a

Pre- and post-operative angiography and illustrative sketch of the situation of a patient harbouring an aneurysm of the left ACM, an aneurysm of the bifurcation of the and two small aneurysms in the posterior wall of the ICA, one at the level of the PCoA and the other at the level of the AChA. The lesions were approached via a left pterional approach in the acute phase (5 hours after bleeding); the ICA bifurcation aneurysm was responsible for the hemorrhage; post-operative angiography confirmed the integrity of a large perforator, originating at the level of the clip excluding the ICA bifurcation aneurysm, and also demonstrated the integrity of both the hypotrophic PCoA and AChA at the level of the clipped lesions.

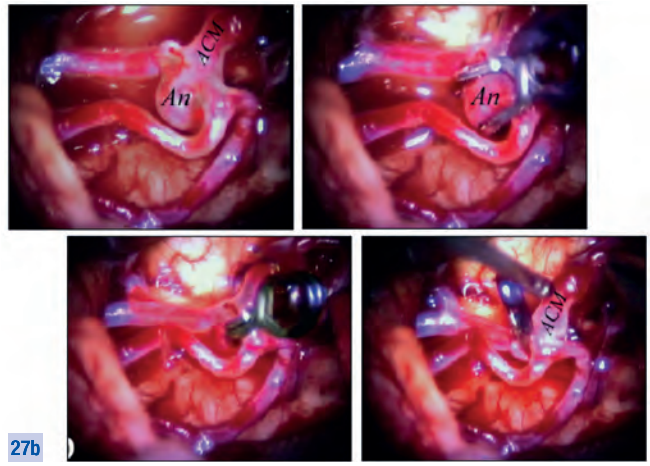

27b

The ACM aneurysm was clipped employing a fully microsurgical technique.

Key to Acronyms (Figs. 27a–d):

3 cn	oculomotor nerve	**ICA**	internal carotid artery
AChA	anterior choroidal artery	**P1**	pre-communicating segment of the posterior cerebral artery
ACM	middle cerebral artery		
An	aneurysm	**post-op**	post-operative
ICA bif	bifurcation of the internal carotid artery	**pre-op**	pre-operative

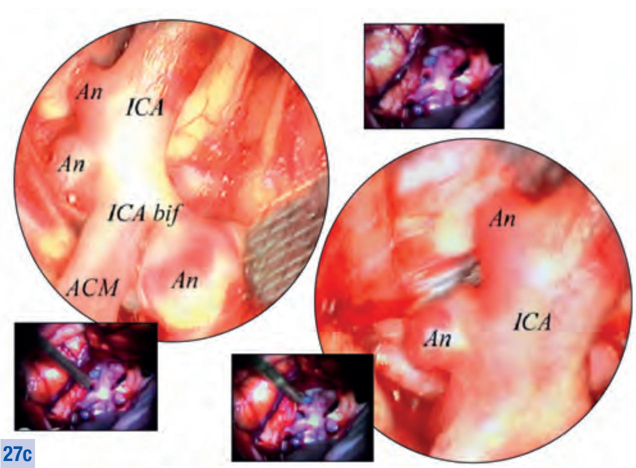

27c

An upward oriented 30°-scope (28162 BOA) was used to explore the situation of the left ICA, demonstrating the lesions much clearer than under pure microsurgical vision.

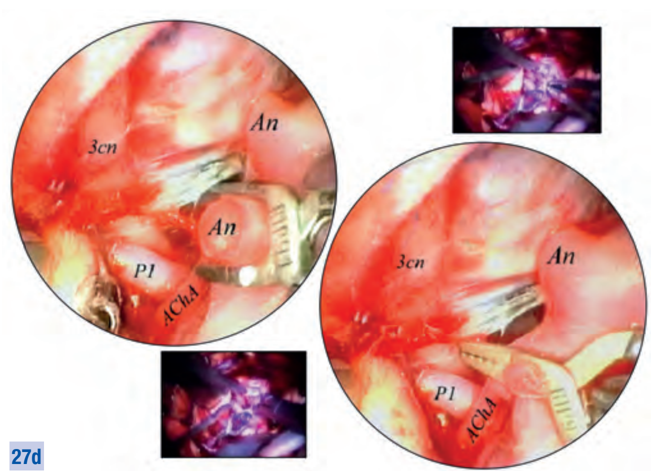

27d

The scope was attached to a mechanical holder (28272 RKB) in a position, not impeding microsurgical maneuvers, and …

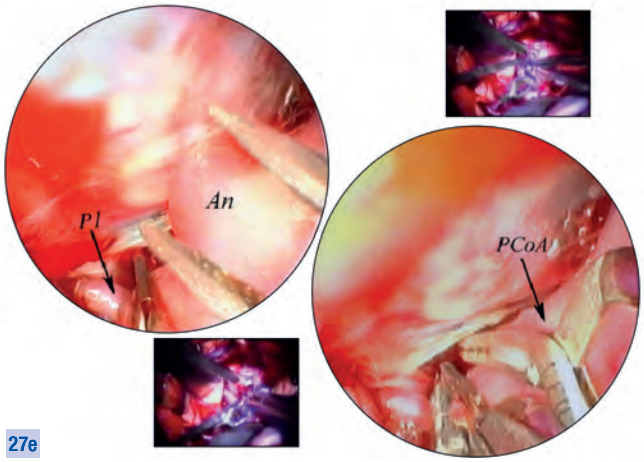

27e

… the small aneurysms, located at the level of the AChA and PCoA, were clipped under endoscopic control.

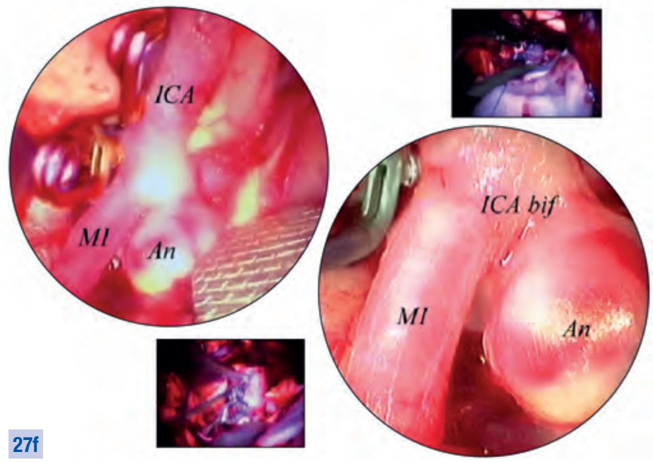

27f

Next, the position of the scope was changed to visualize the ICA bifurcation aneurysm, …

Key to Acronyms (Figs. 27e–h):

ACoA	anterior communicating artery	**M1**	proximal segment of the middle cerebral artery
An	aneurysm	**PCoA**	posterior communicating artery
Ha	Heubner artery	**Pf**	perforators
ICA bif	bifurcation of the internal carotid artery	**P1**	pre-communicating segment of the posterior cerebral artery
ICA	internal carotid artery		

Comment to Case 17

EAM allowed for safe clipping of the lesions with minimal mobilization of the left ICA, preserving all perforators; obviously EAM was not used to surgically manage the aneurysm of the ACM because this superficial lesion does not require this methodology to be treated safely.

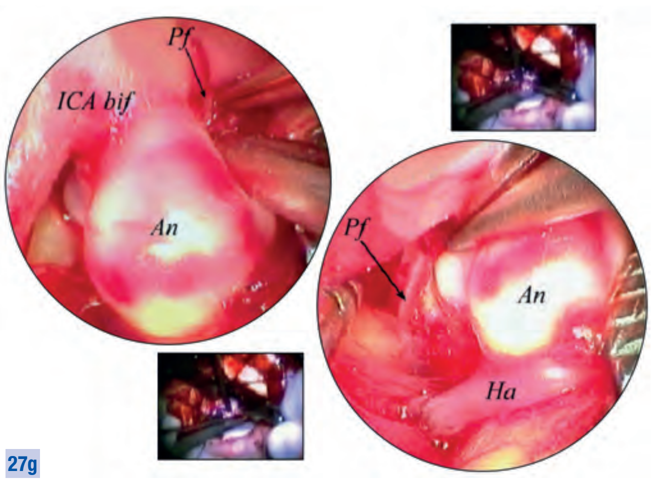

27g

… and again, the mechanical holder (28272 RKB) was used to firmly secure the scope in place: the perforators located medially and laterally to the sac (not visible under pure microscopic vision), as well as a large branch (presumably, the left Heubner artery), strictly adherent to the aneurysmal sac, were safely inspected with minimal mobilization of the sac and parental artery.

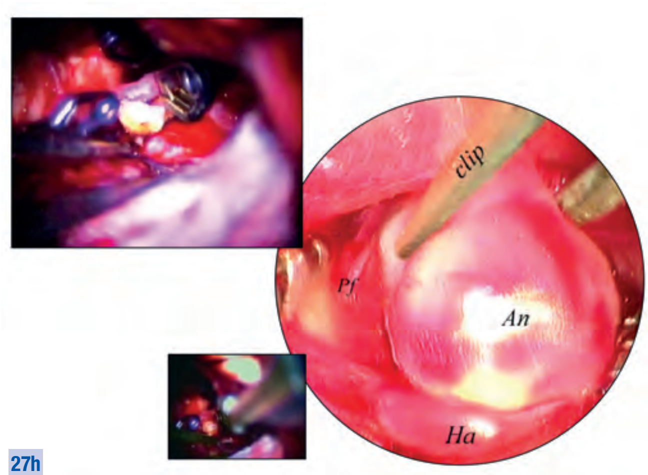

27h

The aneurysm was clipped under direct endoscopic control.

Case 18 (Figs. 28a–h)
Multiple Aneurysms of the Anterior Circulation

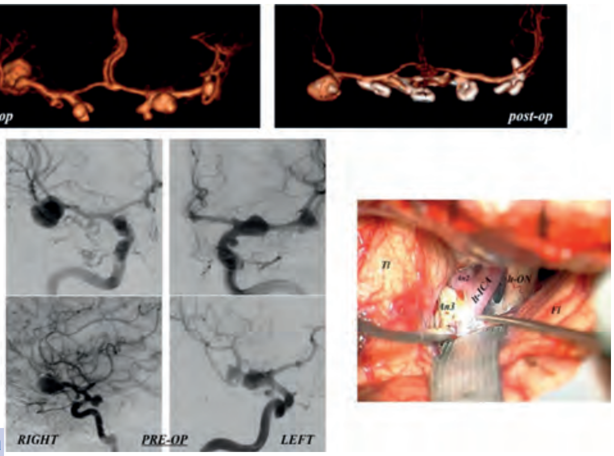

28a

Pre- and post-operative angio-CT 3D recons and pre-operative angiograms of a patient harbouring six unruptured aneurysms of the anterior circulation: an aneurysm of the left middle cerebral artery bifurcation, two aneurysms of the postero-lateral wall of the left internal carotid artery (one at the level of the posterior communicating artery and one at the level of the anterior choroidal artery), an aneurysm of the posterior wall of the right internal carotid artery at the level of the posterior communicating artery, an aneurysm of the proximal tract of the right middle cerebral artery, and an aneurysm of the right middle cerebral artery bifurcation. The patient underwent a standard pterional approach from the left side to treat five aneurysms (the right middle cerebral artery bifurcation aneurysm that was treated in a further procedure via a right pterional craniotomy after eight months – not showed in this case illustration).

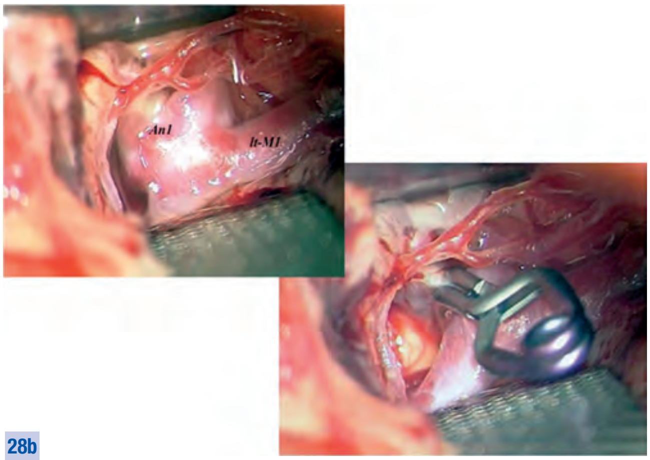

28b

After sylvian fissure opening, the left middle cerebral artery anuerysm was clipped with pure microsurgical techniques.

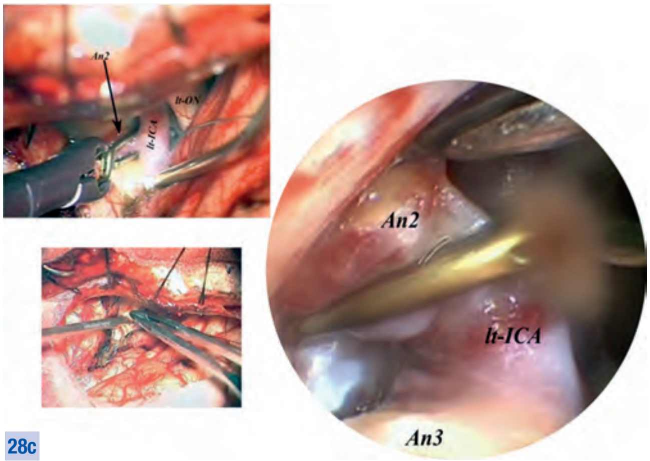

28c

Hereafter, under microscopic vision, a clip was applied to the left ICA/PComA aneurysm. A straight 0°-scope (28162 AUA) was used free-hand to check clip positioning. Endoscopic vision clearly showed that a small remnant of the neck was not included in the clipping.

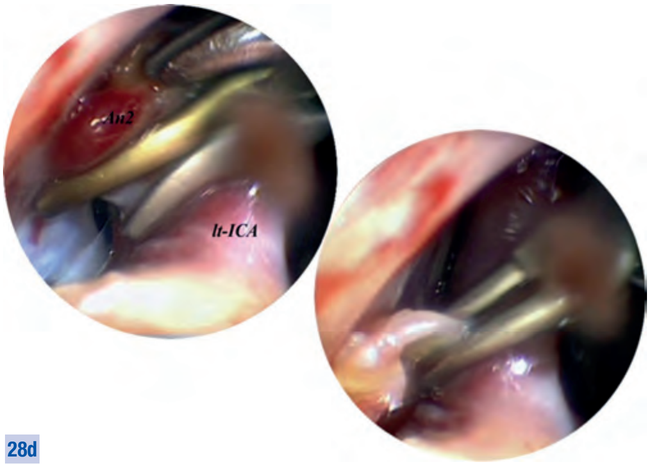

28d

The scope was fixed to a mechanical holder (28272 RKB) and the clip was repositioned under endoscopic control to completely exclude the implant base.

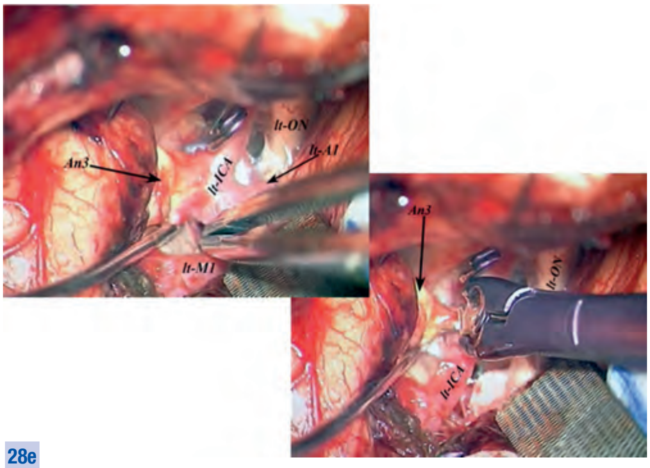

28e

The left ICA/AChA aneurysm was clipped using microsurgical techniques.

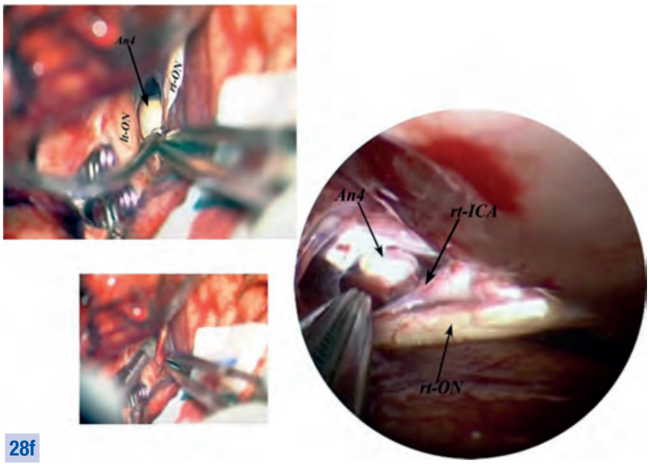

28f

The dissection was continued towards the contralateral side. Passing between the left and the right optic nerves, the right ICA/PComA aneurysm was reached. To avoid excessive manipulation and retraction of the optic nerves, a straight 0°-scope (28162 AUA) was inserted free-hand to inspect the region.

Key to Acronyms (Figs. 28a–h):

A1	pre-communicating segment of the anterior cerebral artery	**art**	temporal branch arising from the proximal tract of the right middle cerebral artery
An1	left middle cerebral artery bifurcation aneurysm	**ICA**	internal carotid artery
An2	left internal carotid artery aneurysm, at the level of the posterior communicating artery	**lt**	left
		M1	proximal segment of the middle cerebral artery
An3	left internal carotid artery aneurysm, at the level of the anterior choroidal artery	**ON**	optic nerve
		post-op	post-operative
An4	right internal carotid artery aneurysm, at the level of the posterior communicating artery	**pre-op**	pre-operative
		rt	right
An5	proximal right middle cerebral aneurysm	**Tl**	temporal lobe
Fl	frontal lobe		

Comment to Case 18

EAM allowed safe clipping of multiple aneurysms of the anterior circulation; as already stated, endoscopic assistence is useful in selected sites, such as the posterior wall of the internal carotid artery.

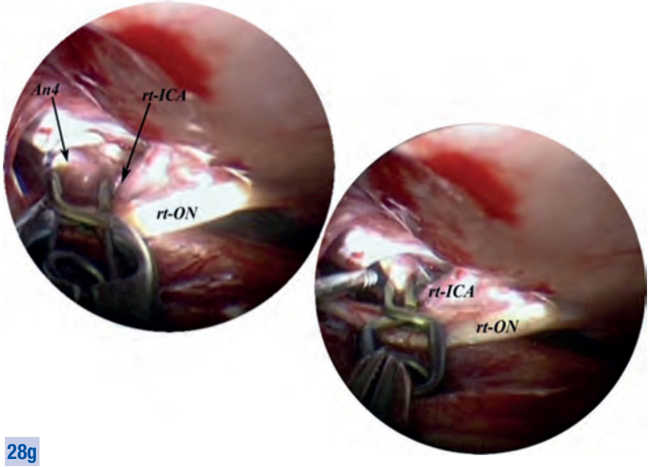

28g

The scope was thereafter fixed to a mechanical holder (28272 RKB) and the aneurysm was clipped passing under the right optic nerve with minimal traumatism of the nerve itself and of the internal carotid artery.

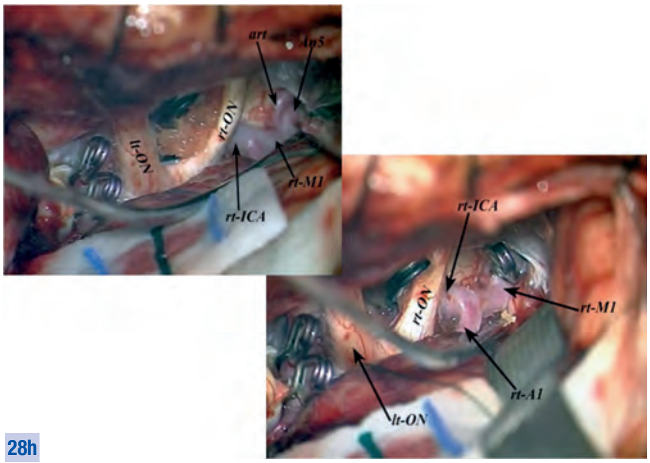

28h

The right proximal middle cerebral artery aneurysm was clipped under direct microscopic vision.

Case 19 (Figs. 29a–f, continued overleaf)
Aneurysm of the Right ACoa Complex, Previously Embolized

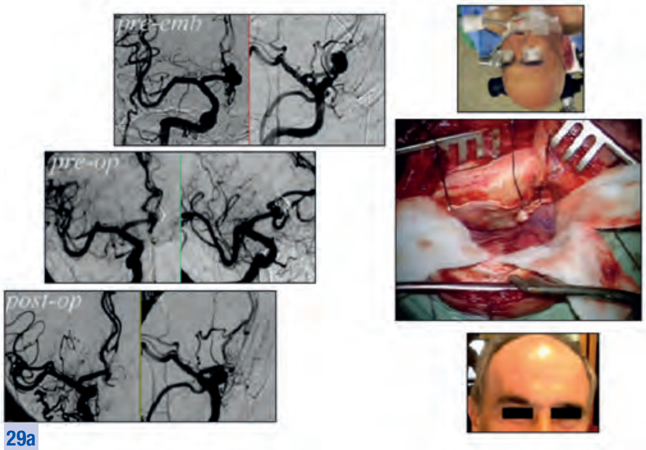

29a

Pre- and post-operative angiograms of an ACoA aneurysm originating from the right anterior cerebral artery (A1): the patient had been embolized twice (for the first time, nine months before surgery, after a subarachnoid hemorrhage, and the second time, four months before the next surgery) but had regrowth; the lesion was approached through a supraorbital eyebrow approach.

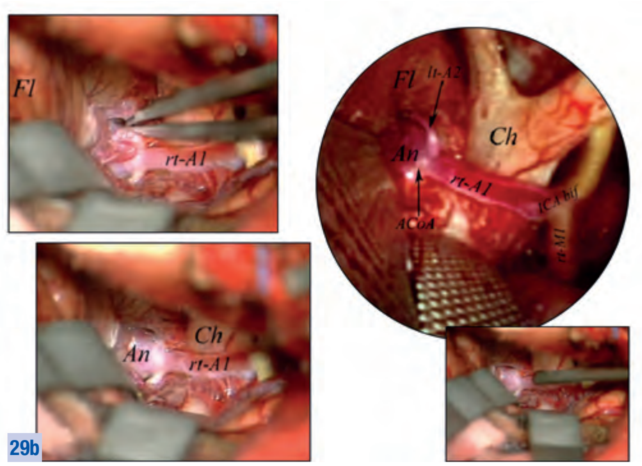

29b

After elevation of the frontal lobe, the right ICA was exposed, presenting atherosclerotic changes at the level of the bifurcation. The right ACoA was dissected to expose the lesion, which was embedded into the deep frontal parenchyma and enclosed by both right and left A2 tracts; a 0°-scope (28162 AUA) was inserted free-hand to inspect the region involved.

Key to Acronyms (Figs. 29a–d):

A1	pre-communicating segment of the anterior cerebral artery	**ICA bif**	bifurcation of the internal carotid artery
		ICA	internal carotid artery
A2	post-communicating segment of the anterior cerebral artery	**lt**	left
		M1	proximal segment of the middle cerebral artery
ACoA	anterior communicating artery	**post-op**	post-operative
An	aneurysm	**pre-emb**	pre-embolization
Ch	chiasm	**pre-op**	pre-operative
Fl	frontal lobe	**rt**	right

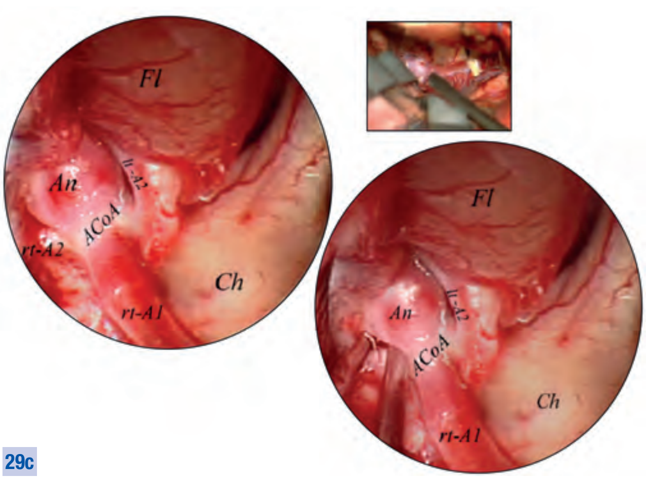

29c

The scope was attached to a mechanical holder (28272 RKB) and the right A2 tract was freed from the medial border of the aneurysm base under endoscopic control.

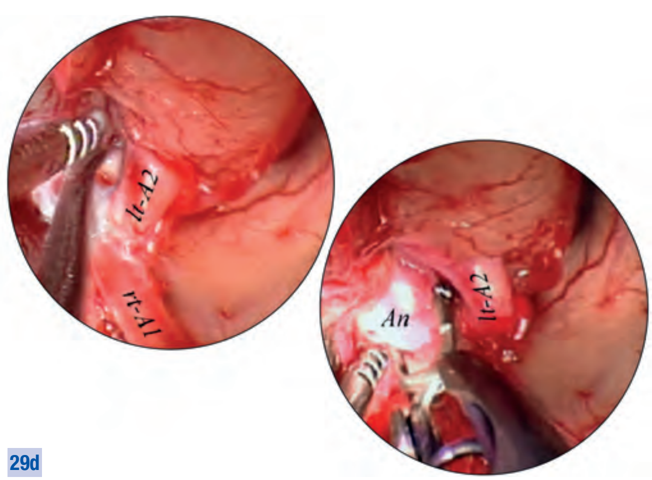

29d

Likewise, the left A2 tract, directly originating from the right A1, was dissected from the lateral border of the basal portion of the aneurysm sac, and a clip was applied under endoscopic control.

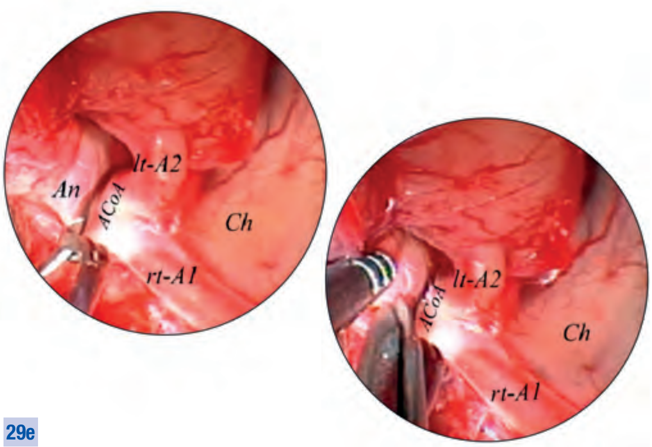

29e

After definitive clipping, the sac was opened with microscissors to confirm complete exclusion.

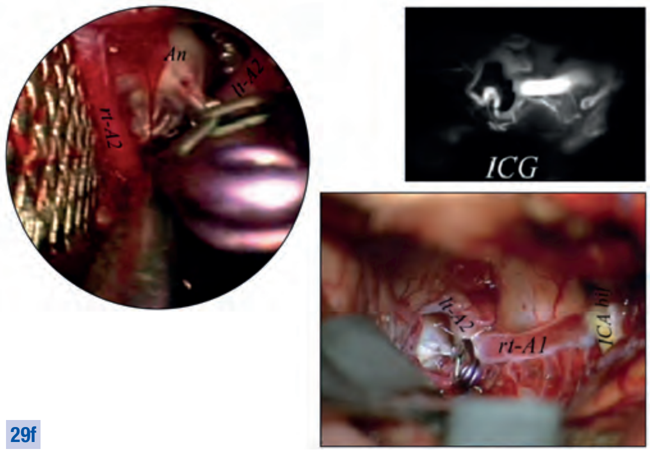

29f

Upon final endoscopic inspection with the free-hand technique complete exclusion of the lesion was demonstrated and additionally confirmed by intraoperative indocyanine green fluoroangiography (ICG).

Key to Acronyms (Figs. 29e–f):

A1	pre-communicating segment of the anterior cerebral artery	**An**	aneurysm
		Ch	chiasm
A2	post-communicating segment of the anterior cerebral artery	**ICA bif**	bifurcation of the internal carotid artery
		lt	left
ACoA	anterior communicating artery	**rt**	right

Comment to Case 19

EAM allowed safe clipping of the lesion through a minimally invasive “key-hole” approach.

Case 20 (Figs. 30a–b)
Aneurysm of the Left PCA-SCA Junctional Portion of the Basilar Artery

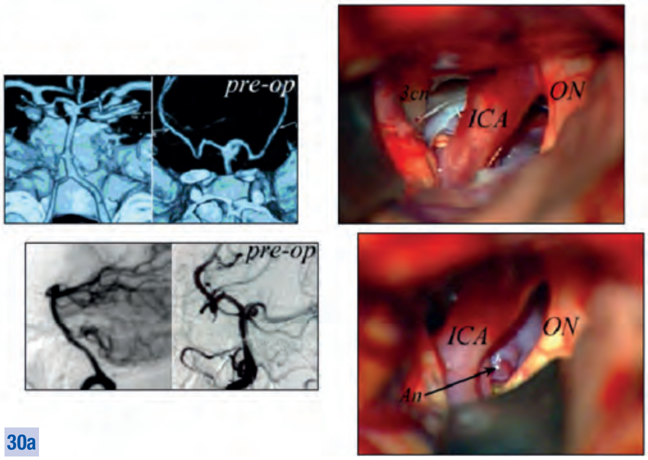

30a

Preoperative angio-CT and preoperative angiograms of the lesions, approached through a left pterional approach (the patient had been operated 1 year before. elsewhere, for a right ICA bifurcation aneurysm and was thereafter operated from the left side after a second bleeding from the distal basilar artery aneurysm).

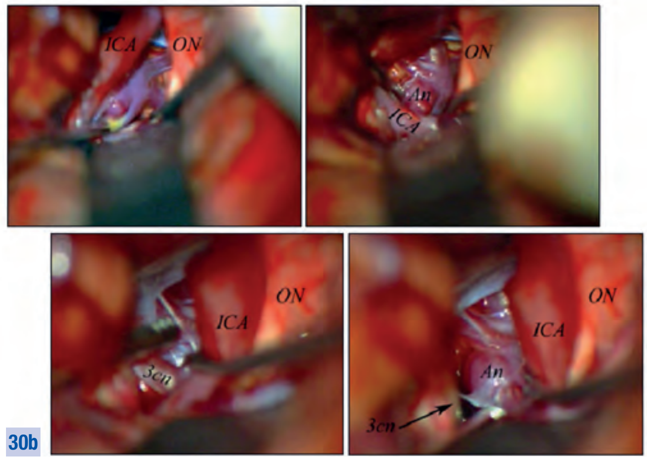

30b

Under microscopic inspection, the aneurysm was exposed, lying in the corridors between ON and ICA, and between ICA and the 3cn: both corridors appeared narrow, and exposure of the lesion required distorsion of the ICA in medial and lateral direction.

Case 20 (Figs. 30c–f) continued from page 55

Aneurysm of the Left PCA-SCA Junctional Portion of the Basilar Artery

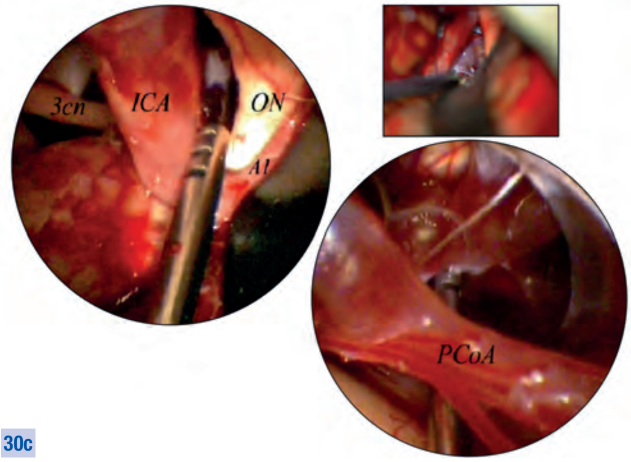

30c

A handheld upward-oriented 30°-scope (28162 BOA) was used to explore the anatomical situation: the aneurysm was mobilized under scopic control, with the micro-suction tip passing behind the PCoA.

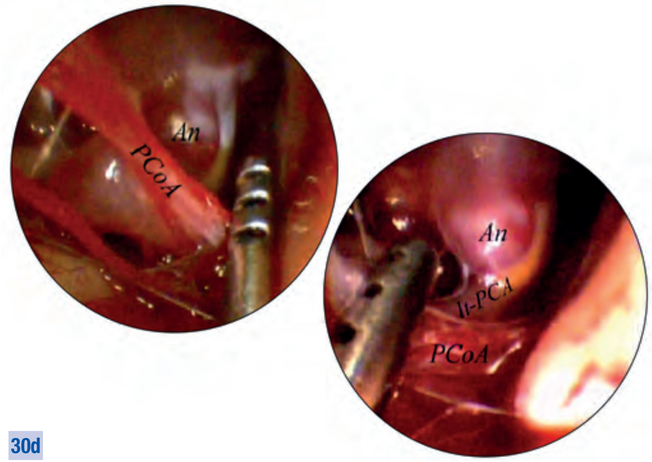

30d

With the suction tip introduced from below and in front of the PCoA, the aneurismal sac and the surrounding vascular circulation were exposed.

Key to Acronyms (Figs. 30a–f):

3 cn	oculomotor nerve	**lt**	left
A1	pre-communicating segment of the anterior cerebral artery	**ON**	optic nerve
		PCA	posterior cerebral artery
An	aneurysm	**PCoA**	posterior communicating artery
ICA	internal carotid artery	**pre-op**	pre-operative

Comment to Case 20

EAM allowed for safe clipping of the lesion, while requiring less manipulation of perilesional vascular structures.

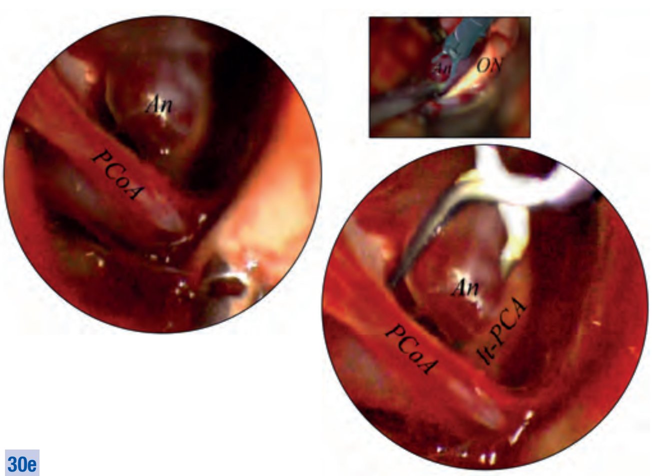

30e

The aneurysm was clipped passing the clip applier through the corridor between ON and ICA, with the scope attached to a mechanical holder (28272 RKB) for control of surgical maneuvers. Comparison between microsurgical and endoscopic views distinctly demonstrated that the endoscope provides a better view of the distal portion of the clip.

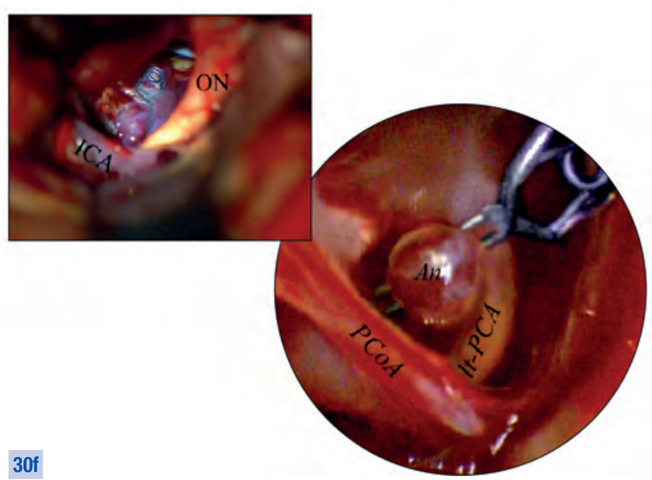

30f

The final endoscopic control allowed to confirm patency of the left PCA which was not clearly visible under the microscope.

Case 21 (Figs.31a–c)
Very Large Thrombosed Aneurysm of the Left PCA-SCA

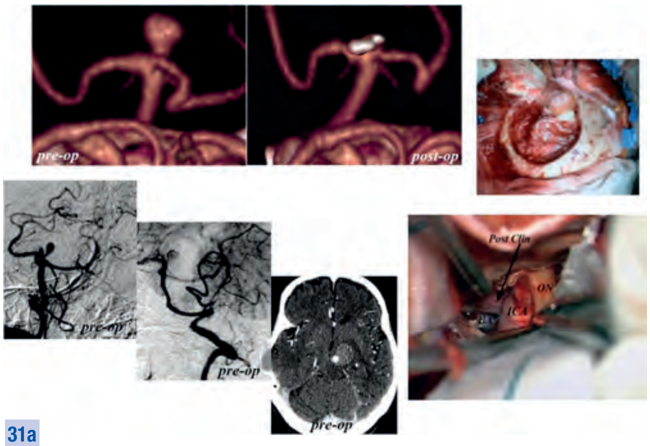

31a

Preoperative angio-CT scan and 3D reconstruction, preoperative angiograms, post-operative angio-CT 3D reconstruction of a very large, mostly thrombosed, unruptured left PCA-SCA aneurysm accessed via a left orbito-pterional approach.

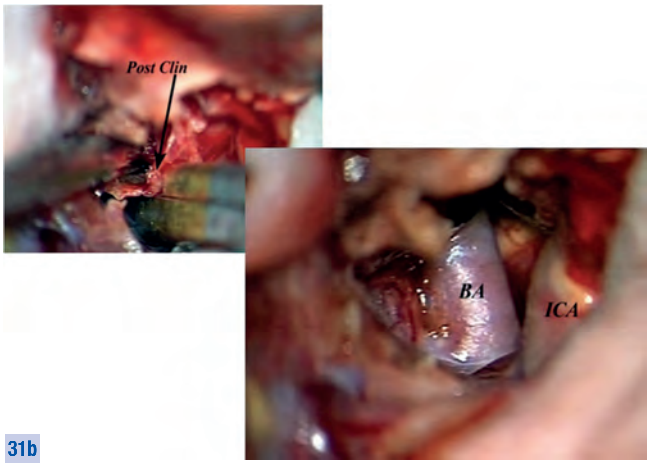

31b

The basilar top was not clearly visible until a posterior clinoidectomy was accomplished.

Key to Acronyms (Figs. 31a–c):

An	aneurysm	**PComA**	posterior communicating artery
ICA	internal carotid artery	**Post Clin**	posterior clinoidal process
BA	basilar artery	**post-op**	post-operative
lt	left	**pre-op**	pre-operative
ON	optic nerve	**rt**	right
PCA	posterior cerebral artery	**SCA**	superior cerebellar artery

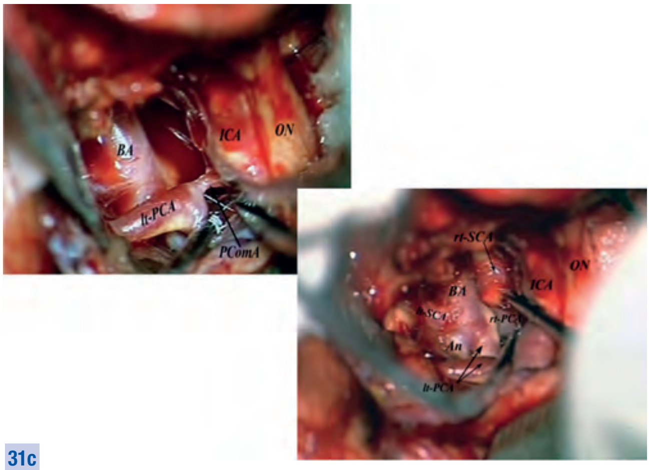

31c

The basilar artery was thereafter approached through the corridor lateral to the internal carotid artery, but the presence of a hypertrophic and anomalous posterior cerebral artery, associated with a short posterior communicating artery, necessitated excessive manipulation and retraction of the artery itself and of the internal carotid artery to visualize the implant base of the aneurysm, located at the angle between the left superior cerebellar artery and the posterior cerebral artery.

Case 21 (Figs.31d–f) continued from page 57

Very Large Thrombosed Aneurysm of the Left PCA-SCA

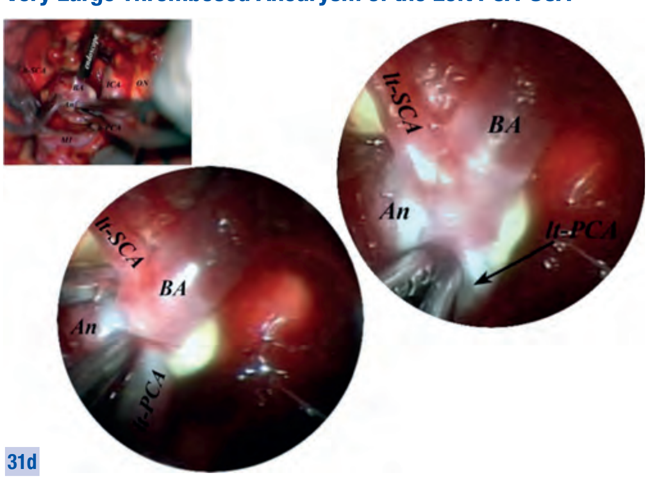

31d

A straight 0°-scope (28162 AUA) was free-hand inserted and thereafter fixed to a mechanical holder (28272 RKB) to visualize the implant base of the aneurysm and to check for any perforators.

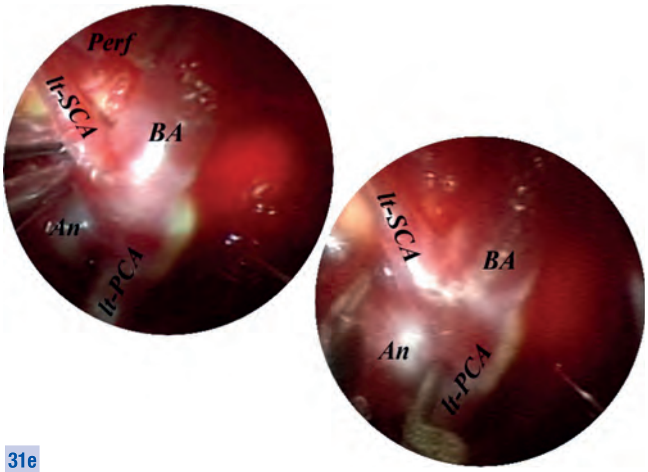

31e

In the next step, it was possible, always under endoscopic control, to place the clip directly at the neck of the aneurysm.

Comment to Case 21

EAM allowed safe clipping of the lesion avoiding undue distortion of perilesional vascular structures and obviating the need for PComA sectioning.

Key to Acronyms (Figs. 31d–f):

An	aneurysm	**ON**	optic nerve
ICA	internal carotid artery	**PCA**	posterior cerebral artery
BA	basilar artery	**Perf**	perforating arteries
ICG	intra-operative indocyanine-green videoangiography	**rt**	right
lt	left	**SCA**	superior cerebellar artery
M1	proximal tract of the middle cerebral artery		

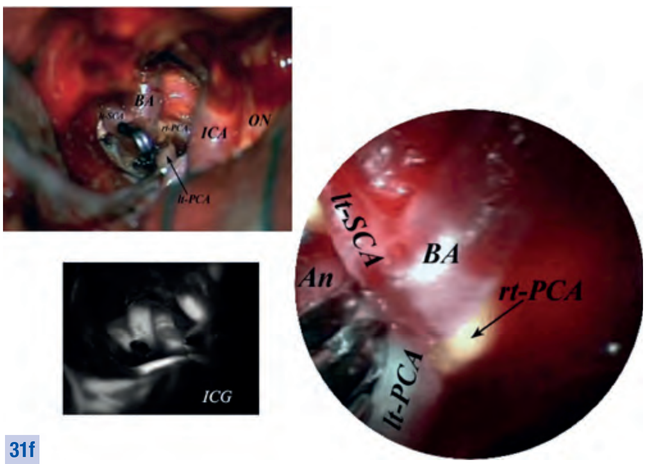

31f

Final endoscopic inspection with the free-hand technique confirmed exclusion of the sac and apparent patency of the perilesional vascular structures, as underpinned by intra-operative indocyanine-green videoangiography.

4.4 Sellar and Parasellar Lesions Approached Using the Transsphenoidal Route

This chapter is based on the senior author's experience of 97 patients who were treated surgically by using the endoscope-assisted transnasal-transsphenoidal approach, most of them for the treatment of pituitary adenomas. We perform the standard rhino-septal approach[82,83] and use endoscopy essentially to control the completeness of removal and sometimes to perform maneuvers in hidden corners not visible through the microscope[84].

Because the pituitary gland is an extra-arachnoid structure, all pituitary adenomas originate in the extra-arachnoid space and expand out of the sella distending the dural ring of the diaphragma sellae, elevating its arachnoid membrane but not penetrating it; thereafter, pituitary adenomas, regardless of size and shape, remain covered by a layer of arachnoid, occasionally markedly thick, separating them from the subarachnoid space[85]. Respect for preserving the integrity of the arachnoid membrane is essential both to protect subarachnoidal structures from undue manipulation and to prevent postoperative cerebrospinal fluid leakage. Accordingly, in most instances, the endoscopic control remains confined to the residual tumor cavity and intracranial structures are not clearly identified (**Fig. 32, Case 22**). Rarely, the dura-arachnoidal interface may be disrupted: in these cases the endoscope will clearly demonstrate the arachnoid perforation, through which the intracranial structures can be inspected (**Fig. 33, Case 23**). Apparently, craniopharyngiomas and other sellar lesions can be completely or partially intra-arachnoid and the arachnoidal plane can be prone to disruption during the procedure: in these cases the subarachnoidal anatomy comes into vision at endoscopic inspection (**Fig. 34, Case 24**).

We have performed endoscope-assisted transsphenoidal procedures with the same scopes as those used for intracranial procedures, but in most instances, they are fitted with specific irrigation and suction sheaths.

We are aware that the pure endoscopic approach may be used for the treatment of these lesions. In fact, the senior author (R.J.G.) has used this methodology in some instances but, for his experience, the standard microsurgical technique results faster and more effective, especially if the lesion is a frankly bleeding one. Accordingly to literature, endoscopic assistance to microsurgery in transsphenoidal approaches allows more effective procedures[86,87]. In any case, in the Department of Neurosurgery of L'Aquila (headed by the senior author), younger surgeons are trained and perform pure endoscopic transsphenoidal approaches using the one- or two-nostril technique [88–92].

In case of chordomas and other tumors originating from the splanchnocranial compartment, secondarily involving the skull base, and in cases of basal cerebrospinal fluid (CSF) fistulas, in the past we have used the conventional microsurgical approach, eventually endoscopically assisted. Nevertheless, in these cases we have progressively shifted to the pure endoscopic approach[93–96]. To perform these procedures we have essentially used the scopes, the irrigation and the suction sheaths normally used for other transsphenoidal EAM procedures.

Case 22 (Figs. 32a–b)
Pituitary Macroadenoma

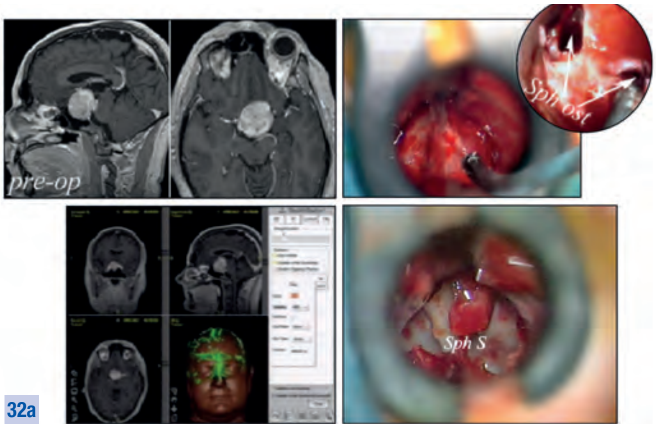

32a

Preoperative MR scan of a pituitary macroadenoma treated surgically with intraoperative neuronavigation; the scope was used during the nasal stage of the procedure to identify the sphenoid ostia, which were enlarged to enable access to the sphenoid sinus.

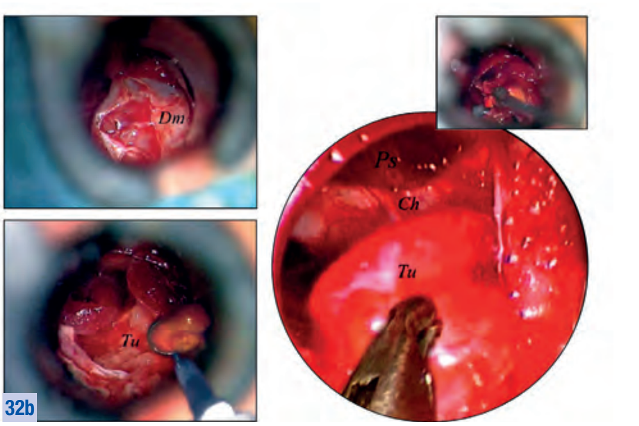

32b

After opening in a cross fashion the sellar dura mater, the tumor was evacuated under microscopic vision; the next step was performed under endoscopic assistance using the upward oriented 30°-scope (28162 BOA) to identify and remove a small remnant.

Key to Acronyms (Figs. 32a–b):

Ch	chiasm	**Sph ost**	sphenoidal ostia
Dm	dura mater	**Sph S**	sphenoid sinus
pre-op	pre-operative	**Tu**	tumor
Ps	pituitary stalk		

Comment to Case 22

EAM allowed for safer and more complete removal of the lesion.

Case 23 (Figs. 33a–b)
Pituitary Macroadenoma

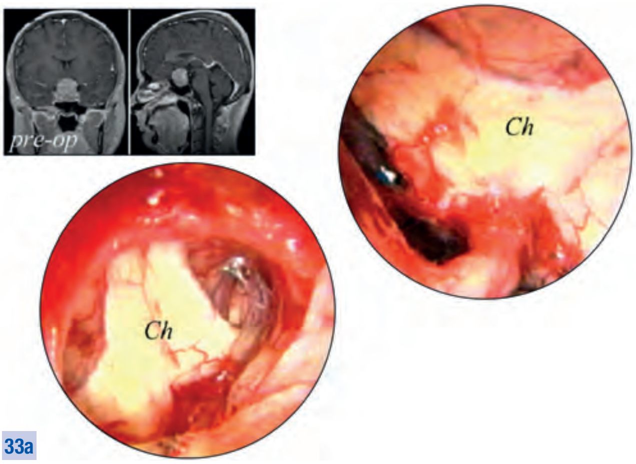

33a

Preoperative MR scans of the lesion. Upon completion of the procedure, endoscopic control with an upward-oriented 30°-scope (28162 BOA) confirmed complete excision of the lesion; …

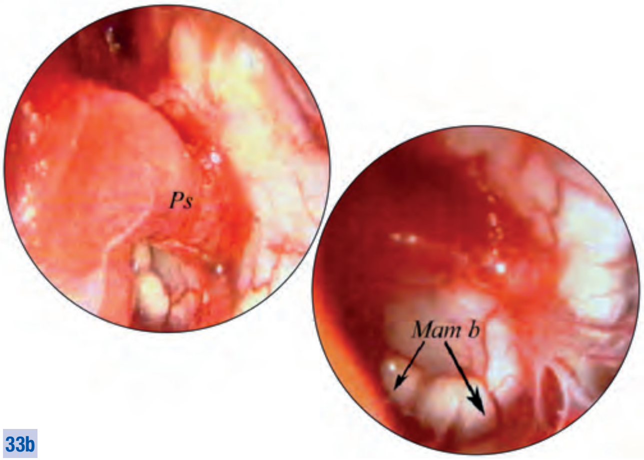

33b

… in the residual cavity the arachnoidal plane was not demonstrated and the chiasm, the pituitary stalk and the mammilary bodies were clearly shown.

Key to Acronyms (Figs. 33a–b):

Ch	chiasm	**pre-op**	pre-operative
Mam b	mammilary bodies	**Ps**	pituitary stalk

Comment to Case 23

EAM readily confirmed completeness of excision, but also provided a beautiful panoramic view of the subarachnoidal structures normally invisible when the arachnoidal plane is intact as it is in most cases.

Case 24 (Figs. 34a–b)
Intrasellar Cystic Craniopharyngioma

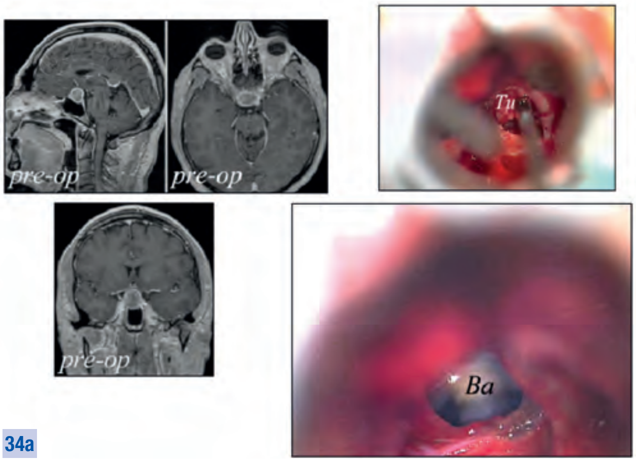

34a

Preoperative MRI scans of an intrasellar cystic craniopharyngioma approached through a rhino-septal approach; complete excision of the lesion was feasible because it was not adherent to suprasellar structures, however, at the end of excision it became obvious, that there was no clear arachnoidal interface with the subarachnoid structures. Moreover, in posterior aspects of the dura mater, a gap appeared through which the distal portion of the basilar artery could be identified.

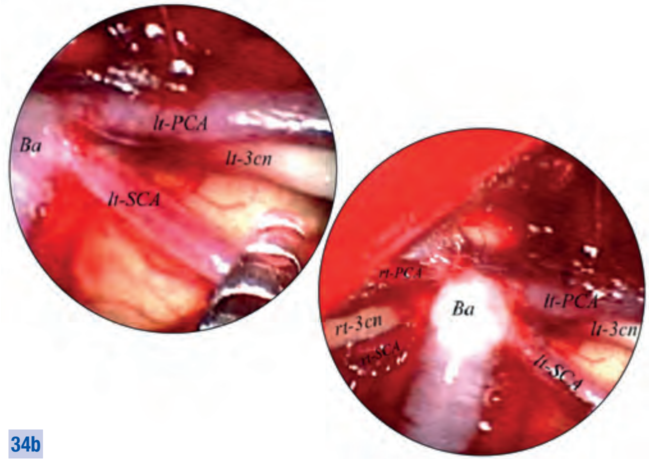

34b

An upward-oriented 30°-scope (28162 BOA) was handheld and provided a clear view of the situation demonstrating both PCA and SCA, and both 3rd cranial nerves passing between them, confirming complete excision of the lesion.

Key to Acronyms (Figs. 34a–b):

3 cn	oculomotor nerve	**pre-op**	pre-operative
Ba	basilar artery	**rt**	right
lt	left	**SCA**	superior cerebellar artery
PCA	posterior cerebral artery	**Tu**	tumor

Comment to Case 24

EAM readily confirmed completeness of excision, but also provided a beautiful panoramic view of the subarachnoidal structures normally invisible when the arachnoidal plane is intact as it is in most cases.

Case 25 (Figs. 35a–b)
Chordoma of the Anterior Splanchnocranial Cavity

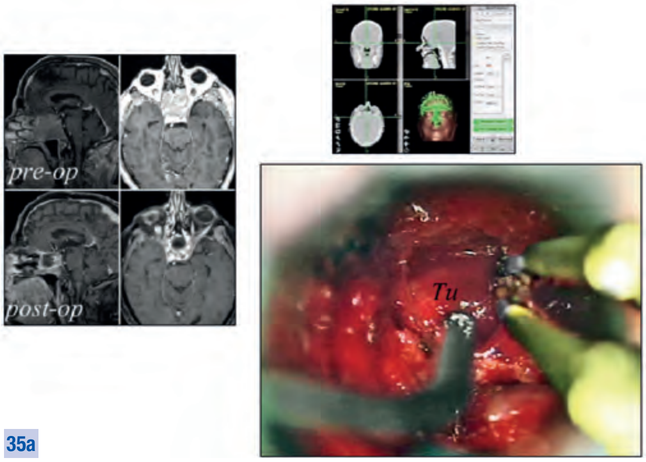

35a

Pre- and post-operative MR scans of a chordoma occupying the entire anterior splanchnocranial cavity. The lesion was treated surgically using a transnasal-transphenoidal approach, assisted by intraoperative neuronavigation. Most surgical maneuvers were performed under microscopic vision; the tumor was mainly aspirated.

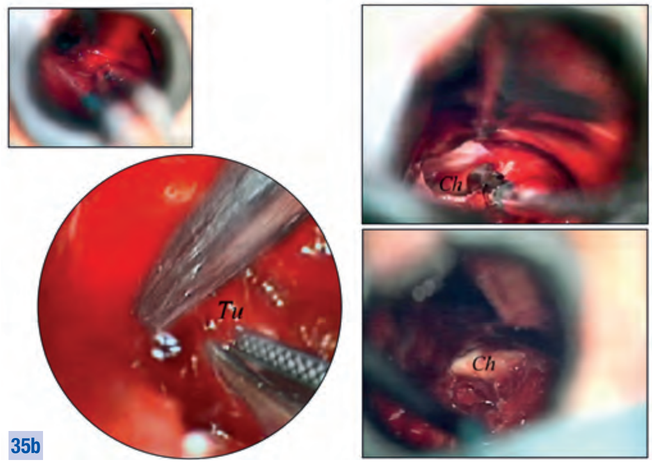

35b

Some surgical maneuvers, mainly those performed in deeply-seated borders of the operative site, were performed under endoscopic vision, using a 0°-scope (28162 AUA) with straight ahead view. In final stages of the procedure, it became evident that the tumor had created a dural gap through which, under microscopic vision, the optic chiasm was visible.

Case 25 (Figs. 35c–d) continued from page 61

Chordoma of the Anterior Splanchnocranial Cavity

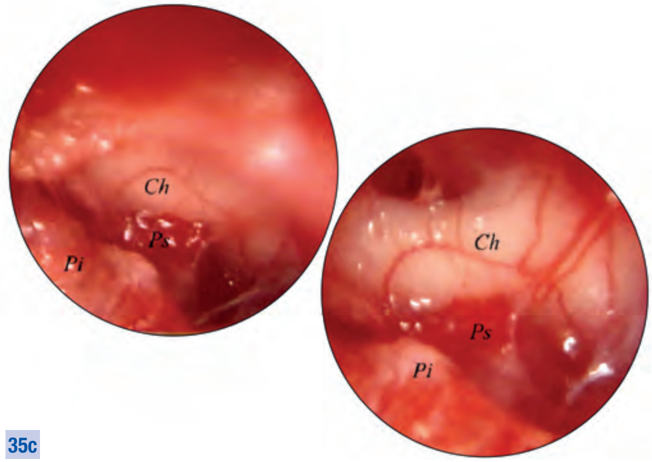

35c

Using an upward-oriented 30°-scope (28162 BOA) it was possible to visualize through the dural gap, the optic chiasm, and …

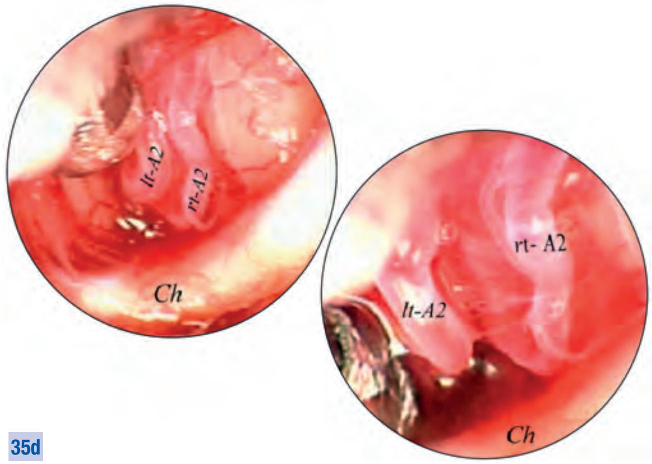

35d

… in its anterior aspects, the A2 tracts of the anterior cerebral artery, confirming complete excision of the tumor.

Comment to Case 25

EAM confirmed the apparent completeness of the exeresis but also allowed to perform some surgical maneuvers.

Key to Acronyms (Figs. 35a–d):

A2	post-communicating segment of the anterior cerebral artery	**post-op**	post-operative
		pre-op	pre-operative
Ch	chiasm	**Ps**	pituitary stalk
lt	left	**rt**	right
Pi	pituitary gland	**Tu**	tumor

Conclusions

Endoscope-assisted microneurosurgery (EAM) is a surgical methodology based on the combined and concurrent use of microsurgical and endoscopic techniques – employed with specialized instrumentation – which has proven to be particularly useful in the treatment of deeply-seated intracranial lesions. The microscope provides illumination and magnification of superficial sectors of the operative field, while the endoscope allows for improved visual control and less traumatizing surgery in deeply located sectors of the operative field.

EAM inherits the potential of reducing iatrogenic trauma and enhances efficacy of the operative procedure, occasionally allowing for less invasive approaches; it is useful in the treatment of cystic and neoplastic lesion located in the arachnoidal spaces of the anterolateral and posterior fossa cisterns and in the fourth ventricle. Besides, it is used effectively in the surgical management of neurovascular conflicts in the cerebellopontine angle and especially of intracranial aneurysms deeply located in focal arterial segments (posterior wall of the internal carotid artery siphoon, internal carotid artery bifurcation, anterior communicating artery-anterior cerebral artery complex and distal portion of the basilar artery). Endoscopic assistence has been shown to be a useful adjunct in the microsurgical treatment of pituitary neoplasms and other expansive lesions of the skull base approached through the transsphenoidal route. EAM requires the use of dedicated scopes and holders and does not require dedicated surgical instrumentation, even though a few specifically designed instruments can considerably facilitate surgical maneuvers.

Lastly, it has to be emphasized that adequate training based on cadaveric dissections and extensive use of the methodology in the operative room is mandatory to achieve adequate expertise.

References

1. APUZZO MLJ, HEIFETZ M, WEISS MH, KURZE T: Neurosurgical endoscopy using the sideviewing telescope. Technical note. J Neurosurg 16:398–400, 1977
2. HALVES E, BUSHE KA: Transsphenoidal operation on craniopharyngiomas with extrasellar extensions. The advantage of the operating endoscope [proceedings]. Acta Neurochir Suppl 28:362, 1979
3. HARDY J: La chirurgie de l'hypophyse par voie transspénoidale. Union Med Can 96:702-12, 1967
4. MATULA C, TSCHABITSCHER M, DAY JD, REINPRECHT A, KOOS WT: Endoscopically assisted microneurosurgery. Acta Neurochir (Wien) 134(3-4): 190-5, 1995
5. PERNECZKY A, FRIES G: Endoscope-assisted brain surgery: part 1-evolution, basic concept, and current technique. Neurosurgery 42(2):219-24, 1998
6. PERNECZKY A, FRIES G: Endoscope-assisted brain surgery: part 2-analysis of 380 procedures. Neurosurgery 42(2):226-31, 1998
7. PERNECZKY A, TSCHABITSCHER M, RESCH KDM: Endoscopic anatomy for neurosurgery. Georg Thieme Verlag, Stuttgart, 1993
8. PERNECZKY A, MULLER-FORELL W, VAN LINDERT E, FRIES G: Keyhole concept in neurosurgery. Georg Thieme Verlag, Stuttgart, 1999
9. HOPKINS HH: Optical principles of the endoscope. In: Berci G (ed). Endoscopy. Appleton- Century-Crofts, New York, 1976
10. LINDER TE, SIMMEN D, STOOL SE: Revolutionary inventions in the 20th century. The history of endoscopy. Arch Otolaryngol Head Neck Surg 123: 1161-3, 1997
11. COCKETT WS, COCKETT ATK: The Hopkins rod-lens system and the Storz cold light illumination system. Urology 51(Suppl 5A):1-2, 1998
12. SCHROEDER HWS, GAAB MR: Intracranial endoscopy. Neurosurg Focus 6(4):E1, 1999
13. PIETRABISSA A, SCARCELLO E, CAROBBI A, MOSCA F: Three-dimensional versus two-dimensional video system for the trained endoscopic surgeon and the beginner. Endosc Surg Allied Technol 2(6):315-7, 1994
14. HOFMEISTER J, FRANK TG, CUSCHIERI A, WADE NJ: Perceptual aspects of two-dimensional and stereoscopic display techniques in endoscopic surgery: review and current problems. Semin Laparosc Surg 8(1): 12-24, 2001
15. RIEGEL T, HELLWIG D, BAUER BL, MENNEL HD: Endoscopic anatomy of the third ventricle. Acta Neurochir Suppl 61:54-6, 1994
16. RESCH KD, PERNECZKY A, TSCHABITSCHER M, KINDEL S: Endoscopic anatomy of the ventricles. Acta Neurochir Suppl 61:57-61, 1994
17. VINAS FC, DUJOVNY N, DUJOVNY M: Microanatomical basis for the third ventriculostomy. Minim Invasive Neurosurg 39(4):116-21, 1996
18. DECQ P, LE GUERINEL C, SOL JC, PALFI S, DJINDJIAN M, NGUYEN JP: Endoscopic anatomy of the third ventricle. Neurochirurgie 46(3):203-8, 2000
19. DECQ P: Endoscopic ventricular anatomy. Morphologie 89(284):12-21, 2005
20. LONGATTI P, FIORINDI A, PERIN A, MARTINUZZI A: Endoscopic anatomy of the cerebral aqueduct. Neurosurgery 61(3):1-5, 2007
21. LONGATTI P, FIORINDI A, FELETTI A, D'AVELLA D, MARTINUZZI A: Endoscopic anatomy of the fourth ventricle. J Neurosurg 109(3):530-5, 2008
22. TSCHABITSCHER M, GALZIO G: Endoscopic Anatomy along the transnasal approach to the pituitary gland and the surrounding structures. In "Endoscopic Endonasal Transsphenoidal Surgery" , de Divitiis E, Cappabianca P (Eds), Springer, Wien New York, 2003, pp 21-39
23. CAVALLO LM, CAPPABIANCA P, GALZIO R, IACONETTA G, DE DIVITIIS E, TSCHABITSCHER M: Endoscopic transnasal approach to the cavernous sinus versus transcranial route: anatomic study. Neurosurgery 56(2):379-89, 2005
24. CAVALLO LM, DE DIVITIIS O, AYDIN S, MESSINA A, ESPOSITO F, IACONETTA G, TALAT K, CAPPABIANCA P, TSCHABITSCHER M: Extended endoscopic endonasal transsphenoidal approach to the suprasellar area: anatomic considerations-part 1. Neurosurgery 61(3):24-33, 2007

25. KASSAM AB, SNYDERMAN CH et al.: The Expanded Endonasal Approach to the Ventral Skull Base: Sagittal Plane. Verlag Endo:Press® Tuttlingen, Germany, 2007
26. CASTELNUOVO P: Endoscopic Cadaver Dissection for Teaching Anterior Skull Base Surgery – An Anatomic-Operative Tutorial on Advanced Techniques of Endoscopic Anterior Skull Base Surgery. Verlag Endo:Press® Tuttlingen, Germany, 2004
27. CAPPABIANCA P, CAVALLO LM, DE DIVITIIS E: Endoscopic Pituitary Surgery – Anatomy and Surgery of the Transsphenoidal Approach to the Sellar Region. Verlag Endo:Press® Tuttlingen, Germany, 2004
28. O'DONOGHUE GM, O'FLYNN P: Endoscopic anatomy of the cerebellopontine angle. Am J Otol 14(2):122-5, 1993
29. M.TSCHABITSHER, R.GALZIO: Central skull base anatomy as seen through the endoscope. In "Cavernous Sinus. A Multidisciplinary Approach to Vascular and Tumorous Lesions", V.V. Dolenc (Ed.), Springer, Wien New York, 2009
30. FROELICH SC, ABDEL AZIZ KM, COHEN PD, VAN LOVEREN HR, KELLER JT: Microsurgical and endoscopic anatomy of Liliequist's membrane: a complex and variable structure of the basal cisterns. Neurosurgery 63(1):ONS1-8, 2008
31. CAPPABIANCA P, CAVALLO LM, ESPOSITO F, DE DIVITIIS E, TSCHABITSCHER M: Endoscopic examination of the cerebellar pontine angle. Clin Neurol Neurosurg 104(4):387-91, 2002
32. MATULA C, REINPRECHT A, ROESSLER K, TSCHABITSCHER M, KOOS WT: Endoscopic exploration of the IVth ventricle. Minim Invasive Neurosurg 39(3): 86-92, 1996
33. REISCH R, PERNECZKY A, FILIPPI R: Surgical technique of the supraorbital key-hole craniotomy. Surg Neurol 59:223–227, 2003
34. VAN LINDERT E, PERNECZKY A, FRIES G, PIERANGELI E: The supraorbital keyhole approach to supratentorial aneurysms: Concepts and technique. Surg Neurol 49:481–490, 1998
35. International Anatomical Terminology. FCAT, Federative Commitee on Anatomical Terminology, Thieme Stuttgart, New York, 1998
36. TANEDA M, KATO A, YOSHIMINE T, HAYAKAWA: Endoscopic-image display system mounted on the surgical microscope.Minim Invas Neurosurg 38:85-86, 1995
37. VAN LINDERT EJ, GROTENHUIS JA, BEEMS T: The use of a head-mounted display for visualization in neuroendoscopy. Comput Aided Surg 9(6):251-6, 2004
38. VAN KOESVELD JJ, TETTEROO GW, DE GRAAF EJ: Use of head-mounted display in transanal endoscopic microsurgery. Surg Endosc. 17(6):943-6, 2003
39. CHEN JC, MOFFITT K, LEVY ML: Head-mounted display system for microneurosurgery. Stereotact Funct Neurosurg. 68:25-32, 1997
40. TEO C: Endoscopy Allows a Keyhole Approach to Many Skull Base Tumors. Neurosurgery 43(3):713, 1998
41. KASSAM A, HOROWITZ M, WELCH W, SCLABASSI R, CARRAU R, SNYDERMAN C, HIRSCH B: The role of endoscopic assisted microneurosurgery (image fusion technology) in the performance of neurosurgical procedures. Minim Invasive Neurosurg 48(4):191-6, 2005
42. BADIE B, BROOKS N, SOUWEIDANE MM: Endoscopic and minimally invasive microsurgical approaches for treating brain tumor patients. J Neurooncol 69(1-3):209-19, 2004
43. KADRI H, MAWLA AA: Endoscopy-assisted microsurgical total resection of craniopharyngioma in childhood. Minim Invasive Neurosurg 49(6):369-72, 2006
44. MAGNAN J, CHAYS A, CACES F, LEPETRE C, COHEN JM, BELUS JF, BRUZZO M: Apport de l'endoscopie de l'angle ponto-cerebelleux par voie retrosigmoide. Ann Otolaryngol Chir Cervicofac. 110(5):259-65, 1993
45. MAGNAN J, CHAYS A, LEPETRE C, PENCROFFI E, LOCATELLI P: Surgical perspectives of endoscopy of the cerebellopontine angle. Am J Otol. 15(3): 366-70. 1994
46. SCHROEDER HW, OERTEL J, GAAB MR: Endoscope-assisted microsurgical resection of epidermoid tumors of the cerebellopontine angle. J Neurosurg 101(2):227-32, 2004

47. DE DIVITIIS O, CAVALLO LM, DAL FABBRO M, ELEFANTE A, CAPPABIANCA P: Freehand dynamic endoscopic resection of an epidermoid tumor of the cerebellopontine angle: technical case report. Neurosurgery 61 (5 Suppl 2): E239-40, 2007
48. CHARALAMPAKI P, FILIPPI R, WELSCHEHOLD S, CONRAD J, PERNECZKY A: Tumors of the lateral and third ventricle: removal under endoscope-assisted keyhole conditions. Neurosurgery 57(4 Suppl):302-11, 2005
49. SOUWEIDANE MM: Endoscopic surgery for intraventricular brain tumors in patients without hydrocephalus. Neurosurgery 57(4 Suppl):312-8, 2005
50. CHARALAMPAKI P, FILIPPI R, WELSCHEHOLD S, CONRAD J: Endoscopic and endoscope-assisted neurosurgical treatment of suprasellar arachnoidal cysts (Mickey Mouse cysts). Minim Invasive Neurosurg 48(5):283-8, 2005
51. TIRAKOTAI W, HELLWIG D, BERTALANFFY H, RIEGEL T: The role of neuroendoscopy in the management of solid or solid-cystic intra- and periventricular tumours. Childs Nerv Syst 23(6):653-8, 2007
52. CAPPABIANCA P, CINALLI G, GANGEMI M, BRUNORI A, CAVALLO LM, DE DIVITIIS E, DECQ P, DELITALA A, DI ROCCO F, FRAZEE J, GODANO U, GROTENHUIS A, LONGATTI P, MASCARI C, NISHIHARA T, OI S, REKATE H, SCHROEDER HW, SOUWEIDANE MM, SPENNATO P, TAMBURRINI G, TEO C, WARF B, ZYMBERG ST: Application of neuroendoscopy to intraventricular lesions. Neurosurgery 62 Suppl 2:575-97, 2008
53. TAMBURRINI G, D'ANGELO L, PATERNOSTER G, MASSIMI L, CALDARELLI M, DI ROCCO C: Endoscopic management of intra and paraventricular CSF cysts. Childs Nerv Syst 23(6):645-51, 2007
54. HOPF NJ, PERNECZKY A: Endoscopic neurosurgery and endoscope-assisted microneurosurgery for the treatment of intracranial cysts. Neurosurgery 43: 1330-1337, 1998
55. PRADILLA G, JALLO G: Arachnoid cysts: case series and review of the literature. Neurosurg Focus 15;22(2):E7, 2007
56. ABDEEN K, KATO Y, KIYA N, YOSHIDA K, KANNO T: Neuroendoscopy in microvascular decompression for trigeminal neuralgia and hemifacial spasm: technical note. Neurol Res. 22(5):522-6, 2000
57. JARRAHY R, BERCI G, SHAHINIAN HK: Endoscope-assisted micro-vascular decompression of the trigeminal nerve. Otolaryngol Head Neck Surg. 123(3):218-23, 2000
58. BADR-EL-DINE M, EL-GAREM HF, TALAAT AM, MAGNAN J: Endoscopically assisted minimally invasive microvascular decompression of hemifacial spasm. Otol Neurotol. 23(2):122-8, 2002
59. EL-GAREM HF, BADR-EL-DINE M, TALAAT AM, MAGNAN J: Endoscopy as a tool in minimally invasive trigeminal neuralgia surgery. Otol Neurotol. 23(2): 132-5, 2002
60. BALANSARD CHF, MELLER R, BRUZZO M, CHAYS A, GIRARD N, MAGNAN J: Nèvralgie du trijumeau: resultats de la decompression vasculaire micro-chirurgicale et endoscopique. Ann Otolaryngol Chir Cervicofac 120(6):330-7, 2003
61. MIYAZAKI H, DEVEZE A, MAGNAN J: Neuro-otologic surgery through minimally invasive retrosigmoid approach: endoscope assisted microvascular decompression, vestibular neurotomy, and tumor removal. Laryngoscope. 115(9):1612-7, 2005
62. TEO C, NAKAJI P, MOBBS RJ: Endoscope-assisted microvascular decompression for trigeminal neuralgia: technical case report. Neurosurgery 59(4 Suppl 2):ONSE489-90, 2006
63. CHEN MJ, ZHANG WJ, YANG C, WU YQ, ZHANG ZY, WANG Y: Endoscopic neurovascular perspective in microvascular decompression of trigeminal neuralgia. J Craniomaxillofac Surg. 36(8):456-61, 2008
64. EBY JB, CHA ST, SHAHINIAN HK: Fully endoscopic vascular decompression of the facial nerve for hemifacial spasm. Skull Base. 11(3):189-97, 2001
65. JARRAHY R, EBY JB, CHA ST, SHAHINIAN HK: Fully endoscopic vascular decompression of the trigeminal nerve. Minim Invasive Neurosurg 45(1):32-5, 2002
66. KABIL MS, EBY JB, SHAHINIAN HK: Endoscopic vascular decompression versus microvascular decompression of the trigeminal nerve. Minim Invasive Neurosurg. 48(4):207- 12, 2005

67. ARTZ GJ, HUX FJ, LAROUERE MJ, BOJRAB DI, BABU S, PIEPER DR: Endoscopic vascular decompression. Otol Neurotol. 29(7):995-1000, 2008
68. KING WA, WACKYM PA, SEN C, MEYER GA, SHIAU J. DEUTSCH H: Adjunctive use of endoscopy during posterior fossa surgery to treat cranial neuropathies. Neurosurgery. 49(1):108-15, 2001
69. RAK R, SEKHAR LN, STIMAC D, HECHL P: Endoscope-assisted microsurgery for microvascular compression syndromes. Neurosurgery 54(4):876-81, 2004
70. CHENG WY, CHAO SC, SHEN CC: Endoscopic microvascular decompression of the hemifacial spasm. Surg Neurol 70 Suppl 1:S40-6, 2008
71. FISCHER J, MUSTAFA H: Endoscopic-guided clipping of cerebral aneurysms. Br J Neurosurg 8(5): 559-565, 1994
72. PERNECZKY A, BOECHER-SCHWARTZ HG: Endoscope-assisted microsurgery for cerebral aneurysms. Neurol Med Chir 38 Suppl: 33-4, 1998
73. TANIGUCHI M, TAKIMOTO H, YOSHIMINE T et al.: Application of a rigid endoscope to the microsurgical management of 54 cerebral aneurysms: results in 48 patients. J Neurosurg 91(2):231-7, 1999
74. KATO Y, SANO H, NAGAHISA S, IWATA S, YOSHIDA K, YAMAMOTO K, KANNO T: Endoscopeassisted microsurgery for cerebral aneurysms. Minim Invasive Neurosurg. 43(2):91-7, 2000
75. KALAVAKONDA C, SEKHAR LN, RAMACHANDRAN P et al.: Endoscope-assisted microsurgery for intracranial aneurysms. Neurosurgery 51(5):1119-26, 2002
76. WANG E, YONG NP, NG I: Endoscopic assisted microneurosurgery for cerebral aneurysms. J Clin Neurosci. 10(2):174-6, 2003
77. KINOUCHI H, MIZOI K: Endoscope-assisted microsurgery for intracranial aneurysms. No Shinkei Geka 32(11):1117-30, 2004
78. KINOUCHI H, YANAGISAWA T, SUZUKI A, et al.: Simultaneous microscopic and endoscopic monitoring during surgery for internal carotid artery aneurysms. J Neurosurg 101(6):989-95, 2004
79. PROFETA G, DE FALCO R, AMBROSIO G et al.: Endoscope-assisted microneurosurgery for anterior circulation aneurysms using the angle-type rigid endoscope over a 3-year period. Childs Nerv Syst 20:811-815, 2004
80. ZHAO J, WANG Y, ZHAO Y, et al.: Neuroendoscope-Assistend Minimally Invasive Microsurgery for Clipping Intracranial Aneurysms. Minim Invasive Neurosurg 49:335-341, 2006
81. GALZIO RJ, DI COLA F, RAYSI DEHCORDI S, RICCI A, DE PAULIS D: Endoscope-assisted microneurosurgery for intracranial aneurysms. Front Neurol 18;4:201 (doi: 10.3389/fneur.2013.00201), 2013
82. GRIFFITH HB, VEERAPEN R: A direct transnasal approach to the sphenoid sinus. Technical note. J Neurosurg 66(1):140-2, 1997
83. JANE JA JR, THAPAR K, KAPTAIN GJ, MAARTENS N, LAWS ER JR: Pituitary surgery: transsphenoidal approach. Neurosurgery 51(2):435-42, 2002
84. KELLY DF, ESPOSITO F, MALKASIAN DR: Endonasal endoscope-assisted microscopic approach. In “Cranial, Craniofacial and Skull Base Surgery”, Cappabianca P, Califano L, Iaconetta G (Eds), Springer-Verlag, Heidelberg London Milan New York, pp 213-224, 2010
85. CIRIC I, ROSENBLATT S, ZHAO JC: Transsphenoidal microsurgery. Neurosurgery 51(1):161-9, 2002
86. KAWAMATA T, ISEKI H, ISHIZAKI R, HORI T: Minimally invasive endoscope-assisted endonasal trans-sphenoidal microsurgery for pituitary tumors: experience with 215 cases comparing with sublabial trans-sphenoidal approach. Neurol Res 24(3):259-65, 2002
87. FAHLBUSCH R, BUCHFELDER M: Transsphenoidal surgery of parasellar pituitary adenomas. Acta Neurochir (Wien) 92(1-4):93-9, 1998
88. JHO HD, ALFIERI A: Endoscopic transsphenoidal pituitary surgery: various surgical techniques and recommended steps for procedural transition. Br J Neurosurg 14(5):432-40, 2000
89. FRANK G, PASQUINI E, FARNETI G, MAZZATENTA D, SCIARRETTA V, GRASSO V, FAUSTINI FUSTINI M: The endoscopic versus the traditional approach in pituitary surgery. Neuroendocrinology 83(3-4):240-8, 2006
90. CAPPABIANCA P, CAVALLO LM, DE DIVITIIS O, SOLARI D, ESPOSITO F, COLAO A: Endoscopic pituitary surgery. Pituitary 11(4):385-90, 2008

91. ANAND VK, SCHWARTZ TH: Endoscopic Skull Base And Pituitary Approaches, A Step-By-Step Guide for Surgical Instruction and Cadaveric Dissection. Verlag Endo:Press® Tuttlingen, Germany, 2010
92. CASTELNUOVO P, LOCATELLI D: The Endoscopic Surgical Technique “Two Nostrils – Four Hands”. Verlag Endo:Press® Tuttlingen, Germany, 2008
93. FRANK G, SCIARRETTA V, CALBUCCI F, FARNETI G, MAZZATENTA D, PASQUINI E: The endoscopic transnasal transsphenoidal approach for the treatment of cranial base chordomas and chondrosarcomas. Neurosurgery 59(1 Suppl 1):ONS50-7, 2006
94. CAPPABIANCA P, CAVALLO LM, ESPOSITO F, DE DIVITIIS O, MESSINA A, DE DIVITIIS E: Extended endoscopic endonasal approach to the midline skull base: the evolving role of transsphenoidal surgery. Adv Tech Stand Neurosurg 33:151-99, 2008
95. CAPPABIANCA P, CAVALLO LM, ESPOSITO F, DE DIVITIIS O, MESSINA A, DE DIVITIIS E: Extended endoscopic endonasal approach to the midline skull base: the evolving role of transsphenoidal surgery. Adv Tech Stand Neurosurg 33:151-99, 2008
96. CASTELNUOVO P, LOCATELLI D: Endoscopic Surgical Management of Cerebrospinal Fluid Rhinorrhea. Verlag Endo:Press® Tuttlingen, Germany, 2008

Endoscope-Assisted Microneurosurgery (EAM) NEW

Recommended Set acc. to GALZIO

Endoscope-Assisted Microneurosurgery (EAM) NEW

Recommended Set acc. to GALZIO

① 28162 AUA		**HOPKINS® Straight Forward Telescope 0°,** diameter 2.7 mm, length 15 cm, **autoclavable**
② 28162 BOA		**HOPKINS® Forward-Oblique Telescope 30°,** enlarged view, diameter 2.7 mm, length 15 cm, direction of view in 12 o'clock position, **autoclavable**
③ 28162 AUS		**Irrigation and Suction Sheath 0°,** for use with HOPKINS® Telescope 28162 AUA and **KARL STORZ** lens irrigation system CLEARVISION® II
④ 28162 BOS		**Irrigation and Suction Sheath 30°,** for use with HOPKINS® Telescope 28162 BOA and **KARL STORZ** lens irrigation system CLEARVISION® II
⑤ 28164 XG		**Suction Tube,** with grip plate and elongated cut-off hole, outer diameter 9 Fr., length 15 cm
⑥ 28164 XM		**Same,** outer diameter 7 Fr.
⑦ 28164 XK		**Same,** outer diameter 5 Fr.
⑧ 28164 PUA		**Dissector,** bayonet-shaped, curved downwards, working length 13.5 cm
⑨ 28164 POA		**Dissector,** bayonet-shaped, curved upwards, working length 13.5 cm
⑩ 28164 HGB		**Micro Hook,** bayonet-shaped, blunt, working length 13.5 cm
⑪ 28164 BPA		**Bipolar Coagulating Forceps,** insulated, bayonet-shaped, blunt, tip 0.7 mm, working length 12 cm, total length 23 cm
⑫ 28164 BPC		**Bipolar Coagulating Forceps,** insulated, bayonet-shaped, blunt, tip 0.3 mm, working length 12 cm, total length 23 cm
⑬ 662362		VANNAS **Micro Scissors,** bayonet-shaped, blade straight, total length 20 cm
⑭ 662365		**Same,** scissor blades curved upwards
⑮ 28272 RKB		**Holding System, autoclavable** including: **Socket,** to clamp to the OR table **Articulated Stand,** L-shaped **Clamping Jaw,** metal, with axial intake

It is recommended to check the suitability of the product for the intended procedure prior to use.

HOPKINS® Telescopes

for Endoscope-Assisted Microneurosurgery (EAM)

Recommended Set acc. to GALZIO

Diameter 2.7 mm, length 15 cm

28162 AUA

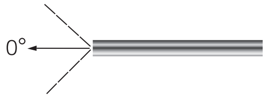

28162 AUA **HOPKINS® Straight Forward Telescope 0°,** diameter 2.7 mm, length 15 cm, **autoclavable,** proximally angled eyepiece and light connection, fiber optic light transmission incorporated, color code: green

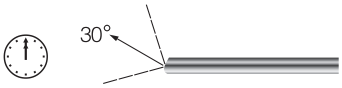

28162 BOA **HOPKINS® Forward-Oblique Telescope 30°,** enlarged view, diameter 2.7 mm, length 15 cm, direction of view in **12 o'clock** position, **autoclavable,** proximally angled eyepiece and light connection, fiber optic light transmission incorporated, color code: red

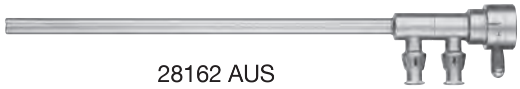

28162 AUS

28162 AUS **Irrigation and Suction Sheath 0°,** oval, 3.5 x 4.7 mm, working length 12 cm, for use with HOPKINS® Telescope 28162 AUA and **KARL STORZ** lens irrigation system CLEARVISION® II

28162 BOS **Irrigation and Suction Sheath 30°,** oval, 3.5 x 4.7 mm, working length 12 cm, for use with HOPKINS® Telescope 28162 BOA and **KARL STORZ** lens irrigation system CLEARVISION® II

Instruments

for Endoscope-Assisted Microneurosurgery (EAM)

Recommended Set acc. to GALZIO

28164 HGB

28164 HGB **Micro Hook,** bayonet-shaped, blunt, working length 13.5 cm

28164 POA **Dissector,** bayonet-shaped, curved upwards, working length 13.5 cm

28164 PUA **Dissector,** bayonet-shaped, curved downwards, working length 13.5 cm

662351

662362 VANNAS **Micro Scissors,** bayonet-shaped, blade straight, total length 20 cm

662365 VANNAS **Micro Scissors,** bayonet-shaped, scissor blades curved upwards, total length 20 cm

Bipolar Coagulating Forceps

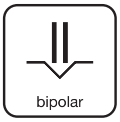

Recommended Set acc. to GALZIO

Bipolar Coagulating Forceps, insulated,
for use with Bipolar High Frequency Cords 847000 or 847000 A/E/M/V

28164 BPA **Bipolar Coagulating Forceps,** insulated, bayonet-shaped, blunt, tip 0.7 mm, working length 12 cm, total length 23 cm

28164 BPC **Same,** tip 0.3 mm

Suction Tubes

Recommended Set acc. to GALZIO

28164 XG

28164 XG	**Suction Tube,** with grip plate and elongated cut-off hole, distal holes, LUER, outer diameter 9 Fr., length 15 cm
28164 XM	**Same,** 7 Fr.
28164 XK	**Same,** 5 Fr.

Holder

For use with CLEARVISION® II irrigation sheaths

28272 RKB

28272 RKB **Holding System, autoclavable**
including:
Rotation Socket, to clamp to the operating table, for use with European and United States standard rails, with lateral clamp for height/angle adjustment of the articulated stand
Articulated Stand, reinforced version, L-shaped, with one central clamp for all five joint functions, height 48 cm, operating range 52 cm
Clamping Jaw, metal, with axial intake, for use with instrument, irrigation and telescope sheaths, clamping range 4.8 up to 12.5 mm

IMAGE1 S Camera System

Economical and future-proof

- **Modular concept for flexible, rigid and 3D endoscopy as well as new technologies**
- **Forward and backward compatibility with video endoscopes and FULL HD camera heads**
- **Sustainable investment**
- **Compatible with all light sources**

Innovative Design

- **Dashboard: Complete overview with intuitive menu guidance**
- **Live menu: User-friendly and customizable**
- **Intelligent icons: Graphic representation changes when settings of connected devices or the entire system are adjusted**
- **Automatic light source control**
- **Side-by-side view: Parallel display of standard image and the Visualization mode**
- **Multiple source control: IMAGE1 S allows the simultaneous display, processing and documentation of image information from two connected image sources, e.g., for hybrid operations**

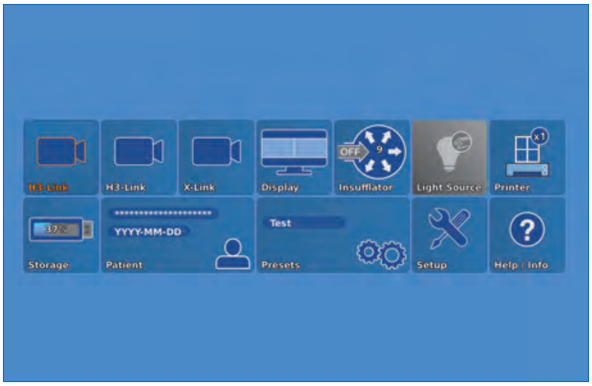

Dashboard

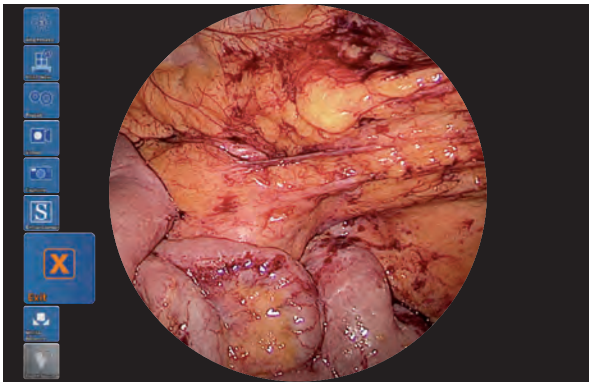

Live menu

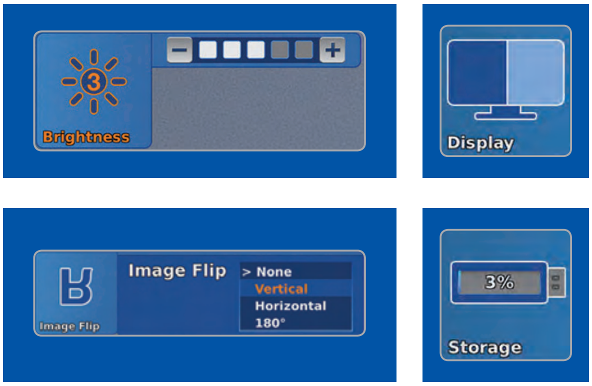

Intelligent icons

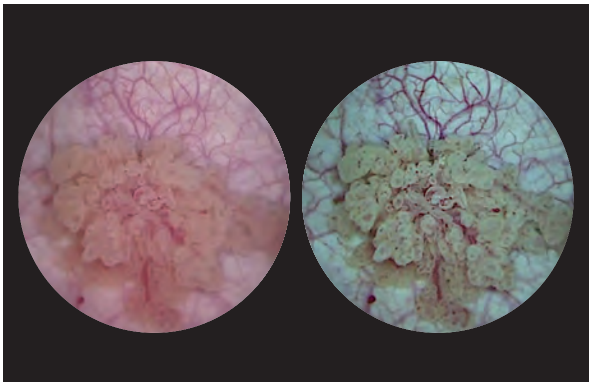

Side-by-side view: Parallel display of standard image and Visualization mode

IMAGE1 S Camera System NEW

IMAGE1 S

Brillant Imaging

- **Clear and razor-sharp endoscopic images in FULL HD**
- **Natural color rendition**
- **Reflection is minimized**
- **Multiple IMAGE1 S technologies for homogeneous illumination, contrast enhancement and color shifting**

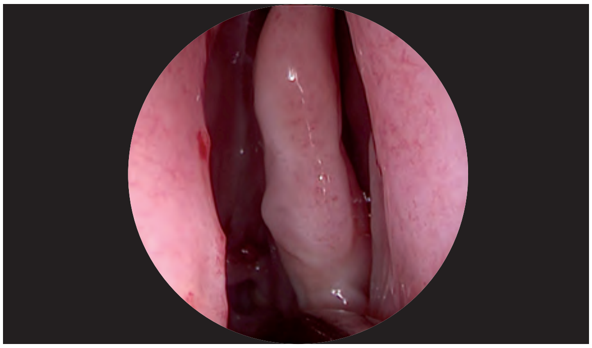

FULL HD image

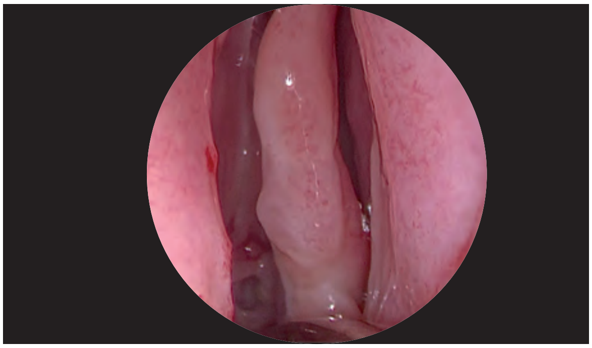

CLARA

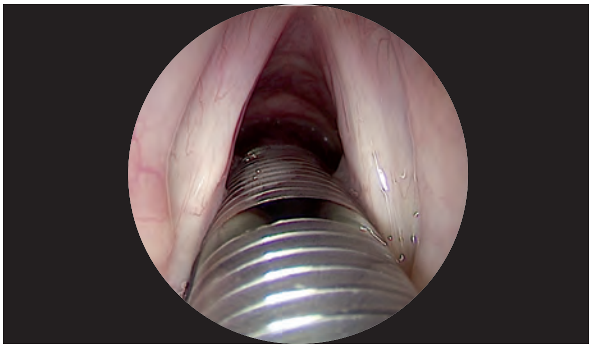

FULL HD image

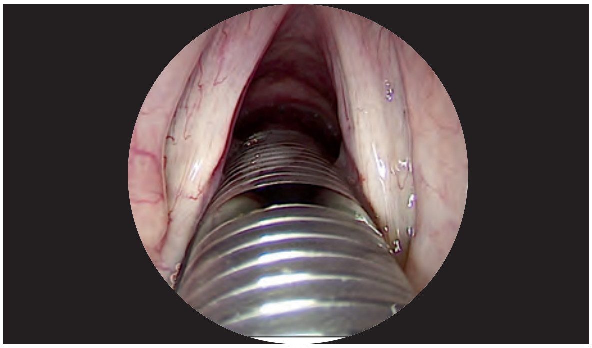

CHROMA

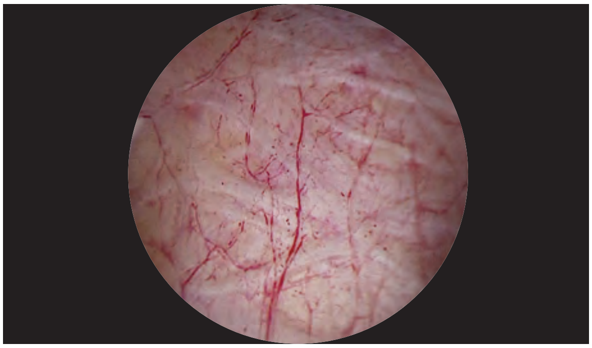

FULL HD image

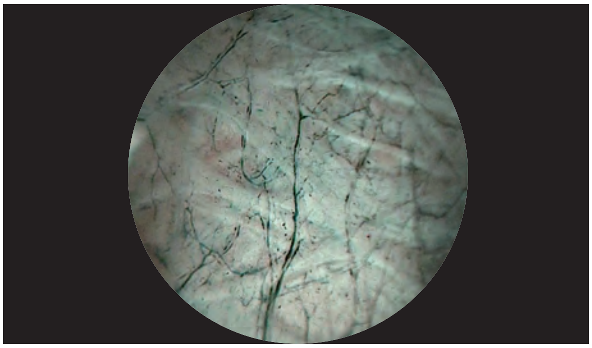

*SPECTRA A**

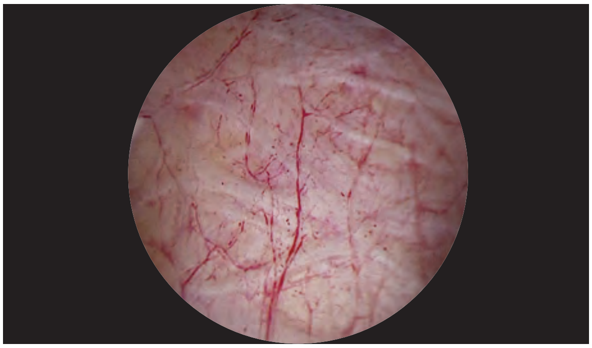

FULL HD image

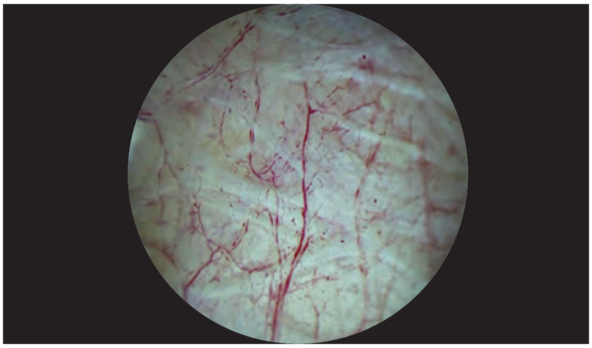

*SPECTRA B***

* *SPECTRA A:* **Not for sale in the U.S.**
** *SPECTRA B:* **Not for sale in the U.S.**

IMAGE1 S Camera System NEW

IMAGE1 S

TC 200EN

TC 200EN* **IMAGE1 S CONNECT**, connect module, for use with up to 3 link modules, resolution 1920 x 1080 pixels, with integrated KARL STORZ-SCB and digital Image Processing Module, power supply 100–120 VAC/200–240 VAC, 50/60 Hz
including:
Mains Cord, length 300 cm
DVI-D Connecting Cable, length 300 cm
SCB Connecting Cable, length 100 cm
USB Flash Drive, 32 GB, USB silicone keyboard, with touchpad, US

***Available in the following languages:** DE, ES, FR, IT, PT, RU

Specifications:

HD video outputs	- 2x DVI-D - 1x 3G-SDI
Format signal outputs	1920 x 1080p, 50/60 Hz
LINK video inputs	3x
USB interface SCB interface	4x USB, (2x front, 2x rear) 2x 6-pin mini-DIN

Power supply	100–120 VAC/200–240 VAC
Power frequency	50/60 Hz
Protection class	I, CF-Defib
Dimensions w x h x d	305 x 54 x 320 mm
Weight	2.1 kg

For use with IMAGE1 S
IMAGE1 S CONNECT Module TC 200EN

TC 300

TC 300 **IMAGE1 S H3-LINK,** link module, for use with IMAGE1 FULL HD three-chip camera heads, power supply 100–120 VAC/200–240 VAC, 50/60 Hz,
for use with IMAGE1 S CONNECT TC 200EN
including:
Mains Cord, length 300 cm
Link Cable, length 20 cm

Specifications:

Camera System	**TC 300 (H3-Link)**
Supported camera heads/video endoscopes	TH 100, TH 101, TH 102, TH 103, TH 104, TH 106 (fully compatible with IMAGE1 S) **22**220055-3, **22**220056-3, **22**220053-3, **22**220060-3, **22**220061-3, **22**220054-3, **22**220085-3 (compatible without IMAGE1 S technologies CLARA, CHROMA, SPECTRA*)
LINK video outputs	1x
Power supply	100–120 VAC/200–240 VAC
Power frequency	50/60 Hz
Protection class	I, CF-Defib
Dimensions w x h x d	305 x 54 x 320 mm
Weight	1.86 kg

* *SPECTRA A:* **Not for sale in the U.S.**
** *SPECTRA B:* **Not for sale in the U.S.**

HD Imaging with Operating Microscopes

Direct Adaption

Direct adaption to the VARIO operating microscope from Carl Zeiss Meditec

With the operating microscope the surgeon always has a perfect view of the operating field. Assistents, OR nurses and students, however, often experience poor video presentation, especially if FULL HD visualization is not available.

KARL STORZ offers a one-stop-shop solution to upgrade any surgical microscope with state-of-the-art FULL HD imaging technology.
To achieve optimal results, all components in the video chain – from the camera system to the monitor – must be of the highest quality.

The most straightforward and professional connection between camera and microscope is the so-called direct adaption.

Here the H3-M COVIEW® microscope camera and the corresponding QUINTUS® TV adaptor are directly connected to the microscope via the C-MOUNT connection.

IMAGE1 S Camera Heads NEW

IMAGE1 S

For use with IMAGE1 S Camera System
IMAGE1 CONNECT Module TC 200EN, IMAGE1 H3-LINK Module TC 300
and with all IMAGE 1 HUB™ HD Camera Control Units

TH 106

TH 106 **IMAGE1 S H3-M COVIEW Three-Chip FULL HD Camera Head,** 50/60 Hz, IMAGE1 S compatible, progressive scan, with C-MOUNT thread for coupling to microscopes, 2 freely programmable camera head buttons, with detachable camera head cable, length 900 cm, for use with IMAGE1 S and IMAGE 1 HUB™ HD/HD

20 2001 31

20 2001 31 **Keypad,** for H3-M camera head, for convenient control of the most important H3-M camera functions, with PS/2 connector, cable length 1 m, alternative to a standard keyboard, for use with H3-M or H3-M COVIEW camera heads, only compatible with IMAGE1 HUB™ HD, not compatible with IMAGE1 S

Specifications:

IMAGE1 S FULL HD Camera Heads	IMAGE1 S H3-M COVIEW
Product code	TH 106
Image sensor	3x ⅓" CCD chip
Dimensions w x h x d	45 x 50 x 60 mm
Weight	240 g
Optical interface	C-MOUNT connection
Min. sensitivity	F 1.9/1.4 Lux
Grip mechanism	C-MOUNT connection
Cable	detachable
Cable length	900 cm

HD Imaging with Operating Microscope

System Components

QUINTUS® – High-Performance TV Adaptor for Operating Microscopes

Unleash the full performance of your operating microscope from CARL ZEISS MEDITEC – with FULL HD imaging solutions from KARL STORZ.

The new QUINTUS® TV adaptor is the perfect interface between the operating microscope and the H3-M COVIEW® FULL HD microscope camera head from KARL STORZ.

The innovative features of QUINTUS® are easy to use, making it one of the most flexible TV adaptors on the market.

Product Features:

- A rotating C-MOUNT connection at the QUINTUS® TV adaptor allows immediate adaption of the camera orientation during mounting.
- The focus control makes it possible to easily achieve parfocality (perfectly sharp camera and microscope images).
- The iris control provides convenient and optimal adjustment of the depth of field.
- Pan (X) function enables adjustment of the horizontal position of the camera image.
- Tilt (Y) function enables adjustment of the vertical position of the camera image. The pan and tilt functions helps the surgeon to adjust the position of the camera image according to his individual needs.
- The QUINTUS® ZOOM model also features a variable focal length f = 43 – 86 mm. This allows the surgeon greater flexibility in choosing the exact zone required for documentation.

Focal length of the QUINTUS® TV adaptor:

The QUINTUS® TV adaptor is available in the fixed focal lengths f = 45 and f = 55 mm or as a zoom model with variable focal length 43 – 86 mm. This provides an optimal FULL HD image in 16:9 in conjunction with the H3-M COVIEW® HD microscope camera head from KARL STORZ.

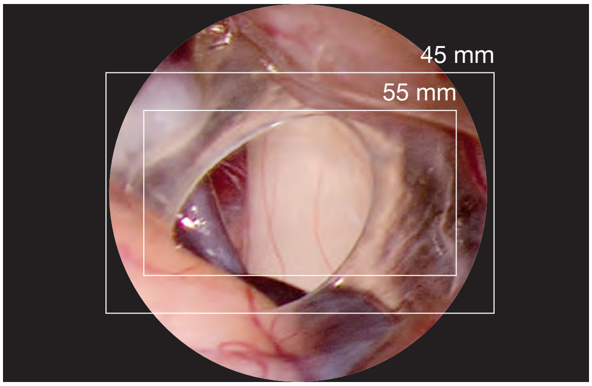

Focal lengths: H3-M COVIEW® *camera image detail sing a QUINTUS® TV adaptor with the fixed focal lengths of 45 and 55 mm.*

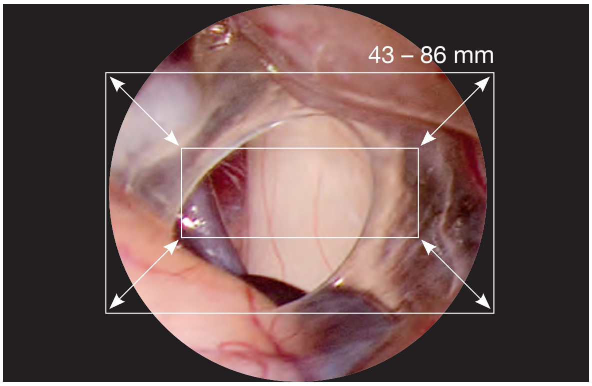

Variable focal length: *Adjustable H3-M COVIEW® camera image detail using a QUINTUS® zoom adaptor with variable focal length of 43 – 86 mm.*

HD Imaging with Operating Microscope

System Components

QUINTUS® TV Adaptor for operating microscopes from CARL ZEISS MEDITEC with fixed focal length

20 9230 45/**20** 9230 55

20 9230 45 — **QUINTUS® Z 45 TV Adaptor,** for CARL ZEISS MEDITEC operating microscopes, f = 45 mm, recommended for IMAGE1 HD H3-M/H3-M COVIEW® camera heads

20 9230 55 — **QUINTUS® Z 55 TV Adaptor,** for CARL ZEISS MEDITEC operating microscopes, f = 55 mm, recommended for IMAGE1 HD H3-M/H3-M COVIEW®, H3, H3-Z as well as IMAGE1 S1 and S3 camera heads

QUINTUS® Zoom TV Adaptor for operating microscopes from CARL ZEISS MEDITEC with variable focal length

20 9230 00 Z

20 9230 00 Z — **QUINTUS® Zoom TV Adaptor,** for CARL ZEISS MEDITEC operating microscopes, with variable focal length f = 43 – 86 mm, for use with all KARL STORZ cameras (SD and HD)

Further accessories for operating microscopes from CARL ZEISS MEDITEC

20 9250 00

20 9250 00 — **Iris,** for ZEISS Pentero®, iris as a necessary extension between the QUINTUS® TV adaptor and the operating microscope ZEISS Pentero®

301513

301513 — **Optical Beamsplitter 50/50,** for use with ZEISS operating microscope or colposcope

Note: Optical beamsplitters for other operating microscopes (i.e. LEICA or Möller-Wedel) are available directly from the manufacturers.

HD Imaging with Operating Microscope

System Components

QUINTUS® TV Adaptor for operating microscopes from LEICA Microsystems with fixed focal length

20 9330 45/**20** 9330 55

20 9330 45 **QUINTUS® L 45 TV Adaptor,** for LEICA Microsystems operating microscopes, f = 45 mm, recommended for H3-M microscope camera head

20 9330 55 **QUINTUS® L 55 TV Adaptor,** for LEICA Microsystems operating microscopes, f = 55 mm, recommended for IMAGE1 HD H3-M/H3-M COVIEW®, H3, H3-Z as well as S1 and S3 camera heads

QUINTUS® TV Adaptor for operating microscopes from LEICA Microsystems with variable focal length

20 9330 00 Z

20 9330 00 Z **QUINTUS® Zoom TV Adaptor,** for LEICA Microsystems operating microscopes, with variable focal length f = 43 – 86 mm, for use with all KARL STORZ cameras (SD and HD)

QUINTUS® TV Adaptor for operating microscopes from Möller-Wedel with fixed focal length

20 9530 45/**20** 9530 55

20 9530 45 **QUINTUS® M 45 TV Adaptor,** for Möller-Wedel operating microscopes, f = 45 mm, recommended for IMAGE1 HD H3-M/H3-M COVIEW® camera heads

20 9530 55 **QUINTUS® M 55 TV Adaptor,** for Möller-Wedel operating microscopes, f = 55 mm, recommended for IMAGE1 HD H3-M/H3-M COVIEW®, H3, H3-Z and S1, S3 camera heads

Note: Optical beamsplitters for other operating microscopes (i.e. LEICA or Möller-Wedel) are available directly from the manufacturers.

IMAGE1 S Camera Heads *NEW*

IMAGE1 S

For use with IMAGE1 S Camera System
IMAGE1 S CONNECT Module TC 200EN, IMAGE1 S H3-LINK Module TC 300
and with all IMAGE 1 HUB™ HD Camera Control Units


TH 100

TH 100 **IMAGE1 S H3-Z Three-Chip FULL HD Camera Head,** 50/60 Hz, IMAGE1 S compatible, progressive scan, soakable, gas- and plasma-sterilizable, with integrated Parfocal Zoom Lens, focal length f = 15–31 mm (2x), 2 freely programmable camera head buttons, for use with IMAGE1 S and IMAGE 1 HUB™ HD/HD

Specifications:

IMAGE1 FULL HD Camera Heads	**IMAGE1 S H3-Z**
Product no.	TH 100
Image sensor	3x ⅓" CCD chip
Dimensions w x h x d	39 x 49 x 114 mm
Weight	270 g
Optical interface	integrated Parfocal Zoom Lens, f = 15–31 mm (2x)
Min. sensitivity	F 1.4/1.17 Lux
Grip mechanism	standard eyepiece adaptor
Cable	non-detachable
Cable length	300 cm

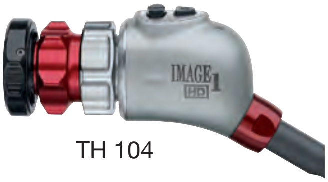
TH 104

TH 104 **IMAGE1 S H3-ZA Three-Chip FULL HD Camera Head,** 50/60 Hz, IMAGE1 S compatible, **autoclavable,** progressive scan, soakable, gas- and plasma-sterilizable, with integrated Parfocal Zoom Lens, focal length f = 15–31 mm (2x), 2 freely programmable camera head buttons, for use with IMAGE1 S and IMAGE 1 HUB™ HD/HD

Specifications:

IMAGE1 FULL HD Camera Heads	**IMAGE1 S H3-ZA**
Product no.	TH 104
Image sensor	3x ⅓" CCD chip
Dimensions w x h x d	39 x 49 x 100 mm
Weight	299 g
Optical interface	integrated Parfocal Zoom Lens, f = 15–31 mm (2x)
Min. sensitivity	F 1.4/1.17 Lux
Grip mechanism	standard eyepiece adaptor
Cable	non-detachable
Cable length	300 cm

Monitors

9619 NB

9619 NB **19" HD Monitor,**
color systems **PAL/NTSC,** max. screen resolution 1280 x 1024, image format 4:3, power supply 100–240 VAC, 50/60 Hz, wall-mounted with VESA 100 adaption,
including:
External 24 VDC Power Supply
Mains Cord

9826 NB

9826 NB **26" FULL HD Monitor,**
wall-mounted with VESA 100 adaption,
color systems **PAL/NTSC,**
max. screen resolution 1920 x 1080,
image fomat 16:9,
power supply 100–240 VAC, 50/60 Hz
including:
External 24 VDC Power Supply
Mains Cord

Monitors

KARL STORZ HD and FULL HD Monitors	19"	26"
Wall-mounted with VESA 100 adaption	9619 NB	9826 NB
Inputs:		
DVI-D	●	●
Fibre Optic	–	–
3G-SDI	–	●
RGBS (VGA)	●	●
S-Video	●	●
Composite/FBAS	●	●
Outputs:		
DVI-D	●	●
S-Video	●	–
Composite/FBAS	●	●
RGBS (VGA)	●	–
3G-SDI	–	●
Signal Format Display:		
4:3	●	●
5:4	●	●
16:9	●	●
Picture-in-Picture	●	●
PAL/NTSC compatible	●	●

Optional accessories:

9826 SF **Pedestal,** for monitor 9826 NB
9626 SF **Pedestal,** for monitor 9619 NB

Specifications:

KARL STORZ HD and FULL HD Monitors	19"	26"
Desktop with pedestal	optional	optional
Product no.	9619 NB	9826 NB
Brightness	200 cd/m² (typ)	500 cd/m² (typ)
Max. viewing angle	178° vertical	178° vertical
Pixel distance	0.29 mm	0.3 mm
Reaction time	5 ms	8 ms
Contrast ratio	700:1	1400:1
Mount	100 mm VESA	100 mm VESA
Weight	7.6 kg	7.7 kg
Rated power	28 W	72 W
Operating conditions	0–40°C	5–35°C
Storage	-20–60°C	-20–60°C
Rel. humidity	max. 85%	max. 85%
Dimensions w x h x d	469.5 x 416 x 75.5 mm	643 x 396 x 87 mm
Power supply	100–240 VAC	100–240 VAC
Certified to	EN 60601-1, protection class IPX0	EN 60601-1, UL 60601-1, MDD93/42/EEC, protection class IPX2

Cold Light Fountains and Accessories

495 NL	**Fiber Optic Light Cable,** with straight connector, diameter 3.5 mm, length 180 cm
495 NA	**Same,** length 230 cm

Cold Light Fountain XENON 300 SCB

20133101-1	**Cold Light Fountain XENON 300 SCB** with built-in antifog air-pump, and integrated KARL STORZ Communication Bus System SCB power supply: 100–125 VAC/220–240 VAC, 50/60 Hz including: **Mains Cord** **SCB Connecting Cable,** length 100 cm
20133027	**Spare Lamp Module XENON** with heat sink, 300 watt, 15 volt
20133028	**XENON Spare Lamp,** only, 300 watt, 15 volt

Cold Light Fountain XENON NOVA® 300

20134001	**Cold Light Fountain XENON NOVA® 300,** power supply: 100–125 VCA/220–240 VAC, 50/60 Hz including: **Mains Cord**
20133028	**XENON Spare Lamp,** only, 300 watt, 15 volt

Equipment Cart

UG 220

UG 220

Equipment Cart
wide, high, rides on 4 antistatic dual wheels
equipped with locking brakes 3 shelves,
mains switch on top cover,
central beam with integrated electrical subdistributors
with 12 sockets, holder for power supplies,
potential earth connectors and cable winding
on the outside,

Dimensions:
Equipment cart: 830 x 1474 x 730 mm (w x h x d),
shelf: 630 x 510 mm (w x d),
caster diameter: 150 mm

inluding:

Base module equipment cart, wide
Cover equipment, equipment cart wide
Beam package equipment, equipment cart high
3x **Shelf,** wide
Drawer unit with lock, wide
2x **Equipment rail,** long
Camera holder

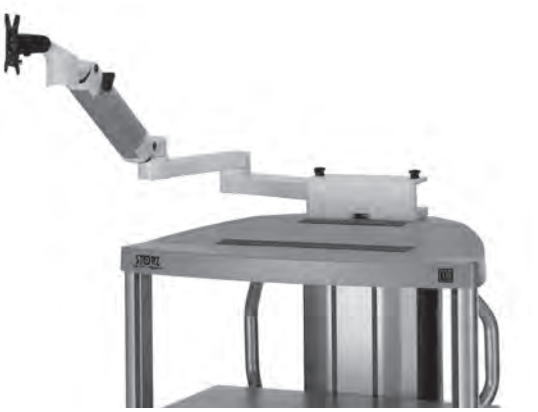

UG 540

UG 540

Monitor Swifel Arm,
height and side adjustable,
can be turned to the left or the right side,
swivel range 180°, overhang 780 mm,
overhang from centre 1170 mm,
load capacity max. 15 kg,
with monitor fixation VESA 5/100,
for usage with equipment carts UG xxx

Recommended Accessories for Equipment Cart

UG 310

UG 310 **Isolation Transformer,**
200 V–240 V; 2000 VA with 3 special mains socket,
expulsion fuses, 3 grounding plugs,
dimensions: 330 x 90 x 495 mm (w x h x d),
for usage with equipment carts UG xxx

UG 410

UG 410 **Earth Leakage Monitor,**
200 V–240 V, for mounting at equipment cart,
control panel dimensions: 44 x 80 x 29 mm (w x h x d),
for usage with isolation transformer UG 310

UG 510

UG 510 **Monitor Holding Arm,**
height adjustable, inclinable,
mountable on left or right,
turning radius approx. 320°, overhang 530 mm,
load capacity max. 15 kg,
monitor fixation VESA 75/100,
for usage with equipment carts UG xxx

Data Management and Documentation

KARL STORZ AIDA® – Exceptional documentation

The name AIDA stands for the comprehensive implementation of all documentation requirements arising in surgical procedures: A tailored solution that flexibly adapts to the needs of every specialty and thereby allows for the greatest degree of customization.

This customization is achieved in accordance with existing clinical standards to guarantee a reliable and safe solution. Proven functionalities merge with the latest trends and developments in medicine to create a fully new documentation experience – AIDA.

AIDA seamlessly integrates into existing infrastructures and exchanges data with other systems using common standard interfaces.

WD 200-XX* **AIDA Documentation System,**
for recording still images and videos,
dual channel up to FULL HD, 2D/3D,
power supply 100-240 VAC, 50/60 Hz

including:

USB Silicone Keyboard, with touchpad
ACC Connecting Cable
DVI Connecting Cable, length 200 cm
HDMI-DVI Cable, length 200 cm
Mains Cord, length 300 cm

WD 250-XX* **AIDA Documentation System,**
for recording still images and videos,
dual channel up to FULL HD, 2D/3D,
including SMARTSCREEN® (touch screen),
power supply 100-240 VAC, 50/60 Hz

including:

USB Silicone Keyboard, with touchpad
ACC Connecting Cable
DVI Connecting Cable, length 200 cm
HDMI-DVI Cable, length 200 cm
Mains Cord, length 300 cm

*XX Please indicate the relevant country code
(DE, EN, ES, FR, IT, PT, RU) when placing your order.

Workflow-oriented use

Patient

Entering patient data has never been this easy. AIDA seamlessly integrates into the existing infrastructure such as HIS and PACS. Data can be entered manually or via a DICOM worklist.
ll important patient information is just a click away.

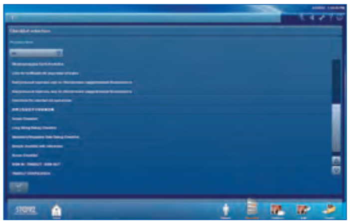

Checklist

Central administration and documentation of time-out. The checklist simplifies the documentation of all critical steps in accordance with clinical standards. All checklists can be adapted to individual needs for sustainably increasing patient safety.

Record

High-quality documentation, with still images and videos being recorded in FULL HD and 3D. The Dual Capture function allows for the parallel (synchronous or independent) recording of two sources. All recorded media can be marked for further processing with just one click.

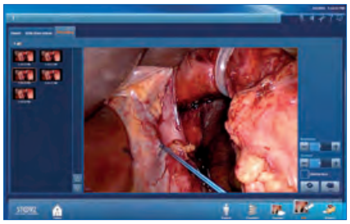

Edit

With the Edit module, simple adjustments to recorded still images and videos can be very rapidly completed. Recordings can be quickly optimized and then directly placed in the report.
In addition, freeze frames can be cut out of videos and edited and saved. Existing markings from the Record module can be used for quick selection.

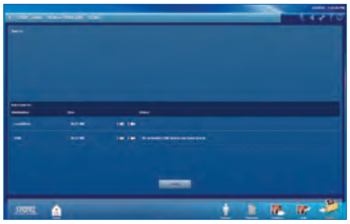

Complete

Completing a procedure has never been easier. AIDA offers a large selection of storage locations. The data exported to each storage location can be defined. The Intelligent Export Manager (IEM) then carries out the export in the background. To prevent data loss, the system keeps the data until they have been successfully exported.

Reference

All important patient information is always available and easy to access. Completed procedures including all information, still images, videos, and the checklist report can be easily retrieved from the Reference module.

Notes: